INFORMATION TO USERS

This manuscript has been reproduced from the microfilm master. UMI films the text directly from the original or copy submitted. Thus, some thesis and dissertation copies are in typewriter face, while others may be from any type of computer printer.

The quality of this reproduction is dependent upon the quality of the copy submitted. Broken or indistinct print, colored or poor quality illustrations and photographs, print bleedthrough, substandard margins, and improper alignment can adversely affect reproduction.

In the unlikely event that the author did not send UMI a complete manuscript and there are missing pages, these will be noted. Also, if unauthorized copyright material had to be removed, a note will indicate the deletion.

Oversize materials (e.g., maps, drawings, charts) are reproduced by sectioning the original, beginning at the upper left-hand corner and continuing from left to right in equal sections with small overlaps.

Photographs included in the original manuscript have been reproduced xerographically in this copy. Higher quality 6" x 9" black and white photographic prints are available for any photographs or illustrations appearing in this copy for an additional charge. Contact UMI directly to order.

Bell & Howell Information and Learning
300 North Zeeb Road, Ann Arbor, MI 48106-1346 USA
800-521-0600

Université d'Ottawa · University of Ottawa

THE EFFECTS OF PARTICULATES ON THE ULTRAFILTRATION OF BILGE (OILY) WASTEWATER CONTAINING NEW OR USED LUBRICATING OIL

By:

Marco Nottegar

A thesis submitted to the Faculty of Graduate and Postdoctoral Studies
in partial fulfilment of the requirements for the degree of
MASTER OF APPLIED SCIENCE
in the Department of Chemical Engineering
University of Ottawa

October 4th, 2000

ABSTRACT

As a result of increasing environmental regulations, navies and the marine industry have been required to install effective Oily Water Separation (OWS) systems capable of providing an effluent containing no more than 15 parts per million (ppm) oil and grease. However, due to the complex nature of bilge water it has proven difficult to develop a system capable of achieving these environmental standards while also addressing the marine constraints of compactness, robustness and automation. This work has investigated the particulate loading of bilge water and the impact of its various components on the effectiveness of a membrane based treatment system. Additionally, various means of minimizing the decline in trans-membrane flux associated with the particulate loading of bilge water were examined.

The oil emulsions created by used diesel engine lubricating oil are different from those created by new diesel engine lubricating oil. Lower trans-membrane flux values were experienced with synthetic bilge water made with used, rather than new, lubricating oil. Flat sheet testing, using membranes with various pore sizes, indicated that a synthetic bilge water made from used lubricating oil contains two primary groups of solute particles. The smaller of these particles is approximately 0.0035 microns in radius and the larger is approximately 0.024 microns in radius. Oil penetration, resulting in severe membrane fouling, was observed with the one microfiltration membrane tested, but not with any of the ultrafiltration membranes.

Pilot scale testing was performed to better simulate shipborne conditions. Two membranes were tested: a ceramic membrane with a pore diameter of 0.005 microns and a polyacrylo nitrile membrane with a Molecular Weight Cut-off of 50,000 Daltons. The average run lasted 24 hours and the membranes were cleaned after each run. The ceramic membrane was found to be prone to fouling. The pure water permeability of the ceramic membrane decreased by approximately 35% over a one month period, while the polymeric membrane maintained its trans-membrane flux over a similar length of time.

Backflushing was tested as a means of trans-membrane flux enhancement. In this particular application only marginal flux enhancements were observed with backflushing. The results were substantially less than theoretically predicted. This result was attributed to the adhesion of the oil emulsion cake layer to the membrane surface. It was found that a membrane pre-filter provided an extremely effective means of reducing the concentration of oil emulsions in the bilge water and therefore improving trans-membrane flux rates.

RÉSUMÉ

Avec le resserrement des normes environnementales, les industries maritimes doivent installer des systèmes d'épuration de l'eau de cale à bord de leurs navires. Ces systèmes doivent être capables de produire un effluent contenant moins de 15 mg/L en huiles et graisses. Toutefois, la nature de cette eau est très complexe. Le développement d'un système capable de rencontrer les normes environnementales tout en respectant les limites d'espace, de solidité et d'automatisation s'avère difficile. Cette étude a examiné la présence de particules et d'émulsions dans l'eau de cale et leur effet sur l'efficacité d'un système de traitement à base de membranes. De plus, divers moyens d'augmenter le flux trans-membranaire lors du traitement d'une eau de cale synthétique ont été étudiés.

Les émulsions créées par une huile usagée de moteur diesel s'avèrent différentes des émulsions produites àpartir d'huiles nouvelles. On observe des flux trans-membranaires inférieurs pour les eaux de cale produites a partir d'huiles usagées comparées a celles produites a partir d'huiles neuves. Les essais impliquant des membranes planes ayant diverses grosseurs de pores ont indiqué que l'eau de cale synthétique faite à partir d'huiles usagées contient deux groupes de particules qui posent un problème de traitement. Ces deux groupes sont caractérisés par des rayons de 0,0035 et 0,024 microns. La pénétration d'huile dans les pores d'une membrane fut observée en microfiltration et non en ultrafiltration.

Des essais à dimension restreints ont été exécutés pour mieux simuler les conditions abord des navires. Deux membranes ont été étudiées; une membrane céramique ayant des pores de 0,005 micron (diamètre) et une membrane en polyacrylonitrile ayant un seuil de coupure de 50,000 Daltons. La durée de chaque essai était de 24 heures et les membranes ont été nettoyées après chaque essai. La perméabilité à l'eau pure de la membrane céramique a diminué d'environ 35% pendant une période d'un mois. Cependant, la membrane polymérique a gardé son flux durant la même période. Des essais à flux inverse de courte durée ont été étudiés en tant que moyen pour réduire

l'entartrage. Les résultats ont été modestes et beaucoup moins que théoriquement prévus. La réduction de la capacité de régénérer le flux est attribuée à l'adhérence de l'émulsion à la surface de la membrane. La présence d'un pré-filtre a augmenter le flux trans-membranaire. Cette augmentation est attribuée à la diminution de la concentration de l'émulsion dans l'eau de cale lors des essais.

ACKNOWLEDGEMENTS

Over the course of completing my Master's of Applied Science, and in particular this thesis, I have been extremely fortunate to have had the help of many individuals. As this list of those who helped me is extremely long I apologise to those that I may have omitted.

First, I wish to thank the support staff within the Department of Chemical Engineering. The staff of technicians was invaluable in providing me with assistance in the design, maintenance and operation of my experimental apparatus. They also provided me with an excellent sounding board of possible means of improving my experimental setup and listened to my constant rants and raves. I also wish to thank the Department's administrative and support staff who were always very willing and cooperative in assisting me in the administrative details associated with my work (or, more accurately, correcting the countless headaches I provided them).

Secondly, I wish to thank those professors who provided me with the necessary instruction in my various environmental studies. I also wish to thank my fellow graduate students who ensured that I learned the correct lessons through their continual, yet friendly, reminders of what our professors were really teaching us.

Thirdly, I owe a huge debt of gratitude to Mr. Dwight Vienot of the Dockyard Laboratory of the Defence Research Establishment (Atlantic). Dwight not only ensured that I received the necessary financial support to complete this Masters program, but also provided me with excellent feedback in how to best examine and present the ideas and concepts associated with my thesis. Dwight's involvement and interest in my works certainly exceeded the limited requirements of the Department of National Defence's Technical Authority.

Fourth, I wish to express my sincere gratitude to my research supervisor, Dr. André

Tremblay of the Department of Chemical Engineering. To Dr. Tremblay I thank you for your endless support and assistance that you provided, throughout this work. It was evident from the onset of my studies and became more and more apparent as I progressed with this project that your interest far exceeded the academic requirements, but extended to my own personal and professional development. I will always remember and appreciate your support, knowing how much you went beyond the normal requirements of an academic advisor.

Finally, I wish to thank my family for their support throughout this work. Their help and encouragement was essential throughout my studies. I greatly appreciated the support and emotional aid provided by both my parents and my wife's parents. However, I owe the greatest debt of thanks to my wife, Christene, and our two sons, Peter and Alex, without whose help I am sure that I would not have been able to complete this thesis. To the many lost days, evenings, and weekends that I spent working on this thesis I can finally answer that "Daddy is finally finished his Masters".

NOMENCLATURE

a_p	=	solute particle radius
C_{bulk}	=	concentration of the bulk solution
C_{cake}	=	concentration within the cake layer
D	=	diffusivity co-efficient
D_{brn}	=	brownian diffusivity
D_{shear}	=	shear diffusivity
J	=	flux
J(t)	=	flux at a given time
$J(t_{ss})$	=	steady state flux
J_{avg}	=	average flux over the length of the non-backflushed portion of a backflush cycle
J_{bf}	=	average flux over the length of a complete operational cycle
J_{PWP}	=	membrane pure water permeate flux
K	=	mass transfer co-efficient
k	=	Boltzmann constant
P_{crit}	=	critical capillary pressure
R	=	resistance
R_{foul}	=	fouling resistance
R_{cake}	=	cake layer resistance
R_{mem}	=	membrane resistance
R_{total}	=	total resistance
$\hat{R}_{cake}$	=	specific cake layer resistance
r_l	=	membrane flow channel (i.e. lumen) radius
r_{oil}	=	oil droplet radius
r_{pore}	=	membrane pore radius
T	=	temperature
t	=	time

t_{bf}	=	time of the backflush
t_{op}	=	time of normal operation (i.e. $t_{total} - t_{bf}$)
t_{total}	=	complete operation cycle time; including both the backflush and normal operation time
t_{ss}	=	time required for the cake layer to achieve steady state
U	=	cross-flow velocity
ΔP	=	transmembrane pressure
δ	=	cake layer thickness
δ_{ss}	=	steady state cake layer thickness
θ	=	contact angle of an oil droplet to a membrane pore
σ	=	oil-water interfacial tension
ϕ	=	solute volume fraction
ϕ_b	=	solute volume fraction of the bulk solution
ϕ_{max}	=	maximum solute volume fraction (at the cake layer)
$\dot{\gamma}$	=	local shear rate
$\eta(\phi)$	=	relative viscosity
$\eta(\phi_b)$	=	bulk relative viscosity
κ	=	shear induced diffusion co-efficient, a dimensionless function of particle volume
μ	=	dynamic viscosity
τ_c	=	time dependent flux decline constant
τ_w	=	wall shear stress
τ_{wo}	=	wall shear stress without a cake layer

ACRONYMS

AWPPA	=	Arctic Waters Pollution Prevention Act
CSA	=	Canada Shipping Act
DND	=	(Canadian) Department of National Defence
IMO	=	International Maritime Organization
MARCORDs	=	Maritime Command Orders (for the Canadian Navy)
MWCO	=	Molecular Weight Cut-Off
OWS	=	Oily Water Separator
PEG	=	Polyethylene Glycol
PEO	=	Polyethylene Oxide
PVDF	=	Polyvinylidene difluoride
ppm	=	parts per million
SPE	=	Solid Phase Extraction
TDS	=	Total Dissolved Solids
TOG	=	Total Oils and Greases
TSS	=	Total Suspended Solids

TABLE OF CONTENTS

Appendices

LIST OF TABLES

LIST OF FIGURES

1.0 INTRODUCTION

The treatment of bilge water required for shipboard overboard discharge has always been a concern for the naval and marine sectors, the requirement for its adequate treatment has become more critical in recent years as environmental regulations have tightened and become better enforced. The current overboard discharge regulations, applicable to Canadian vessels, are primarily detailed in the Canada Shipping Act (CSA, 1999) and in the Arctic Waters Pollution Prevention Act (AWPPA, 1999) which are based upon the International Maritime Organisation (IMO, 1999) regulations. These regulations limit the total content of oil and grease in overboard discharge to be no greater than 100 parts per million (ppm) oil beyond 12 nautical miles off shore, 15-ppm oil within 12 nautical miles of shore, and 5 ppm within coastal waters (CSA, 1999). Additionally, the Canadian Navy is governed by its own regulations, Maritime Command Orders (MARCORDs). MARCORDs preclude Canadian warships from discharging bilge water within 12 nautical miles and require the overboard discharge have an oil content no greater than 15-ppm oil between 12 to 200 nautical miles, and an effluent quality of no more than 100-ppm beyond 200 nautical miles.

In the past, navies and the merchant marine have utilised systems based on and/or accentuating gravity separation (e.g., parallel plate separation). While these systems are effective for the removal of free oil from bilge water they are not particularly adept at the removal of emulsified oil from bilge water (Resera, 1992). Additionally, systems relying upon gravity separation are inherently limited by the extreme motion associated with shipborne applications, resulting in an increase in the quantity of emulsified oil and ultimately lower efficiency. Thus, for a shipborne bilge water treatment system to be effective it must be able to treat free and emulsified oil and deal with other marine requirements such as equipment space limitations, motion, bilge water reductions and system automation.

A major factor in the successful treatment of bilge water is a system's ability to withstand the varied composition of bilge water. Bilge water can and does contain a wide variety of hydrocarbons, such as used and/or unused engine lubricating oils and greases, marine diesel fuel and hydraulic oil. Additionally, a variety of detergents and surfactants may be found in bilge water, which enhance the formation and stability of oil emulsions by their presence and concentration in bilge water. Complicating bilge water treatment are the other miscellaneous contaminants that can be found in bilge water. These contaminants include, but are not limited to, metal oxides (rust particles), asbestos and other insulation particles, refrigerants and general wastes common to municipal treatment facilities (Resera, 1995).

The current Oily Water Separator (OWS) system fitted onboard Canadian Navy Ships is a coalescence system, commercially known as the "SAREX" system. This system can achieve the water quality limits, is compact and independent of motion, but fouls rapidly, making it extremely labour intensive due to the requirement for frequent coalescence filter changes (Resera, 1992). While fundamentally different from a coalescence OWS, a membrane system is also capable of achieving all of the naval/marine requirements, with its primary obstacle successfully meeting all naval requirements being fouling (Resera, 1992). Accordingly, if fouling can be reduced, and therefore membrane efficiency increased, to acceptable levels then a membrane based OWS system can offer a practical solution for bilge water treatment.

This work investigated some fundamental aspects of membrane separation technology in order to provide an effective membrane based shipborne bilge water treatment system. Specifically, this work focused on two prime areas. The first was the development of a better appreciation of how the composition of bilge water affects membrane separation efficiencies (i.e., how its composition impacts the formation of the cake or gel layer and how a membrane is fouled). Methods of flux enhancement were investigated based on a better understanding of this interaction between bilge water and a membrane and how the interaction limits a membrane's flux rate. Membrane flux enhancement was attempted

through the control of operational parameters, such as backflushing.

2.0 BACKGROUND AND LITERATURE REVIEW

2.1 Problem Definition

Onboard ships, wastes, and in particular liquid wastes, collect in a ship's bilges. This resulting "bilge water" has a high oil content, especially bilge water produced in the main machinery spaces, due to the leakage of oils and greases from shipboard machinery. One of the earliest sources of marine pollution is the pollution of the seas by oil, with oily-water discharge regulations first being enacted by the IMO in 1959 (IMO, 1999). Subsequently, due to increasing environmental awareness, the regulations have become more stringent.

In order to effectively treat bilge water a process must be capable of addressing the different oil compositions of this wastewater. Oil is present in bilge water as either free or emulsified oil. The emulsified oil can be further divided into the two categories of mechanical and chemical emulsions. Mechanical emulsions are those created by the physical mixing of oil and water. This can occur due to the movement in a ship's bilge and tanks, and the pumping of bilge water. Chemical emulsions are the result of the addition of detergents and surfactants into the bilge water. These detergents and surfactants are necessary for other shipborne aspects (i.e., ships' husbandry, fire fighting, boiler water treatment, etc...) and ultimately are deposited into a ship's bilge.

The environmental regulations pertaining to oil pollution, for the Canadian marine sector, stem from the following jurisdictions: international - the International Maritime Organization (IMO), and national - the Canada Shipping Act (CSA) and the Arctic Waters Pollution Prevention Act (AWPPA). The Canadian Navy also has their own regulations, as detailed in Maritime Command Orders (MARCORDs). While these regulations are rather complex, their synopsis is as follows (CSA, 1999 and AWPPA, 1999);

a. within Canadian inland waters and various fishing zones (e.g., Grand Banks), undiluted effluent discharged overboard cannot exceed 5 ppm of oil,
b. within 12 nautical miles of Canadian coastline, undiluted effluent discharge overboard cannot exceed 15-ppm of oil,
c. beyond 12 nautical miles off shore, undiluted effluent discharged overboard cannot exceed 100-ppm of oil, and
d. within the Arctic Ocean (i.e., beyond 60° of latitude), no bilge water discharge, unless it is unavoidable and essential to a ship's operation.

While all navies are under no legal obligation to adhere to the CSA, AWPPA or IMO regulations (CSA, 1999) the Canadian Navy has imposed its own restrictions (through MARCORDs) upon the discharge of bilge water (DND, 1999);

a. within 12 nautical miles of land, no effluent shall be discharged,
b. within 200 nautical miles of land, effluent discharge overboard cannot exceed 15-ppm oil, and
c. all Canadian ships will comply with the environmental regulations of other nations.

Therefore in order for Canadian Navy ships to discharge bilge water overboard they must possess an OWS capable of reducing the oil content of bilge water to at least 15-ppm oil. Within Canadian waters, excluding the arctic, an OWS must be capable of reducing bilge water oil content to 5-ppm oil. Assuming that transits within Canadian waters are fairly

short then it would be possible to not discharge bilge water during this interval. Therefore, the most pressing requirement would be to achieve the international standard of no more than 15-ppm oil in effluent discharge. It would also be highly preferable to also achieve an effluent discharge of no more than 5-ppm oil.

Additionally, an OWS not only has to fulfill the environmental regulations, but it must also address unique shipborne concerns. These additional criteria can be summarized as follows;

a. substantial bilge water volumetric reductions are required due to limited physical space,
b. system size, again due to the limited physical space, and
c. system automation; as an OWS is an ancillary system direct operator supervision should be limited.

2.2 Methods of Bilge Water Treatment

2.2.1 Gravity Separation

The most basic method to treat bilge water is by gravity separation. Gravity separation works on the principle that the density differences between water and oil causes these two liquids to separate if placed in a tank, given sufficient residence time. Therefore, an early method of bilge water treatment was the pumping of bilge water into a main collection tank and after a certain amount of residence time the bilge water separates into the oil and water phases. The water phase being more dense would be in the lower portion of the tank and it would be pumped overboard via a suction taken from a low point in the tank. Similarly, the concentrated oil phase would be pumped into a waste oil collection tank and discharged to a shore facility. Gravity separation is based upon Stokes law, therefore the rate of separation is dependent upon the difference in the specific gravities of oil and water (i.e., their density differences), the square of the oil emulsion size and the square of the tank diameter.

However, for a variety of reasons, gravity separation is not an effective means for the onboard treatment of bilge water. First, a reasonably large tank is required to ensure a sufficient residence time in order to effect the separation. Due to a ship's space limitations the size of the tank would be severely limited, and therefore so would the residence time, resulting in insufficient time for both the free oil to separate from the water and for the emulsified oil to coalesce and then separate from the water. Additionally, a ship's continual pitching and rolling does not allow for a uniform oil/water interface to form; therefore the separated oil and water continually re-mix.

In commercially available oily water separators, gravity separation is accentuated by two primary methods coalescence and parallel plate separation as described in the following sections.

2.2.2 Coalescence Separation

Coalescence is the process whereby oil droplets agglomerate together forming larger droplets accentuating gravity separation. The coalescence of oil droplets occurs at the oil-water interface and therefore coalescence increases the occurrence of these interfaces. Various coalescing media can be used to attract and agglomerate small oil droplets causing them to grow sufficiently large, such that they can be gravity separated from bilge water. Whatever media is used it should be oleophylic/hydrophobic in nature, that is, its surface charge attracts oils and repels water. Typical coalescing media include glass fibers, polypropylene, felt and special ceramics (Resera, 1992).

The Canadian Navy has used coalescing separators (trade name – SAREX separator) extensively for their treatment of bilge water. The SAREX system employs (oleophylic/hydrophobic) fine glass fibers as the filter medium and has three coalescence stages, preceded by a gravity separator (on most, but not all, classes of ships) (Resera, 1992). The first coalescing stage has a nominal filtration size of 10 microns, followed by two coalescing stages with nominal filtration sizes of 2 microns. The coalescence of the

oil droplets occurs as the bilge water flows through the coalescing medium. Due to the oleophylic/hydrophobic nature of the medium, oil droplets are retained by the coalescence medium and water is rejected. As more bilge water flows through the units the amount of retained oil increases and the oil droplets subsequently grow in size. When a sufficient amount of oil has been retained the oil droplets become large enough such that their buoyant force exceeds the oleophylic strength of the coalescence media and they separate from the coalescing medium. At this point the oil droplets are sufficiently large to be gravity separated from the bilge water. This process is portrayed in Figure 2.1.

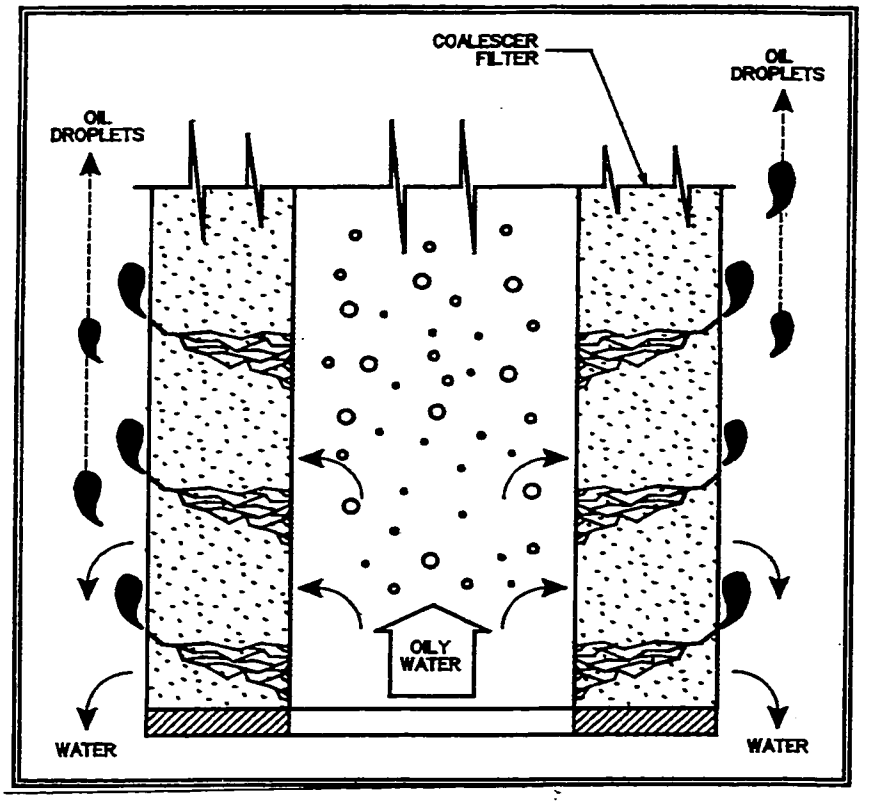

Figure 2.1: Coalescence Separation of Oily-Water (Resera, 1992)

The advantage of coalescence separators is their compactness and the fact that they are unaffected by a ship's motion. However, while they are effective for the separation of oil from bilge water, their use is labour intensive. The variable composition of bilge water

results in their frequent fouling, and the subsequent frequent replacement, of the filter media.

2.2.3 Parallel Plate Separation

Parallel plates can also be used to enhance oil coalescence. These plates provide numerous sloped surfaces which increase the oil-water interfacial area. To enhance the attraction of oil, and reduce the presence of water, at the plates, they are fabricated, or coated, with an oleophylic/hydrophobic material (Resera, 1992). Additionally, due to the numerous plates in the tank, the oil droplets are not required to travel a great distance before encountering a plate. Parallel plate separation uses gravity separation to remove oil from bilge water, but enhances gravity separation by increasing the size of the oil droplets. The size of the oil droplets is increased through the contact of the bilge water with the parallel plates. Due to the oleophylic/hydrophobic nature of the plates and the continual flow of bilge water past the plates, oil accumulates at the surface of the plates. This accumulation continues until the quantity of oil is sufficiently high to be gravity separated from the water phase. The angle of the plates is important to ensure that the bilge water adequately contacts the plates and that the accumulated oil is released from the plates. Accordingly, parallel plate separation enhances both the separation of free and emulsified oil from water. Figure 2.2 provides a schematic description of parallel plate separation.

The degree to which parallel plate separation accentuates gravity separation is a function of the number of plates in the tank (i.e., the ratio between the tank height and the distance between the plates) and the slope of the plates.

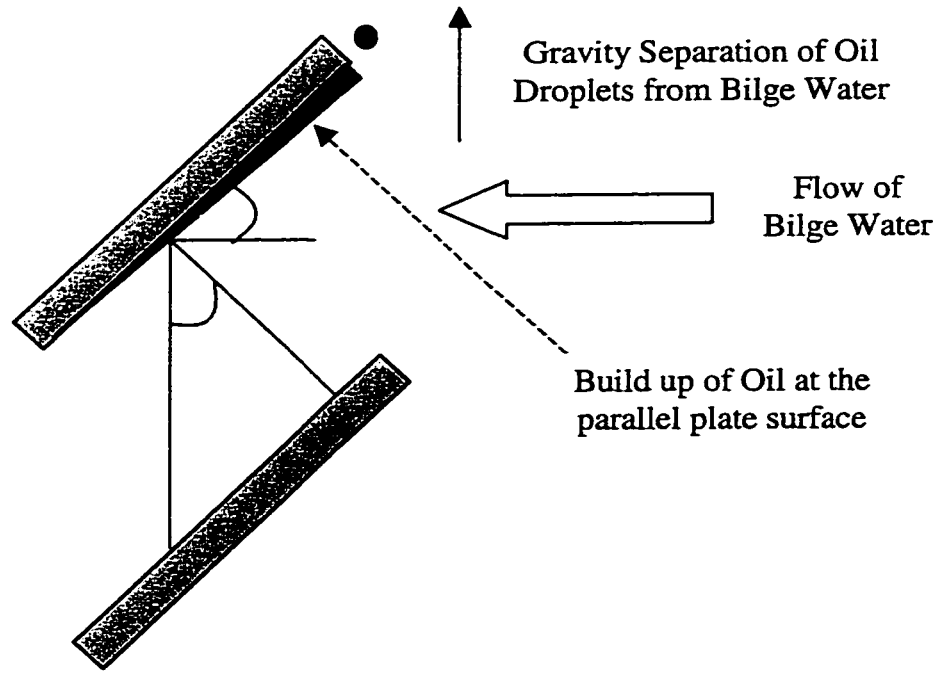

Figure 2.2: Parallel Plate Separation of Oily Water

While parallel plate separation is an effective means of accentuating gravity separation and it is a simple, and therefore easily automated system, it is still not practical for shipborne application for essentially the same reasons as simple gravity separation. That is, while a smaller tank is required as compared to simple gravity separation, the tank is still relatively large and it is adversely affected by the ship's motion. Parallel plate separators have been used throughout the United States Navy, with modest success (NATO, 1994).

2.2.4 Hydrocyclones

Liquid-liquid hydrocyclones are capable of removing free oil and some emulsified oils from oily waste waters. Hydrocyclones utilize centrifugal forces and the density differences between oil and water to separate oil from oily water. Figure 2.3 illustrates the principles of operation of a static hydrocyclone. As seen in Figure 2.3 the oily water enters the cylindrical swirl chamber and its velocity increases as it progresses through the

tapered reducing section. The combination of the swirling flow pattern, pressure drop across the unit and hydrocyclone geometry induce substantial centrifugal forces on the oily water, which results in the migration of the heavier water phase towards the hydrocyclone wall and the lighter oil phase to move towards the central, lower pressure, area. This oil rich centre section is removed via a reject tube located in the centre of the hydrocyclone at approximately a third to half of the hydrocyclone's length.

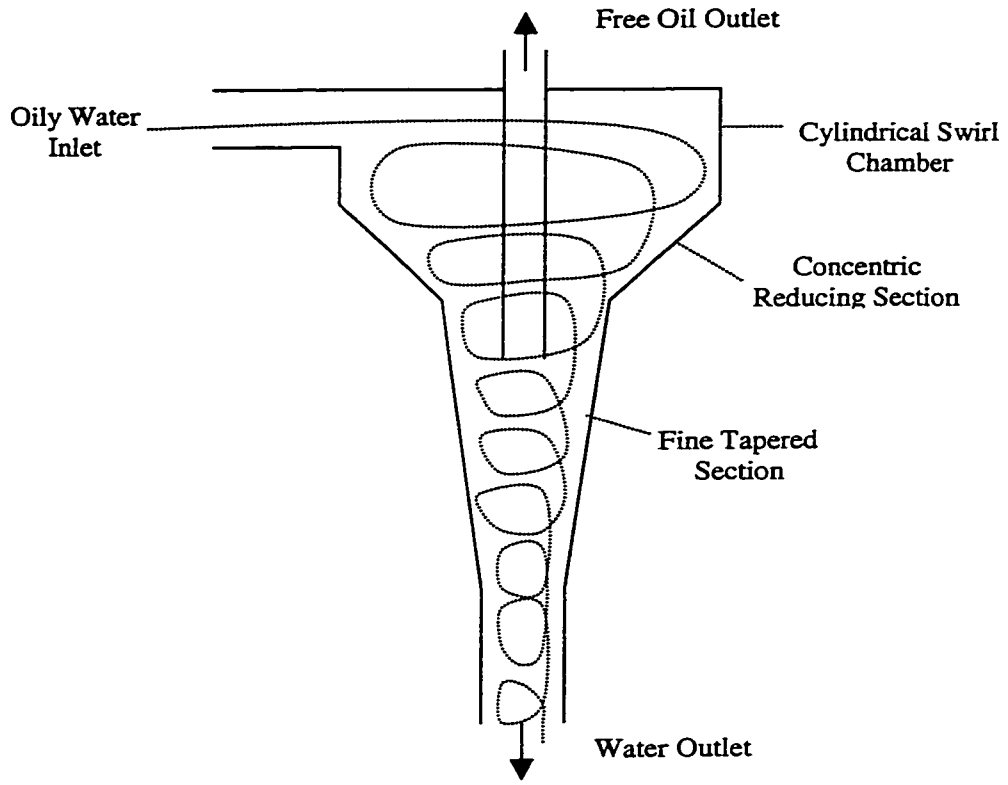

Figure 2.3: Schematic Diagram of a Static Hydrocyclone (Simms, 1994)

Two types of liquid-liquid hydrocyclones are available – static and dynamic. Dynamic hydrocyclones provide somewhat better separation of oils from water as the entire hydrocyclone body is rotated, resulting in higher centrifugal forces. However, this also results in greater maintenance requirements and increased safety concerns related to this movement (Simms, 1994). The combination of these maintenance and safety issues with only a limited improvement in oil separation, do not justify the use of dynamic hydrocyclones over static hydrocyclones for shipborne applications.

While static hydrocyclones are capable of removing oil droplets as small as 7-8 microns, they are most effective for oil droplets greater than 15 microns (Simms, 1994). To effect good separation efficiency a density difference of no less than 0.02 – 0.05 g/mL is required (Simms, 1994). Static hydrocyclones are quite compact and require relatively little maintenance. However, as seen by their separation limitations, static hydrocyclones would be suitable for the removal of free oil, but ineffectual for the removal of emulsified oils.

2.2.5 Membranes

Membrane filtration has been used in a variety of industrial applications, including the treatment of oily waste water. While gravity separation, and processes which accentuate gravity separation, utilize the density differences between oil and water to effect the separation, membrane filtration utilizes the size difference between oil and water to effect the separation. This is achieved through the use of a membrane with a sufficiently small pore size, which will reject the oil present in bilge water. Therefore, for membrane filtration, a satisfactory effluent quality can be dictated by the membrane pore size.

A simple batch membrane system is portrayed in Figure 2.4. It can be seen that a membrane system essentially consists of process tank, a feed pump, membrane and a back pressure valve. While an actual system would have some additional components, such as pre-treatment equipment, it can be seen that a membrane system is not overly complex and therefore can be easily automated. To achieve the necessary bilge water concentration, the feed is recirculated until a desired level of concentration is achieved.

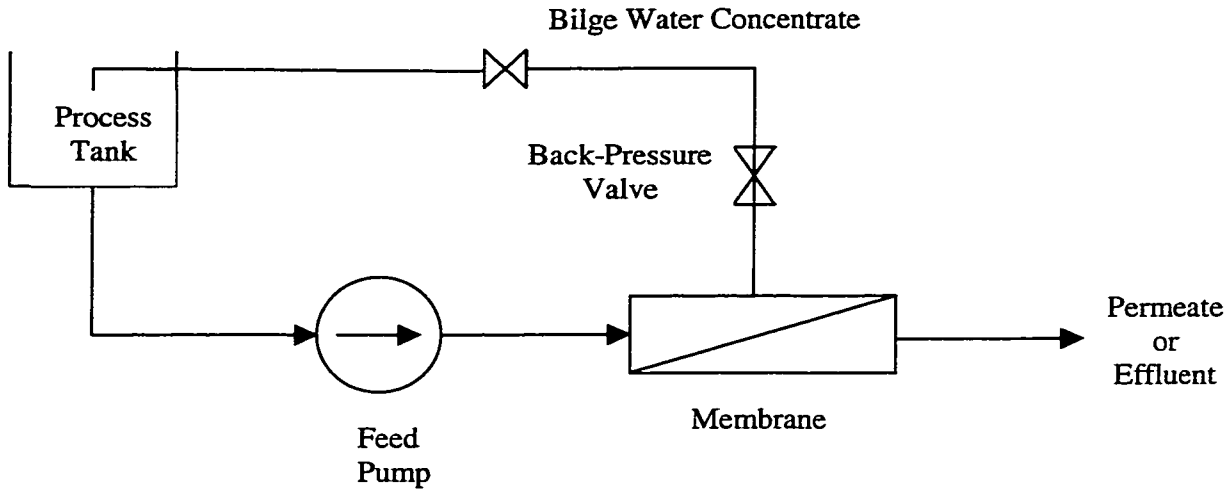

Figure 2.4: Basic Batch Membrane System

Therefore, achieving the required effluent purity and bilge water concentration is relatively easy with a membrane based system. The real challenge for a shipborne membrane system is in providing this degree of treatment and concentration in a sufficiently small system. While a tighter membrane (i.e., a membrane with a smaller pore size) provides a cleaner effluent it also results in lower membrane flux. This obstacle can be overcome by increasing the amount of membrane surface area. However, due to a ship's limited space, membrane area must be balanced against physical space constraints. Additionally, the contaminants found in bilge water can result in membrane fouling and a subsequent reduction in system flux.

Therefore in order for a membrane system to be successful two requirements must be achieved;

a. membrane pore size must balance effluent quality and membrane flux, and
b. membrane fouling must be minimized.

2.3 Physio-Chemical Nature of Bilge Water

The treatment of bilge water is a technically demanding challenge due to the fact that bilge water is not merely oily water. It is contaminated with a wide variety of substances, plus its oil component is often, but not always, emulsified (Marine Engineering Review, 1997). Additionally, it is important to remember that "the composition of bilge water is neither stable nor predictable" (Marine Engineering Review, 1997).

To properly consider the treatment of bilge water it is necessary to examine the impacts of the properties of bilge water. Some of these properties include;

a. composition,
b. oil emulsification,
c. pH, and
d. temperature.

The following description of bilge water characteristics is that of an average sampling. That is, at any given time the composition of bilge water can and does vary widely from this average. Variations from the average composition will pose unique problems to an OWS and therefore it must be designed to accommodate for such extremes. The most variable factor is likely to be the oil in the bilge water, both in terms of the types of oil present and their quantity. For example, the lube oil change of a diesel engine and/or diesel electrical generator can result in substantial influxes of used oil into the bilge in a short period of time.

2.3.1 Composition

Due to the wide variety of components that make up bilge water, plus the fact that its composition will vary from ship to ship and mission to mission, it is virtually impossible to accurately determine the composition of bilge water at any given time. The primary components of bilge water are sea (salt) and fresh water, in approximately equal

proportions. Bilge water contaminants vary widely, with some of the potential contaminants being diesel fuel, lubricants and greases, solvents, bilge cleaners, refrigerants, paints, boiler compound, food products, bacteria and various solid particles (rust, carbon, scale, pipe insulation).

A study (Resera, 1995) conducted on behalf of the Canadian Navy classified bilge water components into the following categories;

a. Total Oils and Greases (TOG),
b. Total Suspended Solids (TSS). TSS were defined as solids larger than 0.45 microns in diameter,
c. Total Dissolved Solids (TDS). TDS were defined as solids smaller than 0.45 microns in diameter,
d. detergents, and
e. sea and fresh water.

The average composition of bilge water was determined to be (Resera, 1995);

a. TOG = 1,284 mg/L,
b. TSS = 502 mg/L,
c. TDS = 17,735 mg/L, and
d. the remainder being water, which was an approximately equal mixture of sea water and potable water.

Each of these characteristics provides some insight into the make up and variability of bilge water.

Total Oils and Grease (TOG). While the average TOG value was found to be approximately 1,300 mg/L it varied from 15 to 7,000 mg/L, based upon a study examining 37 bilge water samples (Resera, 1995). Additionally, TOG provides a somewhat distorted view of the oil content of bilge water as this will include non-harmful oils and greases, such as vegetable oils and animal fats which originate from a ship's

galley. Accordingly, it was found that petroleum based hydrocarbons accounted for approximately 85% of the TOG value (Resera, 1995). The primary types of oils found in bilge water are naval distillate (i.e., marine diesel fuel), naval diesel engine lubricating oil and hydraulic oil (DND, 1996). While the quantity of petroleum hydrocarbons in bilge water is useful, another useful parameter would be an indication of the amount of free and emulsified oil, as differing types of separation processes are more effective for the removal of free or emulsified oil.

Linked to the degree of emulsified oils present in bilge water is the quantity of detergents found in bilge water. Detergents are very much a component of bilge water as they are used onboard ships for a variety of purposes. The quantity of detergents present will have a direct link to the amount of emulsified oils present in solution. The Canadian Navy has estimated the quantity of detergents to be approximately 500 mg/L (DND, 1996). Additionally, while numerous types of detergents are commercially available the Navy has attempted to limit the number used onboard ships. The primary types of detergents found onboard Canadian Navy vessels are CLEANBREAK (a petroleum based, commercially available, detergent), ZOK-27 (a water based, commercially available, detergent) and a corrosion removing compound (containing phosphoric and oxalic acids) (DND, 1996).

Total Suspended Solids (TSS). As with TOG the quantity of TSS also varied significantly, ranging from 0 to 2,750 mg/L, with an average of approximately 500 mg/L. For membrane separations the size of the TSS will be orders of magnitudes larger than the membrane pore size (based upon the usage of an ultrafiltration membrane, i.e. a pore size no greater than 0.01 microns) and therefore will have minimal impact upon the membrane flux rate.

Total Dissolved Solids (TDS). The average value of the TDS suggests that it is essentially the salts found in sea water, since sea water has an average salt content of approximately 35,000 mg/L and sea water comprises 50% of the water component of

bilge water. However, the Canadian Navy study found that TDS ranged from 700 to 32,050 mg/L, with the average content being approximately 17,700 mg/L (Resera, 1995). The upper end of this range, 32,050 mg/L, would suggest that the TDS are comprised of more than just sea salts. Examples of other possible TDS sources may be rust particles and carbonaceous sediment found in the lubricating oil from diesel engines.

In order to have a standard against which to quantify all OWS the Canadian Navy identified the following as its standard bilge water cocktail, including the prime constituents of each of the major categories (DND, 1996):

a. TOG = 2000 ppm. Composed of 50% naval distillate, 40% naval unused diesel engine lubricating oil and 10% naval hydraulic oil;
b. Suspended Solids = 500 ppm. Composed of 80% insulation lagging dust, 10% ferric or ferrous oxide and 10% carbon black;
c. Detergents = 500 ppm. Composed of 50% CLEANBREAK, 40% ZOK-27 and 10% corrosion removal compound; and
d. Water = remaining 99.7%. Composed of a 50/50 mixture of fresh and sea water.

2.3.2 Oil Phases

Oil present in bilge water comprises three distinct phases (Cheryan, 1986);

a. free oil (i.e., oil which is easily separable from the water phase of bilge water),
b. unstable oil/water emulsions, and
c. stable oil/water emulsions.

The specific size and quantity of the oil/water emulsions are created by a number of factors including imposed shear (from pumping and pipe runs), oil concentration, oil to surfactant ratio, interaction with filtering media (Lipp et al., 1988) and ship's motion.

Mechanical emulsions are formed by pumping bilge water, turbulent flow in piping and any other devices in the bilge system that break up oil droplets into smaller droplets. The size of the oil droplets created by mechanical emulsion varies depending on the amount of agitation created and the composition of the bilge water. It is estimated that mechanical emulsions can create oil droplets as small as 0.5 microns (Resera, 1992). Mechanical emulsions can be reduced by using slow turning/low shearing positive displacement pumps and by using pipes of sufficient size to avoid excessive agitation and turbulence.

Chemical emulsions are caused by the presence of detergents, emulsifying agents, or surfactants present in bilge water. While unfortunate for the treatment of the bilge water these compounds serve legitimate shipborne purposes (Resera, 1992), including;

a. removal of oil from bilge deck plates and ladders to reduce the risk of fires and personnel injury due to slipping, and
b. cleaning of machinery/parts for necessary repairs/maintenance.

Accordingly, it is not possible to eliminate the use of detergents, emulsifying agents or surfactants from shipborne use.

Lipp et al. (1998) studied the size of oil emulsions in water, created by mineral oils with surfactants, couplers, corrosion inhibitors and other additives. Their study used various oil to surfactant ratios, including a ratio of 4:1, the same ratio used by the Canadian Navy in its makeup of synthetic bilge water. They noted that the size of oil emulsions were dependent upon both the oil concentration and the oil to surfactant ratio, but they observed that the oil to surfactant ratio had a much greater impact upon emulsion size.

For oily waters with concentrations ranging from 2 to 40% and a surfactant ratio of 4:1 the size of oil emulsions were very consistent, having a range of 0.0175 microns to 0.175 microns, in radius. When the oil concentration was increased beyond 40%, up to 50%,

the size (radius) of the oil emulsions also increased, ranging from 0.0275 to 0.225 microns (Lipp et al., 1988). Further complicating the issue of emulsions is the fact that the quantity and number of different detergents/emulsifying agents/surfactants present in bilge water will affect the quantity and size of oil emulsions (Bil'dyikevich and Dmitrieva, 1989).

Therefore, based upon the types of oils present in bilge water and their approximate size, oil coalescers can adequately process free and mechanically emulsified oils. However, they are likely inadequate to treat chemical (i.e. stable) emulsions. The same could be stated of a parallel plate OWS. A hydrocyclone could provide fast and effective treatment for free oil, however it would not be effective for any type of emulsified oils. A membrane based OWS would be very well suited for emulsified oils, particularly the stable chemical emulsions. However, membrane systems are at greater risk of fouling when experiencing gross slugs of oil (NATO, 1994). Therefore it would appear that an optimal system would use a combination of methods, taking advantages of each particularly system's strength, space permitting.

2.3.3 pH

As the major component in bilge water is sea water it is expected that bilge water would be slightly acidic. This is precisely what has been observed, as a Canadian Navy study found various bilge waters to have an average pH of approximately 6.5. The pH was relatively consistent for various bilge waters as it ranged from 5.3 to 7.6, with only a small percentage (18%) below a pH value of 6 (Resera, 1992). Accordingly, pH is not a concern when dealing with bilge water treatment using membrane technologies, as commercially available membranes can easily tolerate these pH conditions. Polymeric membranes, which are not as robust as inorganic membranes, generally can tolerate a pH range of 4 to 10 (KOCH Membrane Systems Incorporated technical literature, 1997 and Osmonics technical literature, 1999).

2.3.4 Temperature

The temperature of bilge water is primarily affected by the temperature of sea water, the temperature of the main machinery spaces and the energy transferred to the bilge water by bilge system equipment (e.g., pumps). Prior to a ship sailing bilge water temperature will assume that of the ambient sea temperature and then warm as it is heated by the ambient temperature within the main machinery spaces and through equipment heat gains. Accordingly, the temperature of bilge water can range from 2°C to 35°C, depending on where in the world's oceans a ship may be deployed.

This temperature range is not expected to cause any difficulties with membrane performance, as all membranes can tolerate this temperature range. Inorganic membranes are capable of being exposed to boiling water without experiencing any degradation, while organic membranes generally cannot withstand temperatures beyond 45°C.

The impact that temperature will have upon performance is that of flux enhancement. It is commonly known that for every 1°C increase in temperature a membrane's water flux increases by approximately 3 per cent (ASTM Standard D 5090-90, 1991). However, it is unknown how the oil in the bilge water will react as the temperature changes.

2.3.5 Uniqueness of Bilge Water

Oily water is currently produced in the automotive, machining and petroleum industries. Numerous studies have been conducted on the treatment of these waste solutions. However, limited research has focused on bilge water. While oily and produced waters, originating in the petroleum industry, are oily water solutions, they are not identical in nature to bilge water. Accordingly, it cannot be expected that the simple application of an oily water or produced water treatment system will successfully fulfill all the

requirements of a naval bilge water treatment system. This is due to the fact that these systems do not address the unique challenges of treating bilge water and are likely to result in a system with limited capabilities, as experienced by the Canadian and U.S. Navies with the SAREX OWS and parallel plate systems, respectively (NATO, 1994).

One of the unique factors associated with bilge water is its variability, in terms of both oil concentration and composition. Produced water (from oil fields) and industrial oily waters are much more predictable, particularly with respect to composition, as they do not have the varied source of contaminants that exists for bilge water. This unpredictability is a serious problem for the design of a bilge water treatment system because one aspect in membrane selection is choosing a membrane to separate the various compounds. However, if the solution composition or component quantities are continually changing it is difficult for a particular membrane to always perform effectively. The main problem associated with this variance in composition will likely be increased membrane fouling.

Also, the difference in composition between bilge water and oily or produced water is another factor dictating a unique bilge water treatment system. As an example, in produced water the presence of sand can provide a beneficial effect. The sand can result in reduced membrane fouling as the sand may gently scour the membrane, removing substances adhering to the surface.

Another unique variable associated with bilge water treatment is the size of the oil droplet/emulsion. As described in section 2.3.2, oil emulsions can be as small as 0.0175 microns in radius. Accordingly, it would appear that for membranes, the simple answer would be to select a membrane with a sufficiently small pore size. However, the problem with the use of a tighter membrane is reduced membrane productivity. Therefore, membrane selection must optimize oil retention and productivity.

Oily and produced water treatment systems provide a good starting point for the design of a bilge water treatment system, however, without addressing the unique characteristics of bilge water it is doubtful that they will provide optimal treatment solutions for bilge water. Accordingly, the unanswered questions for bilge water treatment are most likely to be membrane pore size, cake or gel properties at the surface of the membrane and fouling due to pore plugging or blinding.

3.0 THEORY

Membrane performance is governed by a variety of factors. Some of these are; the membrane's ability to separate solutes, its intrinsic resistance to flux, system operating conditions such as transmembrane pressure and cross-flow velocity and solution/mixture characteristics such as viscosity and solute fraction. An understanding of the relative contributions and mechanisms of the various resistive components can provide insight into what aspect of system resistance should be targeted in order to increase a membrane system's efficiency.

For liquid separation, permeate flux (J) is known to be a function of transmembrane pressure (ΔP), fluid viscosity (μ) and the system's overall resistance (R_{total}) to permeation. Membrane flux can be expressed in terms of resistances as follows (Mulder, 1995);

$$J = \frac{\Delta P}{\mu R_{total}}. \tag{3.1}$$

The total system resistance is the cumulative effect of the system's various resistive components. These resistive components are;

a. membrane resistance - R_{mem},

b. filter cake (or gel or membrane boundary) layer resistance - R_{cake}, and

c. resistance due to membrane fouling - R_{foul}.

The total system resistance can be expressed as (Mulder, 1995),

$$R_{total} = R_{mem} + R_{cake} + R_{foul}. \tag{3.2}$$

3.1 Membrane Resistance

In ultrafiltration (UF) and microfiltration (MF) applications, the permeate flux for a new membrane in the absence of any solutes or particulates is solely limited by membrane resistance. This is commonly referred to as a membrane's "pure water permeate" flux (J_{PWP}). Pure water permeation of pure water, through a clean membrane, is expressed as (Eykamp, 1995),

$$J = \frac{\Delta P}{\mu R_{mem}}. \tag{3.3}$$

3.2 Concentration Polarization

During membrane separations, concentration polarization occurs at the surface of the membrane. Concentration polarization is the build up of solute particulates at the membrane surface causing the solute concentration to be greater at the surface of the membrane than in the bulk solution. This results in the build-up of a cake, or gel, layer at the membrane surface. This cake layer continues to grow, resulting in a reduction in permeate flux, until steady-state conditions result. When the cake layer achieves its steady-state condition the flow of solute towards the cake layer equals the diffusion of solute away from the cake layer plus the permeation of solute through the membrane. This cake layer phenomena is depicted in Figure 3.1 (Matsurra, 1994).

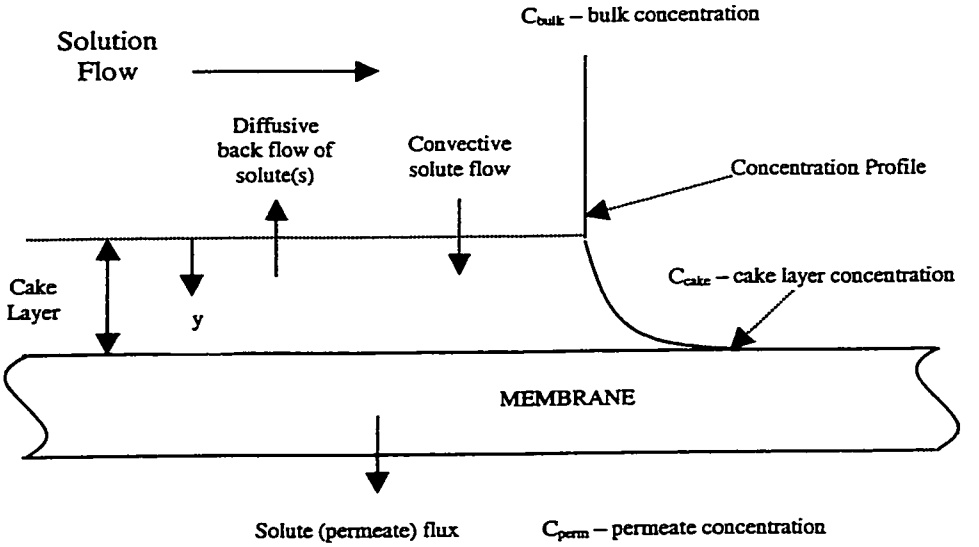

Figure 3.1: Concentration Polarization (Matsuura, 1994).

Conducting a mass balance for the solute around the cake layer provides the following equation (Matsuura, 1994),

$$JC_{bulk} = D\frac{\partial C}{\partial y} + JC_{perm}, \tag{3.4}$$

where D is the diffusion coefficient of the solute within the boundary layer.

Rearranging and integrating equation 3.4 provides (Matsuura, 1994),

$$\ln\left(C - C_{perm}\right) = \frac{J}{D}y + Cst. \tag{3.5}$$

This integration constant (*Cst*) can be determined by examining the integration limit at the start of the boundary layer, where the solute concentration is equal to the bulk solute concentration (i.e., at $y = 0, C = C_{bulk}$) (Matsuura, 1994). Therefore,

$$Cst = \ln\left(C_{bulk} - C_{perm}\right). \tag{3.6}$$

The other limit of integration occurs at the membrane surface, when the boundary layer is the entire cake layer thickness. At the membrane surface the solute concentration is its maximum (i.e., at $y = \delta, C = C_{cake}$). Substituting both of these integration limits into equation 3.5 and rearranging the equation provides (Matsuura, 1994),

$$\frac{C_{cake} - C_{perm}}{C_{bulk} - C_{perm}} = \exp\left(J * \frac{\delta}{D}\right). \tag{3.7}$$

Assuming that the solute concentration in the permeate is negligible provides the following equation for membrane flux,

$$J = \left(\frac{D}{\delta}\right)\ln\left(\frac{C_{cake}}{C_{bulk}}\right). \tag{3.8}$$

Where the mass transfer coefficient (K) is defined as (Matsuura, 1994),

$$K = \frac{D}{\delta}. \tag{3.9}$$

Accordingly, membrane flux can be described in terms of mass transfer coefficient and solute concentrations (Porter, 1990),

$$J = K \ln\left(\frac{C_{cake}}{C_{bulk}}\right). \tag{3.10}$$

The degree of concentration polarization will be affected by the mass transfer conditions in the flow channel above the membrane, the flux through the membrane and membrane pore size, with limiting cases being for large and small pores. For membranes with relatively large pores (i.e. a high pore size to particulate ratio) the flux rate will be high and therefore the effect of concentration polarization will also be high. For membranes with relatively small pores membrane flux will be low and therefore the degree of concentration polarization will also be low (Mulder, 1995).

It can be seen from equations 3.8 and 3.9 that both the flux and mass transfer coefficient are directly proportional to the diffusivity of the solute particles in the cake layer and inversely proportional to the cake layer thickness.

3.3 Cake Layer Resistance

As described above the cake layer is the result of concentration polarization. It is a thin film, lying directly on the membrane surface. This cake layer provides additional filtration properties and its resistance can be described as (Davis, 1992),

$$R_{cake} = \hat{R}_{cake}\delta\,, \tag{3.11}$$

where $\hat{R}_{cake}$ is the specific cake layer resistance and δ is the cake layer thickness.

Several means of evaluating the specific cake layer resistance exist, one of which is estimation by means of the Blake-Kozeny equation (Davis, 1992),

$$\hat{R}_{cake} = \frac{37.5\phi_{\max}^2}{a_p^2(1-\phi_{\max})^3}, \tag{3.12}$$

where $\phi_{\max}$ is the maximum solute volume fraction of the cake layer and a_p is the radius of the solute particle. The cake layer thickness can be determined from the maximum solution volume fraction and solute particle size. For rigid spheres the maximum solute volume fraction is known to be 0.58 (Sethi and Wiesner, 1995) therefore the only remaining variable required to determine the specific cake layer resistance is the solute particle radius.

If a solution, such as bilge water, is composed of a range of different particle sizes the cake layer will be composed of the particle with the minimum diffusivity. Accordingly, by determining a solution's minimum diffusivity its critical particle size can be identified.

Total diffusivity is the sum of the Brownian (D_{brn}) and Shear (D_{shear}) diffusive components, which are defined as (Davis, 1992),

$$D_{brn} = \frac{kT}{6\pi\mu a_p}, \tag{3.13}$$

$$D_{shear} = \dot{\gamma} a_p^2 \kappa, \tag{3.14}$$

where k is the Boltzmann constant, T is temperature, $\dot{\gamma}$ is the local shear rate and κ is the coefficient of induced diffusivity.

The local shear rate is the velocity gradient within the cake layer and can be expressed as (Davis, 1992),

$$\dot{\gamma} = \frac{\tau_w}{\mu\eta(\phi)}, \tag{3.15}$$

where τ_w is the wall shear stress and $\eta(\phi)$ is the relative viscosity.

For flow in a membrane flow channel (i.e., a membrane lumen) of circular cross section the wall shear stress and the relative viscosity are defined as (Sethi and Wiesner, 1995),

$$\tau_w = \frac{4U\mu\eta(\phi_b)}{r_l - \delta} = \frac{\tau_{wo} r_l^3}{(r_l - \delta)^3}, \tag{3.16}$$

$$\eta(\phi) = \left(1 + \frac{1.5\phi}{1 - \frac{\phi}{0.58}}\right)^2, \tag{3.17}$$

where U is the cross-flow velocity and r_l is the radius of the membrane flow channel.

The coefficient of shear induced diffusion is a dimensionless function of the volume fraction of the solute particles and has been determined empirically for rigid spheres to be (Sethi and Wiesner, 1995),

$$\kappa = 0.33\phi^2(1 + 0.5e^{8.8\phi}). \tag{3.18}$$

A system's variables that can alter the cake layer's diffusivity are the cross-flow velocity and the solute concentration (i.e., the concentration of oil in bilge water). Figure 3.2 is an example of diffusivity versus particle size, for a solute volume fraction, within the cake layer, of 0.29, a cross-flow velocity of 0.9 m/s and an oil concentration of 250 mg oil/L. (Appendix A provides a detailed derivation of the data points associated with Figure 3.2.)

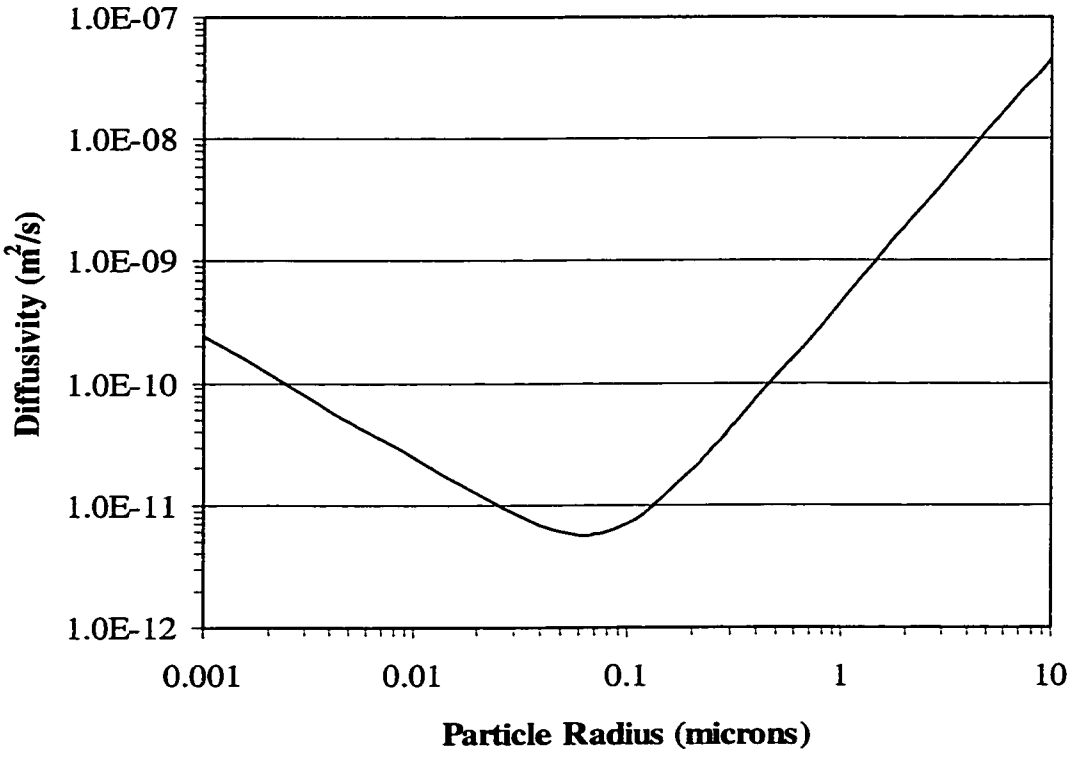

Figure 3.2: Effect of Particle Size on Cake Layer Diffusivity

As seen from Figure 3.2 the critical particle radius, associated with a minimum diffusivity, is below 0.1 micron – approximately 0.065 micron. While it is impossible to identify a precise critical solute particle size, it is reasonable to expect that the range of critical solute particle sizes for microfiltration and ultrafiltration will be approximately 0.01 to 0.1 microns. Sethi and Wiesner also determined a similar critical solute particle size range for somewhat different system variables.

3.4 Oil Droplet Fouling

The are a number of different mechanisms which can cause membrane fouling. While it is well beyond the scope of this paper to examine all of these mechanisms, one that is of particular importance to bilge water treatment is the fouling that may be caused by the entry of oil droplets into a membrane's pores, resulting in their subsequent blockage.

This type of fouling can occur when the operating pressure achieves or exceeds the critical capillary pressure (P_{crit}) required to force oil droplets into and through membrane pores. This can result in either reduced flux, decreased permeate quality, or both. The mechanism for this fouling is displayed in Figure 3.3, with the key variables being the contact angle of the oil droplet to the membrane pore (θ), the oil-water interfacial tension (σ), and the radii of the oil droplet (r_{oil}) and the pore (r_{pore}).

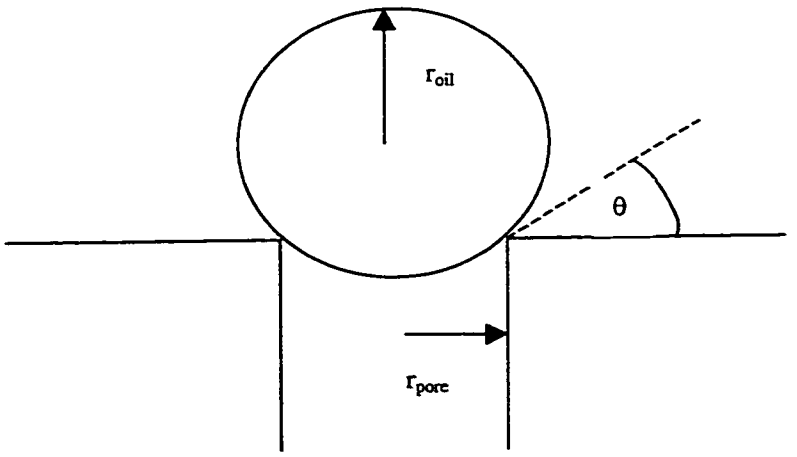

Figure 3.3: Oil Droplet Fouling of Membrane Pores (Nazzal and Wiesner, 1996)

This critical capillary pressure can be expressed as (Nazzal and Wiesner, 1996),

$$P_{crit} = \left(\frac{2\sigma\cos\theta}{r_{pore}}\right)\left[1-\frac{2+3\cos\theta-\cos^3\theta}{4(\frac{r_{oil}}{r_{pore}})^3\cos^3\theta}-(2+3\sin\theta-3\sin^3\theta)\right]^{0.33} . \qquad (3.19)$$

Using equation 3.19 the critical pressure for different sized oil droplets and membrane pore sizes can be determined. In section 2.3.2 it was identified that oil emulsions are not expected to have a radius less than 0.0175 microns (Lipp et al, 1988). The smallest oil emulsion presents the most likely occasion for observing oil droplet pore plugging. Accordingly, Figure 3.4 provides the critical pressures required for the most likely opportunity to observe oil droplet pore plugging. (Appendix B provides a detailed derivation of the data points associated with Figure 3.4.)

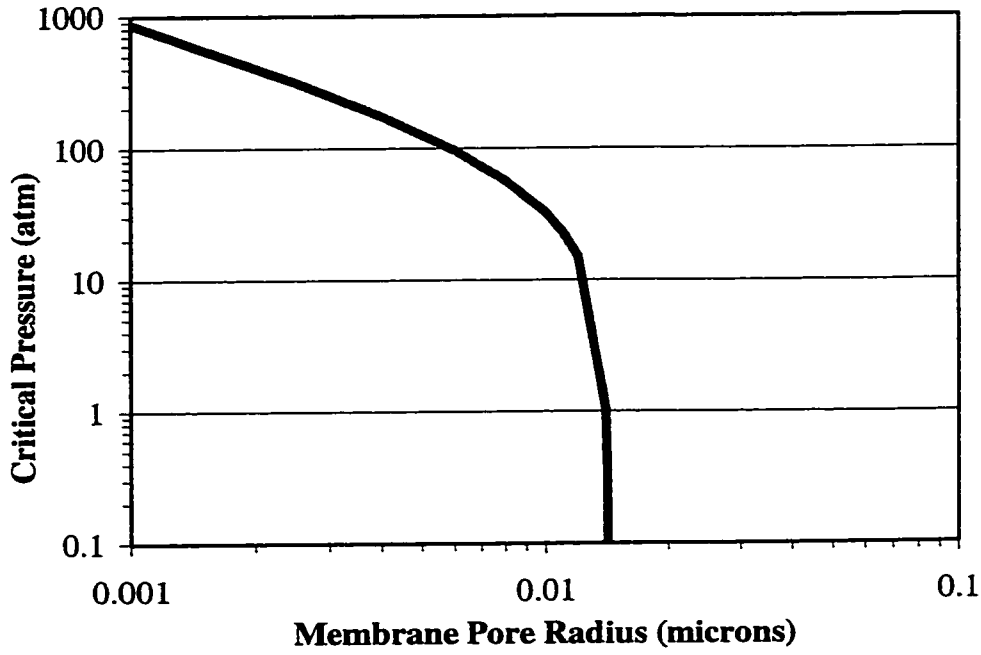

Figure 3.4: Oil Droplet Pore Plugging

Ultrafiltration does not normally exceed transmembrane pressures of 3 to 4 atmospheres (approximately 300 to 400 KPa). At these pressures it can be observed from Figure 3.4 that, even for the smallest oil emulsion of 0.0175 micron radius, the membrane's pore must have a radius of no less than (approximately) 0.015 microns in order for oil droplet pore plugging to occur. This size of membrane pore is well within the microfiltration range. Additionally, for this fouling to occur with even relatively open ultrafiltration, the transmembrane pressure would have to be quite excessive - at least 100 atmospheres - which is well beyond the operational ultrafiltration pressures. Accordingly, this type of fouling is only theoretically predicted to be problematic for microfiltration membranes. In fact, this is precisely what has been reported, that oil droplet pore plugging has been noted for microfiltration, but not for ultrafiltration, membranes (Bodzek and Konieczny, 1996).

3.5 Time Dependent Permeate Flux

Another critical parameter that must be examined is operating time. As a membrane system is operated the flux will decline as the cake, or gel, layer builds up on the surface of the membrane. However, the flux decline associated with the cake layer resistance will remain constant once the cake layer achieves its steady-state conditions (Davis, 1992).

While the effects of fouling upon membrane resistance are difficult to quantify, the effects of the cake layer on the system flux rate are relatively predictable. Until the cake layer achieves its steady-state conditions the flux can be expressed as a function of the pure water permeate flux and the associated time decay. This can be generically expressed as (Mulder, 1995),

$$J(t) \propto J_{PWP} t^{m}, \tag{3.20}$$

where J_{PWP} is the pure water permeate flux, t is the length of time that the system has been in operation and t^m is the decay in pure water flux associated with this time of system operation.

The value of m is always less than zero and it is a function of a membrane's cross-flow velocity (Mulder, 1995). The greater the cross-flow velocity the more the value of m will approach zero.

While difficult to predict due to the unique membrane/solution interactions, a more detailed time dependent flux model has been predicted as (Davis, 1992),

$$J(t) = \frac{J_{PWP}}{\left(1 + \frac{2t}{\tau_c}\right)^{0.5}}, \tag{3.21}$$

where τ_c is the time constant associated with membrane flux decline. The membrane flux decline is defined as (Davis, 1992),

$$\tau_c = \frac{R_{mem}(\phi_{\max} - \phi_b)}{J_{PWP}\hat{R}_{cake}\phi_b}, \tag{3.22}$$

where $\phi_{\max}$ and ϕ_b are the maximum solute volume fraction within the cake layer, and the bulk solute volume fraction, respectively.

To minimize this time dependent flux reduction it is necessary to remove, or at least minimize, the cake layer. Many methods exist to minimize cake layer thickness. For obvious reasons it is preferable to have an in situ method of cake layer minimization. One such method is backflushing. Backflushing is the effect of driving 'clean water' (e.g., permeate) back through the membrane at a pressure exceeding the normal transmembrane pressure. This results in lifting the cake layer off the membrane. A

backflush is applied for a short period of time in a given operating cycle (e.g., a 5 second backflush in a 120 second operating cycle). Accordingly, instead of a steady-state cake layer forming on the membrane, the membrane has a transitional cake layer which continually ranges in thickness from a minimum thickness directly after the backflush to a maximum thickness just prior to backflushing. During backflushing, the membrane will have a negative flux as the flow through the membrane is reversed. This negative flux will increase during the duration of the backflush as the cake layer is removed, resulting in increased permeation through the membrane. Figure 3.5 depicts the effect of backflushing.

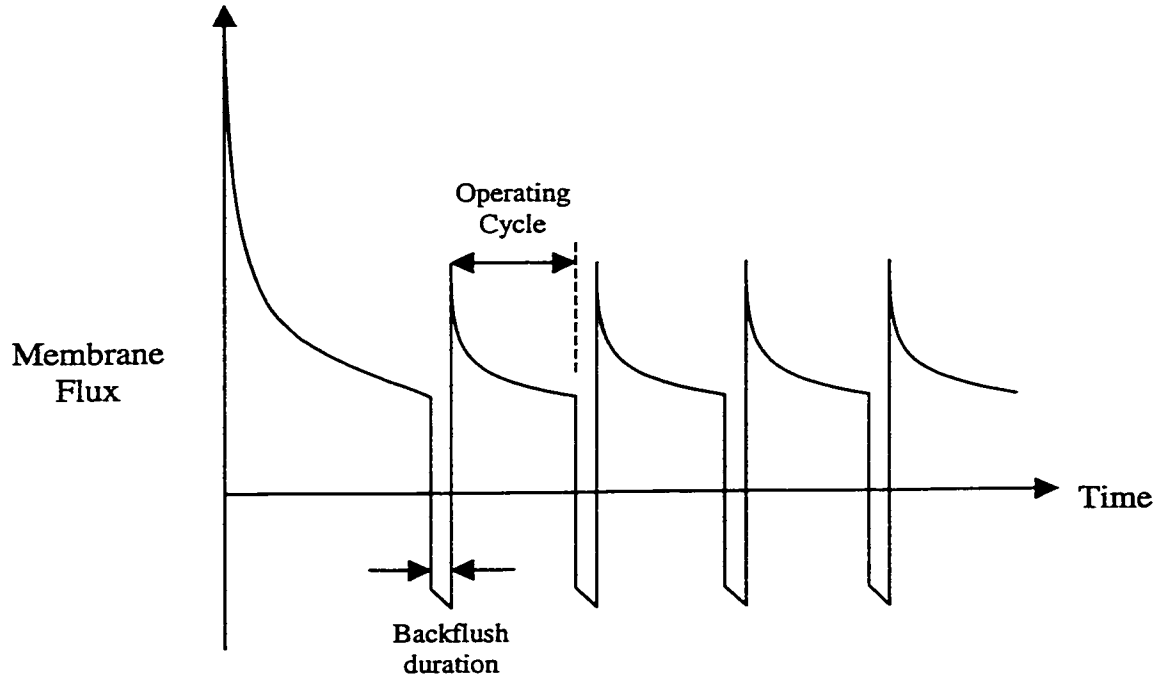

Figure 3.5: Effect of Backflushing

Therefore to effectively utilize membrane backflushing to overcome the time related flux decline it is beneficial to have a backflush operating cycle no greater than the time required for the cake layer to achieve steady state. It would also be beneficial to backflush as early in the operating cycle as possible, in order to minimize the growth of the cake layer. This time required to achieve the steady-state cake layer can be

determined by solving equation 3.21 using the steady-state flux and then rearranging it to identify the time required to achieve this steady-state cake layer.

This steady-state cake layer time is,

$$t_{ss} = \left(\frac{\tau_c}{2}\right)\left[\left(\frac{J_{PWP}}{J(t_{ss})}\right)^2 - 1\right], \tag{3.23}$$

where t_{ss} is the time required to achieve the steady-state cake layer and $J(t_{ss})$ is the flux during steady-state cake layer conditions.

The amount of backflushing must be balanced against the loss of membrane flux during the actual backflushing. Therefore the average backflushed flux, including the lost operational time attributable to the backflushing, is the product of the average flux and the percentage of system time when permeate is produced, i.e. operating time divided by the sum of the operating time and the backflushing time.

Thus the average backflush flux can be expressed as the product of the average flux and the fraction of the total cycle devoted to permeate production,

$$J_{bf} = J_{avg}\left(\frac{t_{total} - t_{bf}}{t_{total}}\right) = J_{avg}\left(\frac{t_{op}}{t_{total}}\right). \tag{3.24}$$

Where J_{bf} is the average flux during a complete cycle, including time for backflushing, J_{avg} is the average flux during a cycle, excluding backflushing, t_{bf} is the duration of the backflush, t_{op} is the duration of normal operation (i.e., the time during which permeate is being created) and t_{total} is the sum of t_{bf} and t_{op}.

For conditions where the operating cycle is less than the time required to achieve a steady-state cake layer the average flux can be defined as (Sethi and Wiesner, 1995),

$$J_{avg} = \frac{1}{t_{total}} \int_0^{t_{total}} J(t)dt . \tag{3.25}$$

If the operating time exceeds the steady-state time then the expression for the average flux becomes (Sethi and Wiesner, 1995),

$$J_{avg} = \frac{1}{t_{total}} \left[\int_0^{t_{ss}} J(t)dt + (t_{total} - t_{ss}) J(t_{ss}) \right]. \tag{3.26}$$

The average flux can be solved for by substituting equation 3.21 into either 3.25 or 3.2. Accordingly, for conditions whereby the operating cycle is less than the time required to achieve a steady-state cake layer the average flux can be expressed as (Sethi and Wiesner, 1995) (detailed derivation of equations 3.27 and 3.28 are provided in Appendix C),

$$J_{avg} = \frac{J_{PWP}\tau_c}{t_{total}} \left[\left(1 + \frac{2t_{total}}{\tau_c} \right)^{0.5} - 1 \right]. \tag{3.27}$$

Similarly, when the operating cycle is greater than the time required to achieve a steady-state cake layer the average flux can be expressed as (Sethi and Wiesner, 1995),

$$J_{avg} = \left(\frac{1}{t_{total}}\right) \left[J_{PWP}\tau_c \left(\left(1 + \frac{2t_{ss}}{\tau_c} \right)^{0.5} - 1 \right) + (t_{total} - t_{ss}) J(t_{ss}) \right]. \tag{3.28}$$

Therefore the average backflush flux can be determined by substituting these two equations into equation 3.25. Thus the average backflush fluxes, for operating cycle less than and exceeding the steady-state cake layer time are;

$$J_{bf} = \left(\frac{J_{PWP}\tau_c t_{op}}{t_{total}^2} \right) \left[\left(1 + \frac{2t_{total}}{\tau_c} \right)^{0.5} - 1 \right], \quad \text{where } t_{op} < t_{ss}, \quad (3.29)$$

$$J_{bf} = \left(\frac{t_{op}}{t_{total}^2} \right) \left[J_{PWP}\tau_c \left(\left(1 + \frac{2t_{ss}}{\tau_c} \right)^{0.5} - 1 \right) + (t_{total} - t_{ss}) J(t_{ss}) \right], \quad \text{where } t_{op} > t_{ss}. \quad (3.30)$$

3.6 Cake Layer Accumulation and Removal

Conducting a mass balance around the cake layer (Figure 3.1) allows one to determine the rate of rate of solute accumulation at the membrane surface. Due to concentration polarization, the cake layer will have a maximum solute concentration (i.e., maximum solute volume fraction) and therefore the overall solute accumulation is the product of the maximum solute concentration and the rate of cake layer accumulation. The components of this overall solute accumulation are the rate of solute moving towards the membrane surface, the rate of increase in the cake layer thickness, and the decrease in the cake layer due to permeation through the membrane. This can be expressed as,

$$J\phi_b + \frac{d\delta}{dt}\phi_b - J\phi_p = \frac{d\delta}{dt}\phi_{\max}, \quad (3.31)$$

where ϕ_b, ϕ_p and $\phi_{\max}$ are the solute volume fractions in the bulk solution, in the permeate and the maximum fraction in the cake layer, respectively.

Assuming that the quantity of solute in the permeate is minimal the above equation is simplified to,

$$J\phi_b + \frac{d\delta}{dt}\phi_b = \frac{d\delta}{dt}\phi_{\max}. \tag{3.32}$$

In the absence of fouling the total resistance is the sum of the membrane and cake layer resistance. Utilizing equation 3.11, equation 3.32 can be re-written in terms of the cake layer thickness (δ) as,

$$\frac{d\delta}{dt} = \frac{C}{R_{mem} + \hat{R}_{cake}\delta}, \tag{3.33}$$

$$\text{where: } C = \frac{\Delta P \phi_b}{\mu(\phi_{\max} - \phi_b)}.$$

Re-arranging equation 3.33 to isolate the cake layer thickness and time provides,

$$R_{mem}d\delta + (\hat{R}_{cake}\delta)d\delta = Cdt. \tag{3.34}$$

Integrating equation 3.34 over the limits of no cake layer to its steady-state thickness for the respective times of zero and the steady-state time provides,

$$0.5\hat{R}_{cake}\delta_{ss}^2 + R_{mem}\delta_{ss} - Ct_{ss} = 0. \tag{3.35}$$

Therefore equation 3.35 can be solved for the steady-state cake layer thickness as,

$$\delta_{ss} = \frac{(R_{mem}^2 + 2C\hat{R}_{cake}t_{ss})^{0.5} - R_{mem}}{\hat{R}_{cake}}. \tag{3.36}$$

Similar to the above development the amount of cake layer removed, by means of backflushing, can also be determined. This development also starts with the mass balance around the membrane. Assuming that the solute volume fraction in permeate is negligible, the overall flux rate associated with backflushing is the sum of the solute removed and the solute remaining in the cake layer. This can be expressed as,

$$\frac{d\delta}{dt}\phi_{\max} + J_{bf}\phi_{\max} = \frac{d\delta}{dt}\phi_b . \tag{3.37}$$

The following expression is obtained when equation 3.37 is solved for the remaining cake layer thickness (δ),

$$\delta = J_{bf}t\left(\frac{\phi_{\max}}{\phi_b - \phi_{\max}}\right). \tag{3.38}$$

Since the bulk solute volume fraction is very small in comparison to the maximum solute volume concentration, it can be seen that the solute volume term is essentially equal to minus one and therefore the above equation can be simplified; expressing the cake layer removal as being,

$$\delta = -J_{bf}t . \tag{3.39}$$

4.0 EXPERIMENTAL METHODOLODY

4.1 Flat Sheet Testing

Flat sheet testing was conducted in accordance with the schematic representation provided in Figure 4.1. The prime components of the system are a piston pump, 4L reservoir, stir cell, flat sheet membrane coupon and the pressure relief valve. The pump drew bilge water from the reservoir, feeding the stir cell. The valve downstream of the stir cell did not control the pressure, but rather was a relief valve ensuring system pressure did not exceed 517KPa (75psi). The system's operating pressure, of 345KPa gauge (50psig), was maintained by the pump cycling on and off. The operation of the pump was computer controlled, using LABVIEW (National Instruments) software, which is a commercially developed software package for experimental control. A suspended stir bar in the cell ensured the rotational movement of the bilge water in the cell. The flat sheet testing was conducted as a batch process. That is, a batch of bilge water was prepared in the bilge water tank for each experimental run.

The system provided adequate pressure control, maintaining a pressure of 345KPa gauge (50psig) plus or minus 7KPa (1psi). A temperature control system was also employed whereby the stir cell was partially submerged in a temperature controlled bath. The system temperature was recorded via the bilge water temperature in the bilge water reservoir. All calculations were corrected to 25°C.

Flux rates were determined using a remote auto sampler which was fed with permeate from the stir cell. The auto sampler was controlled by a computer program, which allowed for a choice of sampling times. During the experimental runs, samples were taken every hour for the first five hours and then every two hours for the next 20 hours. The sampling times could be altered, if desired. Additionally, the duration of sampling could be altered, up to a maximum of 59 minutes. The sampling duration time was altered to maximize the amount of permeate collected for each membrane.

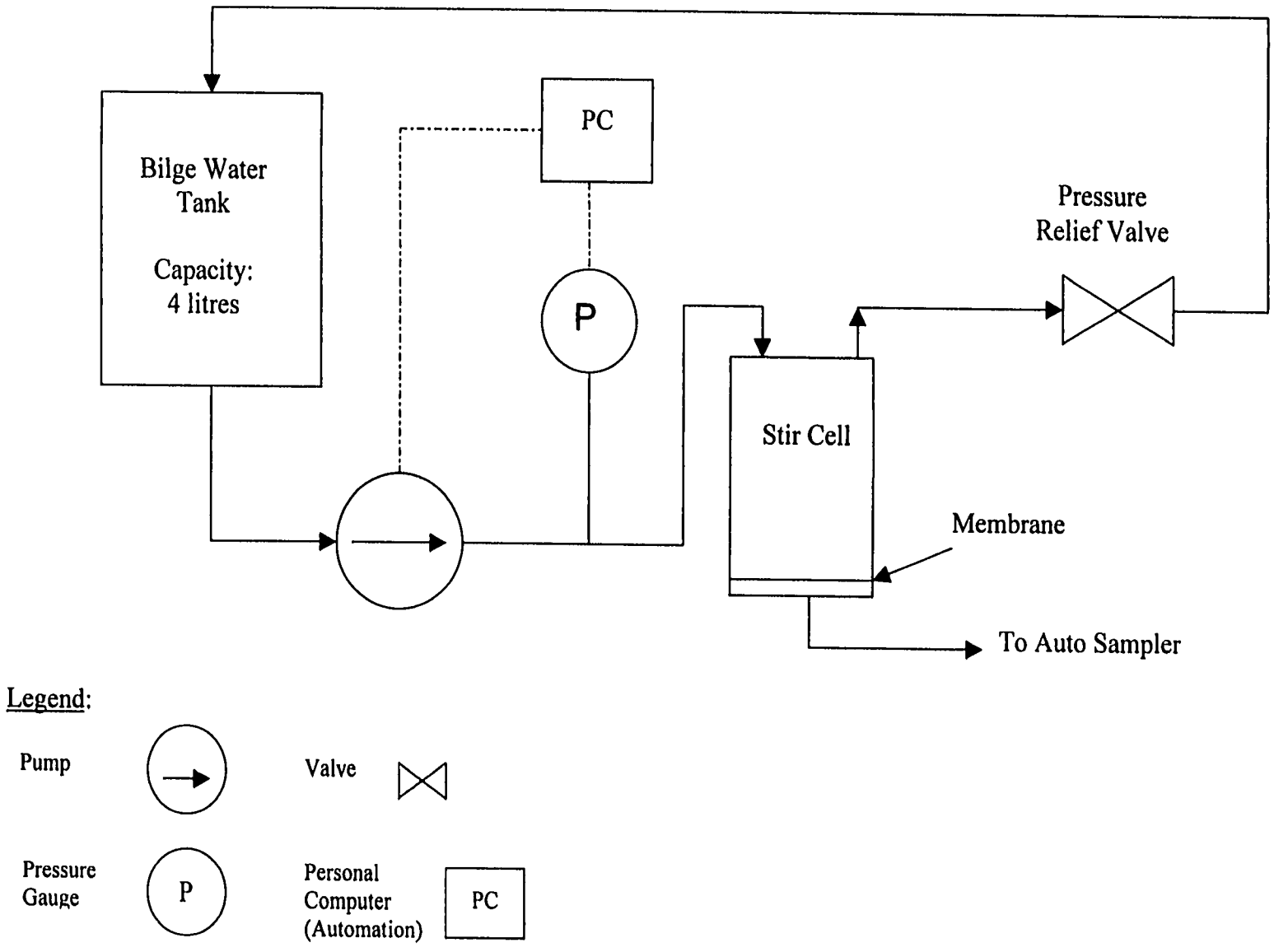

Figure 4.1: Flat Sheet Experimental Set-up

It was not practical to test permeate quality due to the small quantities of permeate produced.

Various commercial flat sheet membranes were used. They were obtained from KOCH (Ann Arbor, Michigan, USA) and OSMONICS (Minnetonka, Minnesota, USA). The details of the flat sheet membranes are provided in Table 4.1. The primary reason for the selection of these membranes was to ensure a thorough examination of the range of membrane pore sizes which could be employed for the treatment of bilge water. In many cases some details, such as the material forming the selective layer, were not available.

Additionally, the membranes' selectivity were not always expressed in the same manner by the manufacturers; that is, most of the membranes had their selectivity expressed in terms of Molecular Weight Cut-Off (MWCO), while others were given in terms of pore radius. The correlation between MWCO and pore radius is dependent upon the polymer used to determine the MWCO. For polyethylene glycol (PEG) and polyethylene oxide (PEO) the correlation between MWCO and pore radius is (Tremblay, 1992)

$$\text{pore radius (microns)} = \frac{0.026068 * MWCO(Daltons)^{0.5} - 0.015}{1000} \qquad (4.1)$$

Table 4.1: Details of the Flat Sheet Membranes Used

Manufacturer	Name	Selective Layer Material	Selectivity	
			MWCO (Daltons)	Pore Radius (microns)
OSMONICS	GH	not available – proprietary information	2,500	0.0018
OSMONICS	GK	not available – proprietary information	3,500	0.002
OSMONICS	GM	not available – proprietary information	8,000	0.0033
OSMONICS	GN	not available – proprietary information	10,000	0.0037
OSMONICS	QW	not available – proprietary information	30,000	0.0064
OSMONICS*	QX	not available – proprietary information	3,600,000	0.05
KOCH	M100	polyvinylidene diflouride (PVDF)	20,000	0.0052
KOCH	M180	PVDF	50,000	0.0082
KOCH	P707	PVDF with a negative surface charge	150,000	0.0143

* The OSMONICS QX membrane was identified as having a membrane pore size (diameter) ranging from 0.01 to 0.1 microns.

4.2 Pilot Scale Studies

Membrane modules were tested in the pilot plant set-up as detailed in Figure 4.2. The flows through the system are depicted as follows;

a. routine flow of bilge water and permeate is depicted by the bold flow line;
b. hashed flow line depicts backflushing, and
c. light flow lines depict membrane by-pass or over pressure release safety line.

This pilot plant system consisted of a 200L reservoir tank providing feed for a rotary vane pump (PROCON, Murfreesboro, Tennessee, USA), which in turn fed the membrane module. A backpressure valve, mounted after the membrane module, maintained the system's operating pressure. This valve was pneumatically operated and computer controlled. This provided for extremely fine system pressure control, within 0.7KPa (0.1psi). The transmembrane pressure was normally at 206KPa gauge (30psig). However, for certain runs conducted at higher cross-flow velocities the lowest system pressure attainable was 220KPa gauge (32psig). All experimental data were corrected to 206KPa gauge (30psig) as per ASTM standard D5090-90: Standardizing Ultrafiltration Permeate Flow Performance.

The temperature of the bilge water was controlled to 25°C. The initial bilge water temperature was approximately 23°C and was heated up to this temperature by means of the thermal energy imparted by the system's main pump. To ensure the bilge water temperature did not exceed 25°C a cooling coil, supplied with cold tap water, was inserted in the bilge water holding tank. The passage of cold water through the cooling coil was controlled by a computer controlling a pneumatic valve. Once the bilge water warmed to the 25°C temperature set point the system was able to maintain the temperature of the bilge water to within plus or minus 0.1°C.

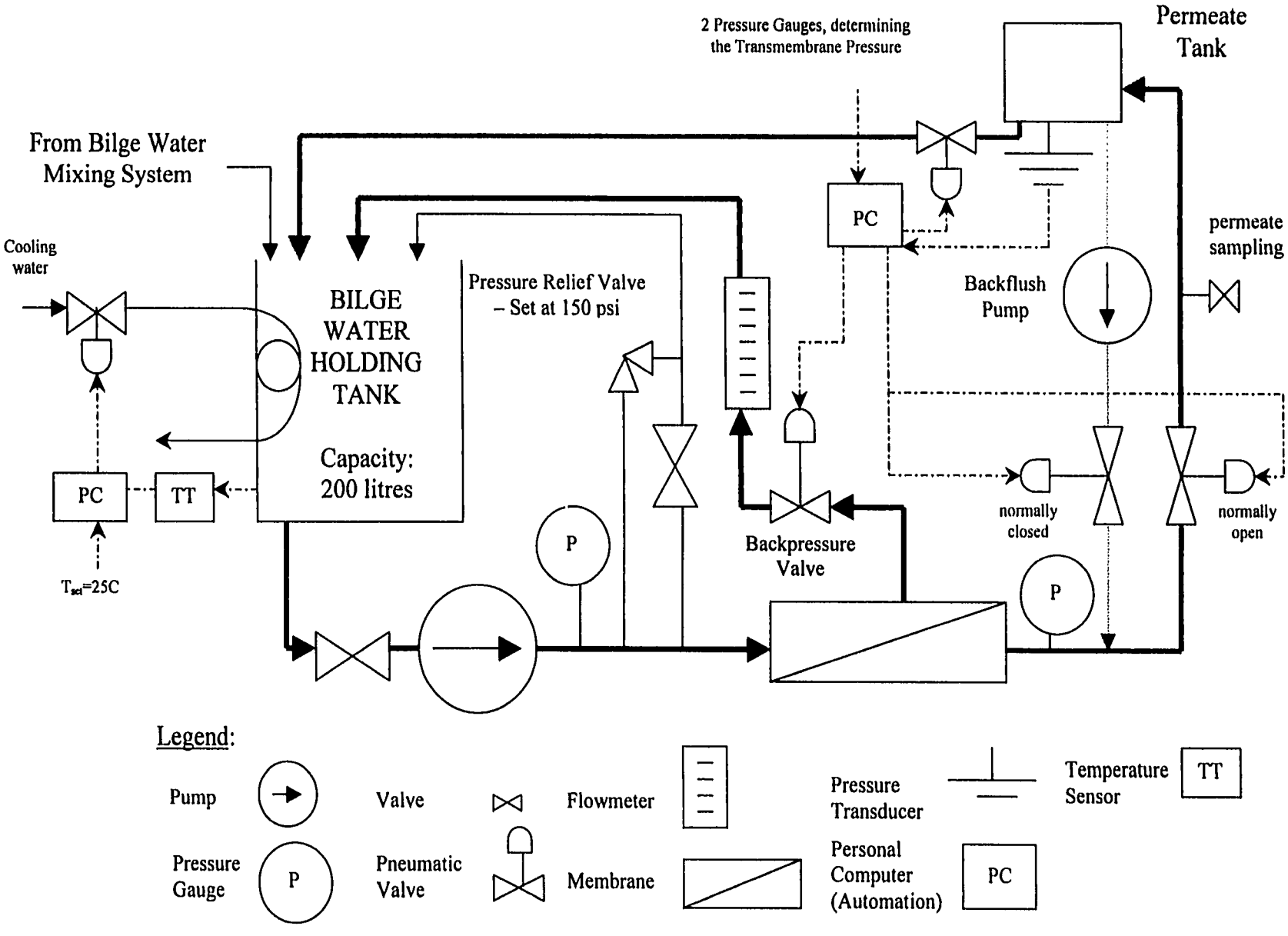

Figure 4.2: Pilot Scale Experimental Set-up

The flux values for the data obtained in the earlier portions of the experimental runs, when the bilge water had not achieved a temperature of 25°C, were corrected to 25°C as per ASTM standard D5090-90: Standardizing Ultrafiltration Permeate Flow Performance.

The rate of permeate flux from the membranes was determined by means of mounting a pressure transducer to the base of the permeate tank. This allowed for the recording of pressure levels in the permeate tank, which were converted to permeate tank heights and then to permeate tank volumes.

The system also provided backflushing to the membrane module, using a pneumatic diaphragm pump. This pump drew a suction from the permeate tank feeding the membrane module from the permeate side, through to the feed side, and was continually operated at a pressure of 241KPa gauge (35psig). While the backflush pump was constantly operated at 241KPa the backflushing of permeate to the membrane was controlled by means of a valve located between the diaphragm pump and the membrane module. This valve was normally in the closed position; i.e. it ensured no backflushing of permeate through the membrane. During the backflushing operation the valve was opened and permeate was backflushed through the membrane. This valve was operated in conjunction with the valve between the membrane module and the permeate tank which was normally open and closed during backflushing operation, thus ensuring the flow of backflushed permeate through the membrane. The total operational cycle time and the backflushing times were computer controlled.

After every experimental run the membrane module was removed from the pilot scale system and cleaned. The membranes were cleaned with a detergent specifically formulated to regenerate membranes fouled during oily wastewater treatment processes. The detergent was produced by KOCH Membrane Systems Incorporated (Ann Arbor, Michigan, USA) and has the commercial name of KLD II – KOCH KLEEN. KLD II is a strongly basic cleaner; however its exact formulation is not known due to its proprietary

nature. (A 1 percent solution of KLD II has a pH ranging from 10 to 11.5.) The membrane regeneration procedure was to wash the membranes with a water-KLD II solution. The concentration of the KLD II in the wash water was 5 mL/L of water. Additionally, the water was heated in order to enhance the washing process. For the polymeric membrane the cleaning solution was heated to 40°C ± 2°C and used for approximately 30 minutes or when the temperature of the cleaning solution dropped to below 30°C. For the ceramic membrane the cleaning solution was heated to 65°C ± 5°C and used for approximately 45 minutes or when the temperature of the cleaning solution dropped to below 40°C. These washes were conducted at high cross-flow velocities (in excess of the operational cross-flow velocities) and low pressures (between 3 to 5 psi). For either membrane numerous cleaning cycles were conducted in order to regenerate (as best as possible) the membrane to its original conditions, with a minimum of three cleaning cycles being conducted per membrane.

Pressure, temperature, operational cycle time and backflushing time were controlled using LABVIEW (National Instruments) software.

The main feed pump's speed was manually controlled and operated at approximately 60% capacity.

The following membrane modules were tested in the pilot plant experimental set-up:

a. CERAMEM (Waltham, Massachusetts, USA) LMA-0005-PS ceramic membrane (from this point on referred to as the CERAMEM LMA membrane):

Material:	silica selective layer on an alumina substructure,
Membrane Selectivity:	pore radius of 0.0025 microns (equating to an approximate MWCO of 9,300 Daltons),
Membrane Configuration:	tubular,
Membrane Dimensions:	length of 0.325m,

60 square flow channels with a diameter of 2mm, which provides a total membrane surface area of approximately 0.14m^2 (1.5ft^2); and

b. KOCH (Ann Arbor, Michigan, USA) CM polymeric membrane (from this point on referred to as the KOCH CM membrane):

Material:	polyacrylo nitrile,
Membrane Selectivity:	MWCO of 50,000 Daltons (equating to an approximate pore radius of 0.0082 microns),
Membrane Configuration:	hollow fibre,
Membrane Dimensions:	length of 0.417m, approximately 65 fibres with a diameter of 1.143mm, which provides a total membrane surface area of approximately 0.093m^2 (1ft^2).

In order to conduct the experimental runs within the transmembrane pressure range of 206 – 220 KPa the cross-flow velocities, for each of the membrane modules, was restricted to a particular range. The cross-flow velocity used for the CERAMEM LMA membrane ranged from 1.04 m/s to 1.74 m/s (which equated to a volumetric flow rate ranging from 15 to 25 L/min). For the KOCH CM membrane the cross-flow velocity ranged from 3.12 m/s to 3.75 m/s (which equated to a volumetric flow rate ranging from 12.5 to 15 L/min). The difference in cross-flow velocities was the result of the difference in the cross-sectional area of the two modules. The CERAMEM LMA module had a cross-sectional area of approximately $2.40*10^{-4}$ m^2 (60 channels * 0.002m X 0.002m square flow channel). Whereas, the KOCH CM module had a cross-sectional area of approximately $6.67*10^{-5}$ m^2 (65 fibres * $(1.143*10^{-3}m)^2$ diameter fibre * $\pi/4$). As a result of the substantial difference in cross-sectional area between the two modules it is

expected that the cross-flow velocities, for similar transmembrane pressures, were substantially different.

4.3 Bilge Water Preparation

The overall composition of the synthetic bilge water was as follows;

a. 2000-ppm oils,
b. 500-ppm detergents and surfactants - 500 ppm, and
c. with the remainder being water (approximately 99.75%).

The oils were composed of the following Canadian Navy standard oils;

a. 50% naval distillate (diesel fuel),
b. 40% naval diesel engine lubricating oil, and
c. 10% hydraulic oil.

The detergents and surfactants were composed of the following Canadian Navy standard detergents and surfactants;

a. 90% Canadian Navy standard oil and grease detergent (CLEANBREAK), and
b. 10% Canadian Navy standard corrosion removal compound (OSTREM Rust Stain Remover).

The water was composed of a 50/50 mixture of fresh (potable) and sea water.

The synthetic bilge water was prepared in a separate tank and was mixed for approximately two hours. The synthetic bilge water was then allowed to settle for approximately 24 hours to ensure separation of the free and emulsified oil states. The bilge water, less the free oil, was then pumped to the main experimental setup. The purpose of ensuring no free oil being used in the experiments was to simulate the removal of the free oil phase. This free oil phase would be removed with some form of

pretreatment in an actual system: for example, a hydrocyclone or a parallel plate separator.

The synthetic bilge water was altered to study the effect of particular key components upon membrane separation efficiency.

The lubricating oil used in the composition of the synthetic bilge water was varied in different batches of bilge water. Either new or used diesel engine lubricating oil was used in the preparation of bilge water. New naval distillate and hydraulic oil were always used.

Additionally, the prime surfactant used was altered - either CLEANBREAK or SEACLEAN (LBG Industries, Mansonville, Quebec) were used. CLEANBREAK is the only accepted oil and grease surfactant within the Canadian Navy (NDHQ/DMSS4, 1996). However, it is expected that despite this requirement to only use CLEANBREAK it is likely that other surfactants may be employed. Accordingly, SEACLEAN was used in the make-up of selected bilge water runs. It should be noted that CLEANBREAK and SEACLEAN are both produced by the same manufacturer, with their difference being in their emulsification strength. SEACLEAN is identified as being a more powerful emulsification agent than CLEANBREAK, as identified in the Material Safety Data Sheets of these two surfactants.

Sea water was prepared in accordance with ASTM standard D1141-90: Standard Specification for Substitute Ocean Water.

4.4 Oil and Grease Testing

It is important to note that the definition of oil and grease, as pertaining to water and wastewater treatment, is rather vague. The term "oil and grease" applies to a wide variety of organic substances including hydrocarbons, esters, oils, fats, waxes and high

molecular weight fatty acids (Sawyer et al., 1994). Four standard methods, based upon 1,1,2-trichloro-1,2,2-trifluorethane (Freon-113) extraction exist, and each of these methods extracts differing degrees of the "oils and greases" from water and therefore each method provides different results. This is critical as it is necessary to identify the method of "oil and grease" determination being used when identifying the oil and grease content in water. Unfortunately, neither the Canada Shipping Act nor the Arctic Waters Pollution Prevention Act identify a method for oil and grease determination.

The four standard methods for oil and grease testing all rely upon an initial extraction from water by Freon-113. However, the use of Freon-113 is prohibited by the Montreal Protocol. Therefore Freon-113 extraction could not be used for the extraction of oils and greases from water and an alternative method of testing had to be identified. In lieu of Freon-113 the US EPA has authorized the use of hexane liquid-liquid extraction (method 1664). In fact, originally both hexane and Freon-113 were listed as acceptable solvents for oil and grease extraction, however Freon-113 was the preferred solvent since it is less of an explosive hazard (Sawyer et al., 1994). Hexane liquid-liquid extraction was tried but the presence of surfactants (which are likely to be present in the membrane permeate) lead to the formation of an emulsified layer between the hexane and water phases. This difficulty with hexane liquid-liquid extraction has been documented and solid phase extraction (SPE) has replaced many liquid-liquid extraction methods for the determination of organics in solution (Stone, 1998). Specifically, reverse-phase SPE has been used to remove non-polar compounds from polar compounds, such as water (Beney et al., 1996). Accordingly, it was decided to utilize solid phase extraction for the determination of the oil content of water.

Prior to using solid phase extraction for the determination of the oil content in water it was necessary to identify the most appropriate SPE material and assess its accuracy and precision. According to Beney et al., octadecyl (C_{18}) or octyl (C_8) bonded silica reverse phase SPE is appropriate for the extraction of non-polar compounds from water. Preliminary tests were conducted with both of these SPE materials and it was determined

that the octadecyl (C_{18}) SPE was the better extractant. SPE tubes with a volume of 6mL and 500mg of octadecyl adsorbent were used (SUPELCO, Oakville, Ontario).

The basic extraction method utilised to recover oil from permeates and other waters consisted of a three-step procedure. The first step was to condition the SPE tubes. This consisted of flushing them with 5mL of hexane and 5 mL of methanol, the solvents used to extract the oil from the SPE tubes, followed by flushing the SPE tube with 5mL of a 50/50 mixture of sea and fresh water. Once the tubes were conditioned the bilge water permeate was extracted by use of a vacuum. The adsorption of the oil onto the SPE packing was evidenced by the formation of a ring of extracted oil. The final step was extracting the adsorbed oil from the SPE tubes by washing them with organic solvents. Five 5mL washes of both hexane and methanol were conducted for each SPE tube. The solvents were forced through the packing by air pressure. The extracted material was collected in aluminium weighing dishes and the organic solvents were allowed to evaporate.

Based upon a study comparing the effectiveness of oil and grease extraction, for a variety of wastewaters using octadecyl (C_{18}) reverse phase SPE and hexane liquid-liquid extraction, it was found that the SPE extraction had an average recovery of 107% $\forall$ 76% while the hexane liquid-liquid extraction had an average recovery of 100% $\forall$ 121% (Stone, 1998).

Using the octadecyl (C_{18}) reverse phase solid phase extraction a number of calibration extractions were conducted with varying amounts of new diesel lubricating oil, ranging from 22 to 141 mg/L. Figure 4.3 presents these results. From these trials it was found that the oil recovered through this solid phase extraction method related to known quantity of oil in accordance with the following equation:

$$\text{oil content} = 1.25SPE - 9.9 \quad \text{mg/L} \tag{4.2}$$

where *SPE* is the quantity of recovered oil, in mg, as removed from the octadecyl reverse phase material.

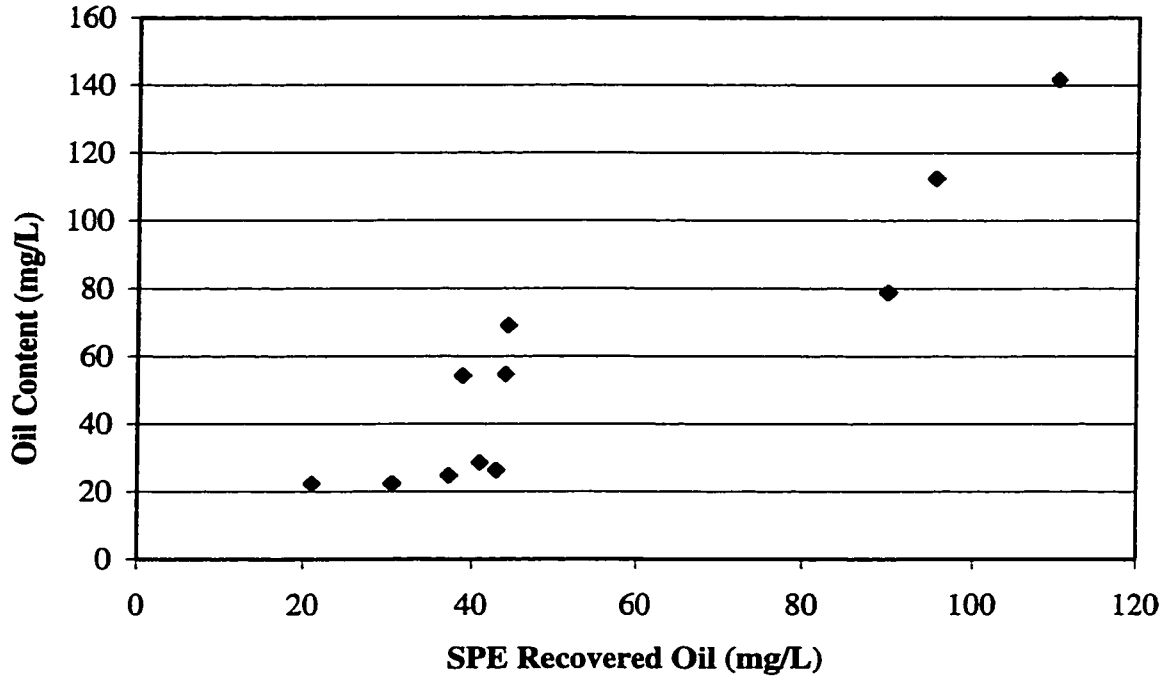

Figure 4.3: Results of SPE Trials for Oil Extraction from Water

Admittedly, the precision of this method is poor, but it is comparable to that of hexane liquid-liquid extraction, as identified by Stone.

To achieve these recovery levels two SPE cartridges were used in series, with the first SPE tube extracting approximately twice as much oil as the second SPE tube.

5.0 RESULTS AND DISCUSSION

Experimental work was conducted with both flat sheet membranes and membrane modules. Testing commenced with the flat sheet membranes in order to assess the effect of membrane pore size (molecular weight cut-off) on membrane flux rates. Following this initial evaluation, pilot plant testing was conducted using membrane modules to observe longer term phenomena and other treatment options which could not be examined with flat sheet membranes.

5.1 Flat Sheet Testing

The key objective of flat sheet testing was to examine the effect of nominal membrane pore size on membrane flux when treating bilge water. Flat sheet testing also provided insight as to whether the flux was dominated by the membrane or the cake layer resistive components. Due to the small quantities of bilge water used during flat sheet testing, and subsequently the smaller quantities of permeate produced, it was not possible to evaluate permeate quality.

As described in section 4.1 the "G", "Q", "M" and "P" series of ultrafiltration membranes were examined. These membranes were fabricated of different material and had different pore size and pore size distributions.

To assess the impact of bilge water composition on membrane flux certain flat sheet experimental runs were conducted with a modified synthetic bilge water composition. The synthetic bilge water was prepared in accordance with the method described in section 4.3, with the following two exceptions:

a. either new or used lubricating oil was employed in the synthetic bilge water preparation. These two mixtures will be referred to as new bilge water and used bilge water respectively; and

b. the surfactant was also varied. Primarily, CLEANBREAK was employed, but in some experimental runs SEACLEAN was employed. These surfactants created oil emulsions of differing stability.

The operational parameters held constant were pressure and stir cell rotational velocity. Unless stated otherwise the transmembrane pressure was 345 KPa gauge (50 psig). The temperature of the bilge water varied somewhat throughout the experimental runs. Its initial temperature was as low as 22°C, but was then heated to and maintained at a temperature of 25°C ± 1°C, by means of the temperature controlled bath in which it was submerged. All permeate volume data and subsequent flux rate calculations were corrected to 25°C in accordance with ASTM standard D5090-90: Standardizing Ultrafiltration Permeate Flow Performance.

The experimental data were analysed through an examination of the various resistive component values and the impact of the bilge water's oil concentration on membrane flux.

5.1.1 Solute Particulate Sizes

The experimental runs were conducted over a 24 hour period. However, a closer examination of the experimental results revealed that some of the membrane experienced sharp and sudden flux declines. These flux declines occurred very early in the experimental runs, usually within the first 2 hours of operation. In order to mitigate the effects of membrane fouling, and thereby examine a truer representation of the cake layer, membrane flux within this earlier period of the experimental runs was examined. Figure 5.1 provides a synopsis of the various flat sheet membrane experimental runs, after one hour of operation. Table 5.1 presents the flux and resistive component values for the various membranes. (Appendix E details how the resistive component values were determined.)

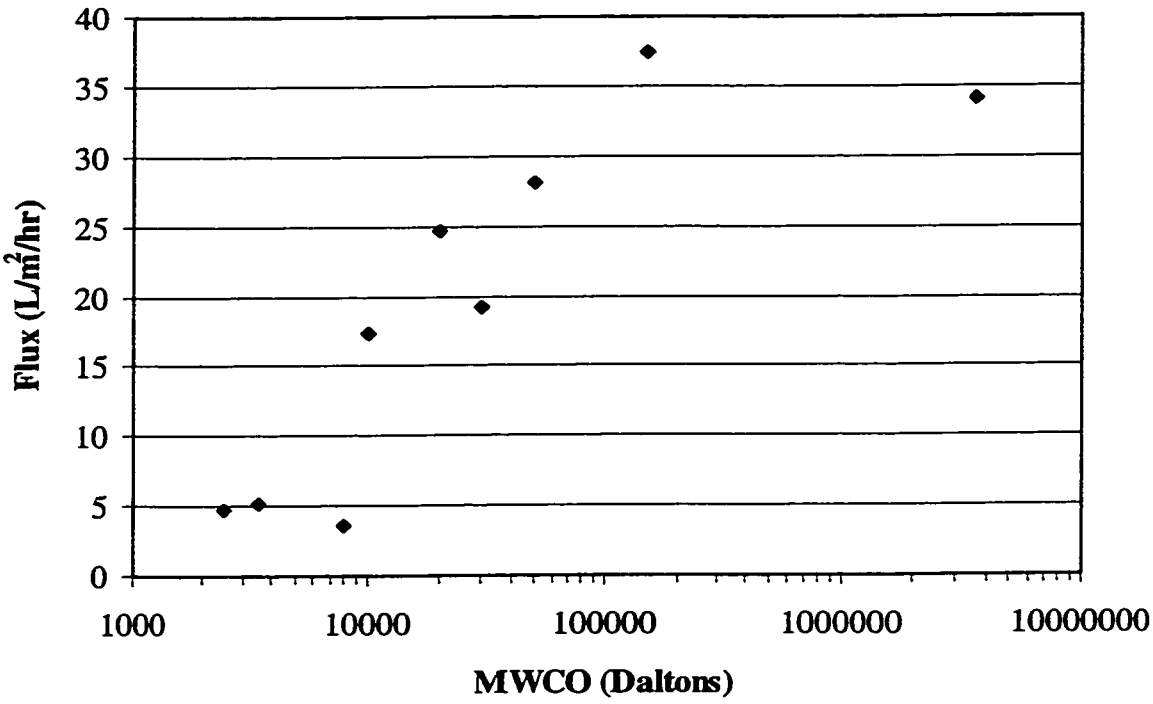

Figure 5.1: Flat Sheet Flux Results, after 1 hour, at 345 KPa

The cake layer resistance, in simple terms, is defined as the product of the specific cake layer resistance and cake layer thickness, as defined by equation 3.11. Therefore, differences in the cake layer resistances, identified in Table 5.1, are due to either changes in the specific cake layer resistance, the cake layer thickness or both of these variables. For each of the various membranes, the specific cake layer resistance is a relatively constant value, as it is defined by the solute particulate size and the solute volume fraction of the cake layer (equation 3.12). However, the cake layer thickness varies with membrane pore size, as it is defined by the membrane resistance (which is determined by the membrane pore size) in addition to the solute particulate size and volume fraction.

Table 5.1: Resistive Component Values for Flat Sheet Membranes

Membrane			PWP Flux at 345 KPa	Flux at 1hour and 345 KPa	Resistive Component	
Name	MWCO (Daltons)	Pore Radius[1] (microns)	($L/m^2/hr$)	($L/m^2/hr$)	Membrane (10^{14} m^{-1})	Cake Layer (10^{14} m^{-1})
GH	2,500	0.0018	6.15	4.75	2.264	0.667
GK	3,500	0.0022	33.10	5.23	0.421	2.241
GM	8,000	0.0033	54.20	3.57	0.257	3.643
GN	10,000	0.0037	105.27	17.39	0.132	0.668
M100	20,000	0.0052	217.31	24.64	0.064	0.501
QW	30,000	0.0064	207.12	19.16	0.067	0.659
M180	50,000	0.0082	245.40	28.16	0.057	0.438
P707	150,000	0.0143	323.50	37.39	0.043	0.329
QX	3,600,000[2]	0.05[2]	438.64	34.18	0.032	0.376

[1] Pore Radius was obtained using equation 4.1 and the fact that MWCO represents 90% separation.

[2] Estimated – Membrane was a microfiltration membrane and was characterized by a pore size range of 0.01 – 0.1 microns, rather than MWCO.

Thus if the solute conditions, size and volume fraction remain constant, then the specific cake layer resistance would not be expected to change. Therefore, for each individual membrane, changes in cake layer resistance should be dictated by changes in the cake layer thickness.

Provided that a membrane can retain the solute particles that it is intended to separate from the solvent (i.e., for bilge water, it is desired to separate oil emulsions and other particulates from water) the cake layer thickness, and therefore its associated resistance, increases as MWCO increases. This is because, as a membrane's pore size increases, the flux of water through the membrane increases. This increase in flux results in a greater degree of concentration polarization at the membrane's surface and therefore a thicker

cake layer. However, as the membrane pore size increases it can no longer retain the smaller particulates and oil emulsions, which in turn results in a decreasing cake layer thickness.

Examination of the cake layer resistances of the various membranes, identified in Table 5.1, does not reveal a continually decreasing cake layer resistance, but two distinct membrane groupings. The division between these two membrane groups appears to be a MWCO ranging between 8,000 to 10,000 Daltons. For membranes with MWCOs less than 8,000 Daltons, the cake layer resistance increases with increasing MWCO. However, when the MWCO exceeds 8,000 Daltons, the cake layer resistance drops significantly and then appears to slowly decline with increasing membrane MWCO.

As described in section 2.3.2 it is expected that an oil emulsion will have a radius no smaller than 0.0175 microns (Lipp et al., 1988). As seen in Table 5.1 only the QX membrane has a nominal pore size greater than this size. Therefore if only oil emulsions were present in the bilge water one would expect to observe an ever increasing cake layer resistance, but this does not occur. This suggests that this unexpected cake resistance trend is due to the presence of another component in the used oil bilge water.

As detailed in section 3.5 the cake layer thickness, and therefore the cake layer resistance, can be theoretically determined through equation 3.36. While this equation contains a number of variables the majority of these variables are either system parameters (e.g., transmembrane pressure) or are dictated by the membrane's properties (e.g., membrane resistance) and therefore are either known or can be easily determined. The unknown variables, in this expression for the cake layer thickness, are the maximum solute volume fraction in the cake layer, the steady-state time and the particle size.

The maximum solute volume fraction in the cake layer is assumed as a constant value of approximately 0.58 – true for non-deformable spheres (Sethi and Wiesner, 1995). While the oil emulsions are deformable it is reasonable to assume that they would remain

spherical and under steady-state conditions their shape would remain constant. With these assumptions and the remaining known variables it is possible to solve for the particle sizes. (Sample calculations are presented in Appendix E.)

The results of this theoretical modeling are displayed in Figure 5.2, which compares the theoretical results against the experimental data. The theoretical results are based on the identification of two critically sized solute elements (radius) of 0.0034 and 0.0241 microns.

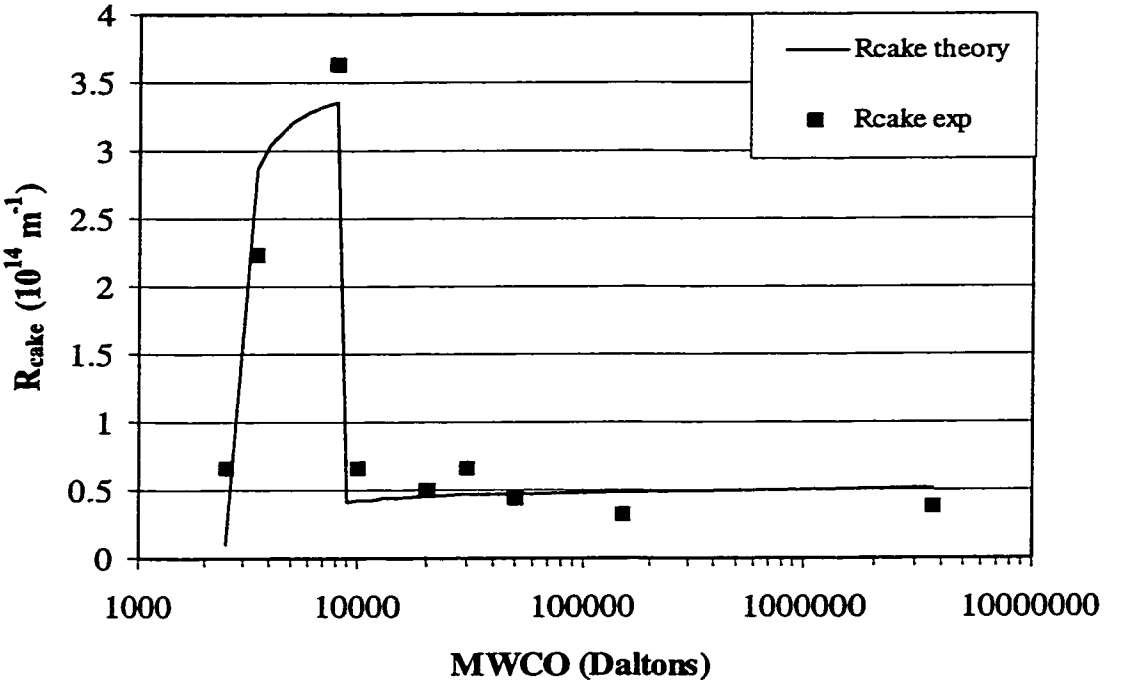

Figure 5.2: Cake Layer Resistance vs. Membrane MWCO

The associated cake layer thickness and time required to achieve this steady-state cake layer, for the various membranes, are presented in Table 5.2. (The determination of these values is presented in Appendix E.) For the tighter membranes, that is those with a MWCO not exceeding 8,000 Daltons, the calculated steady-state cake layer conditions are determined using both the smaller and larger solute particles.

For the membranes with a MWCO greater than 10,000 Daltons the cake layer is formed strictly of oil emulsions. Since the oil emulsions have a range of sizes in the bulk bilge water solution the cake layer will be formed of a critically sized oil emulsion, as dictated by the one having the lowest diffusion coefficient.

Table 5.2: Flat Sheet Steady-State Cake Layer Conditions

Membrane			Steady-State Cake Layer Conditions	
Name	**MWCO (Daltons)**	**Pore Radius (microns)**	**Thickness (microns)**	**Time (seconds)**
GH	2,500	0.0018	4.5	879
GK	3,500	0.0022	15.2	1753
GM	8,000	0.0033	24.7	3841
GN	10,000	0.0037	228.0	7946
M100	20,000	0.0052	170.9	4017
QW	30,000	0.0064	224.9	6672
M180	50,000	0.0082	149.3	3074
P707	150,000	0.0082	112.3	1743
QX	3,600,000	0.05	128.1	2102

The sizes of the solute matter, radii of 0.0034 microns and 0.0241 microns, are important in that they provide clues as to their nature. One of the solute particles must be an oil emulsion, but which one? As identified, from a literature review it is not expected that an oil emulsion will have radius less than 0.0175 microns (Lipp et al., 1988). Therefore it is not likely that the smaller solute particle, radius of 0.0034 micron, is an oil emulsion. Some likely sources of these smaller particles are metallic hydroxides and/or combustion (carbonaceous) particles, all of which can realistically be expected to be in this smaller size range. The larger solute particles are more likely to be oil emulsions, as the determined size of these particles is within the expected size range for oil emulsions.

However, an oil emulsion cannot be expected to retain a constant size. The mixing, associated with pumping, and the presence of surfactants in the bilge water will counteract the agglomeration of oil emulsions and therefore bilge water will become

comprised of oil emulsions of varying sizes. As shown by Lipp et al. the size of an oil emulsion can reasonably be expected to have a radius ranging from 0.0175 to 0.2250 microns, with the emulsion size depending on a number of variables, including oil and surfactant content (Lipp et al., 1988). As described in section 3.3, and graphically represented in Figure 3.2, the diffusivity of the oil emulsions will cause a critically sized oil emulsion to remain within the cake layer. That is, the cake layer should be comprised of the particles/oil emulsions with a minimum diffusivity, as the more diffuse particles will leave the cake layer. This critical size of particle/oil emulsion is determined by the membrane and operating parameters, as explained in section 3.3.

The composition of the cake layer, for used bilge water, is decidedly different for the tighter and the more open membranes. For the tighter membranes it is believed that the cake layer is composed of both the smaller particles and the larger oil emulsions. However, it is felt that the cake layer of the more open membranes is only comprised of the larger oil emulsions. This is depicted in Figures 5.3 and 5.4.

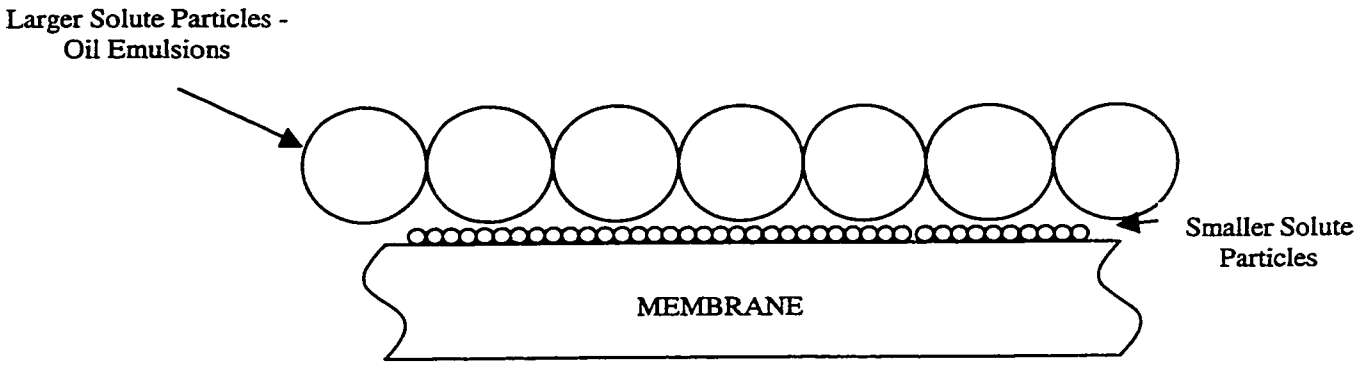

Figure 5.3: Used Bilge Water Cake Layer,
For Membranes With a MWCO < 10,000 Daltons

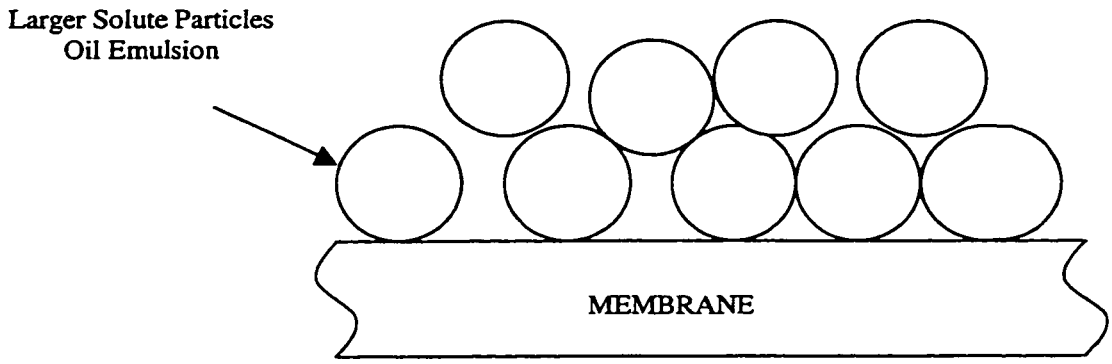

Figure 5.4: Used Bilge Water Cake Layer,
For Membranes With a MWCO > 10,000 Daltons

5.1.2 Effect of Bilge Water Composition

Further evidence of the impact of oil emulsion size on membrane flux was noted when using different surfactants in the bilge water. The stability of the oil emulsions, and therefore their size, is a function of the surfactant found in the bilge water (Lipp et al., 1988). That is, different surfactants will produce emulsions of varying stability. For selected experimental runs two different surfactants (commercial names of CLEANBREAK and SEACLEAN) were used in the composition of the bilge water. CLEANBREAK is reported to create a temporary dispersion of oil particles, which eventually agglomerate and separate from the water, whereas SEACLEAN is formulated to provide a more stable emulsion (LBG Industries Inc. Technical Literature, 1997).

As stated in section 4.1 the flat sheet membranes were tested in stir cells. The oil concentration of the bilge water within the stir cell increased over the duration of the experimental run. However, due to the differing flux associated with each membrane they did not necessarily treat bilge water of equal oil concentrations throughout the length of their experimental runs. Therefore examining concentration versus flux, rather than time versus flux, would provide a better comparison of the various membrane experimental runs. However, it was not possible to determine the oil content of the bilge

water because all of the oil did not become emulsified in the bilge water. As well it was not possible to test the bilge water within the stir cell, as the stir cell did not possess a drain and therefore it was not possible to retrieve its contents.

In lieu of comparing the bilge water's oil concentration during an experimental run it was possible to determine the volume of bilge water treated throughout an experimental run and thus determine the volumetric reduction of the bilge water throughout a run. For the stir cell experimental setup the quantity of synthetic bilge water entering the stir cell is equal to the quantity of permeate leaving the stir cell. Assuming that the permeate has a very small amount of oil in it compared to the feed solution, the volumetric reduction (VR) can be expressed as:

$$VR = \frac{Permeate\ Volume\ at\ a\ given\ time}{Stir\ Cell\ Volume + Permeate\ Volume\ at\ a\ given\ time} \qquad (5.1)$$

From Figures 5.5 and 5.6 it can be noted that membrane flux varies with the type of surfactant used, in some cases rather significantly as seen in Figure 5.6.

As SEACLEAN creates a more stable, and therefore smaller, oil emulsion it is expected that its specific cake resistance and thus its cake layer resistance would be greater than that for bilge water containing CLEANBREAK. However, as evidenced by Figures 5.5 and 5.6, the bilge water containing SEACLEAN produces a greater flux (and therefore a lesser cake layer resistance) than the bilge water made with CLEANBREAK. Therefore the impact of a surfactant on oil-water interactions is greater than merely its effect upon oil emulsion stability and size. One possibility may be that the emulsions formed in the bilge water made with CLEANBREAK were sufficiently unstable such that they agglomerated together in the cake layer, where they were present in a greater concentration. This agglomeration may occur in such a manner that the emulsions adhere or smear onto the membrane surface rather than diffuse away, resulting in membrane fouling and therefore reducing flux.

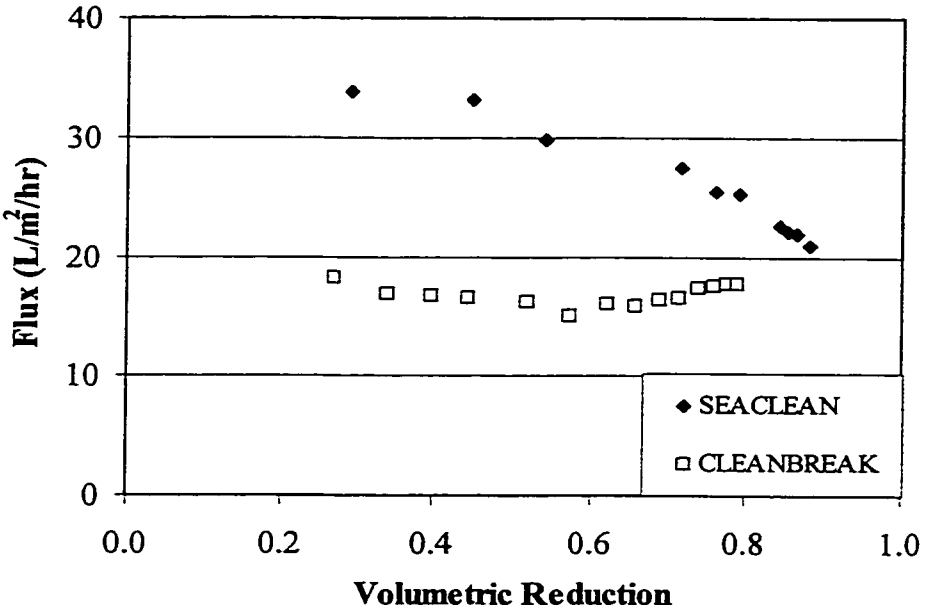

Figure 5.5: Comparison of Detergents in Used Bilge Water, M100 Membrane

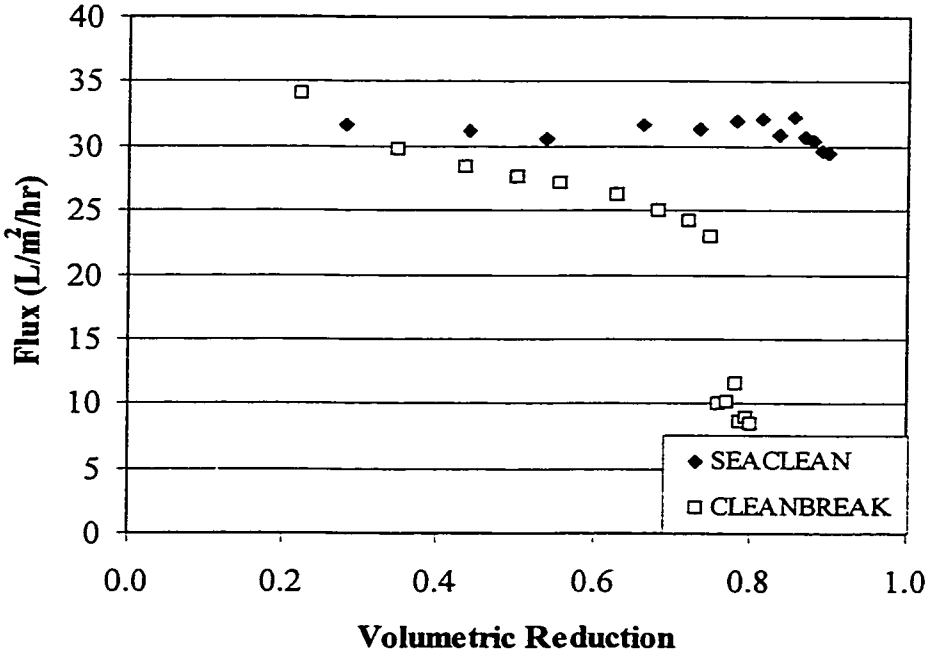

Figure 5.6: Comparison of Detergents in Used Bilge Water, QX Membrane

In addition to varying surfactants another prime source of bilge water variance is the type of lubricating oil present, that is either new (i.e., unused) or used lubricating oil. Certain flat sheet membranes were tested with bilge water composed of new or used lubricating oil in order to examine the effects of the type of lubricating oil on bilge water treatment. The M100 and QX membranes were examined for their flux rates for both new and used bilge water. These experimental results are presented in Figure 5.7 and 5.8 respectively.

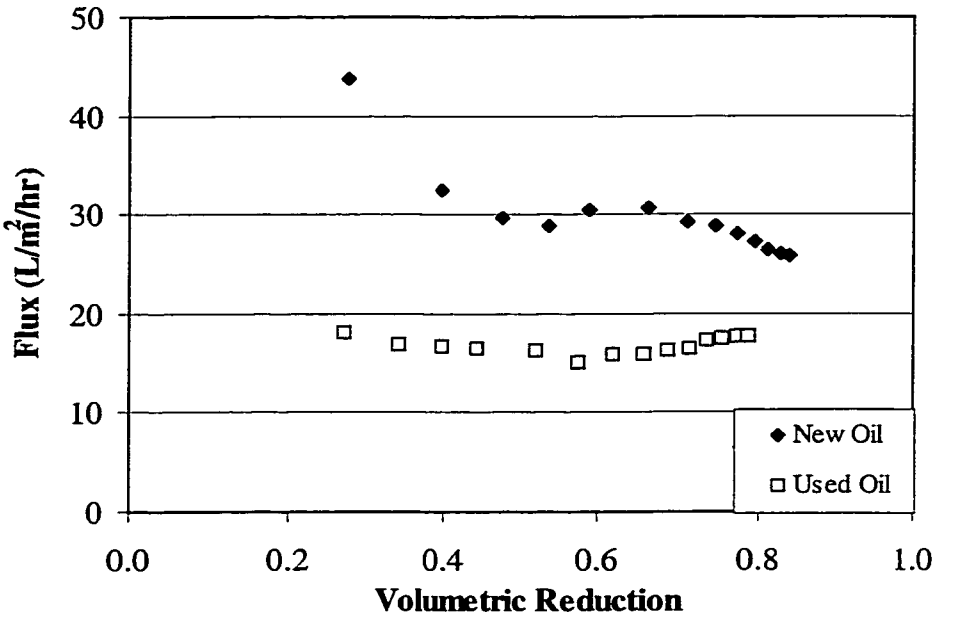

Figure 5.7: Comparison of New and Used Lube Oil in Bilge Water, M100 Membrane

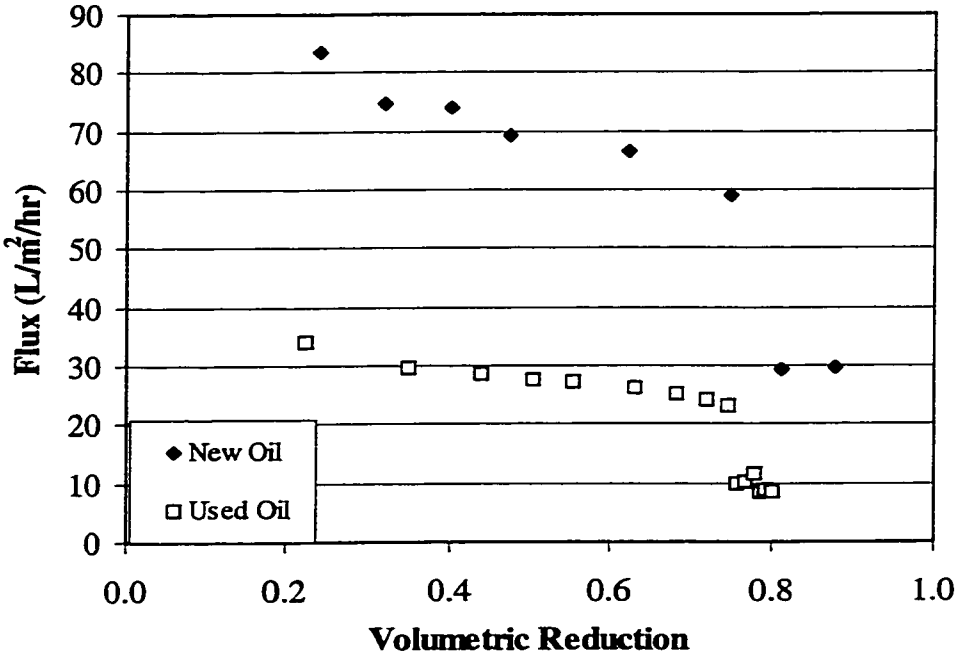

Figure 5.8: Comparison of New and Used Lube Oil in Bilge Water, QX Membrane

As seen from Figure 5.7 and 5.8 it is evident that new bilge water has a higher flux rate than used bilge water; two possible reasons are offered.

The first explanation is based upon the solute particulate difference between new and used bilge water. That is, used bilge water contains smaller solute particulates, in addition to the oil emulsion, whereas new bilge water only contains the oil emulsion.

The second possible explanation is inherent with equation 3.10, which details the impact of concentration polarization effects on membrane flux. That is, membrane flux is dependent on the ratio of the oil concentration in the cake layer and the oil concentration in the bulk bilge water solution. If used lube oil is more soluble in water than new lube oil, then bilge water comprised of used lube oil will have a greater bulk oil concentration than bilge water comprised of new lube oil. This will result in a decreased flux when processing bilge water composed of used lube oil.

5.1.3 Oil Droplet Pore Plugging

As described in section 3.4 oil droplet pore plugging can be experienced at routine microfiltration operating pressures (i.e., pressures not exceeding 200KPa). This phenomenon is not expected to occur for ultrafiltration membranes because the smaller pore sizes associated with ultrafiltration would necessitate a pressure far in excess of typical ultrafiltration operating pressures in order to force oil droplets into their pores. The QX membrane was the only microfiltration membrane tested - the rest were ultrafiltration membranes - and thus is the only membrane that is expected to be susceptible to this phenomenon. Oil droplet pore plugging would be identified by a sharp and severe reduction in membrane flux.

As seen in Figure 5.8 the QX membrane experienced severe membrane flux degradation at increased bilge water concentrations for both new and used bilge waters (CLEANBREAK was the surfactant in these bilge waters). Re-examining Figure 5.6 shows that this flux degradation was not observed for bilge water composed of SEACLEAN surfactant, but it did occur for bilge water composed of CLEANBREAK.

In Figure 5.8 this severe flux reduction was observed for both new and used bilge waters, but it occurred at lower oil concentrations for the used bilge water. Therefore the cake resistance associated with used bilge water may be greater than that for new bilge water.

Microscopic examination of the oil emulsions, created by new and used lubrication oil, are presented in Figure 5.9. From Figure 5.9 it can be seen that the oil emulsions created with the new and used lubricating oil are different. The new lubricating oil creates a simple oil-in-water emulsion. However, the used lubricating oil creates a more complex water-in-oil-in-water emulsion, these types of emulsions are referred to as double emulsions. It has been shown that double emulsions are more stable than simple oil-water emulsions (Ficheux et al., 1998). This increased stability would mean that oil emulsions created with used lubricating oil will not coalesce together as readily as

emulsions created with new lubricating oil and therefore used lube oil emulsions will maintain a higher oil concentration in bilge water, corroborating the hypothesis presented in section 5.1.2. In accordance with the concentration polarization phenomena (equation 3.4), an increased bulk (emulsified) oil concentration would result in a reduced flux with bilge water composed of used lubricating oil.

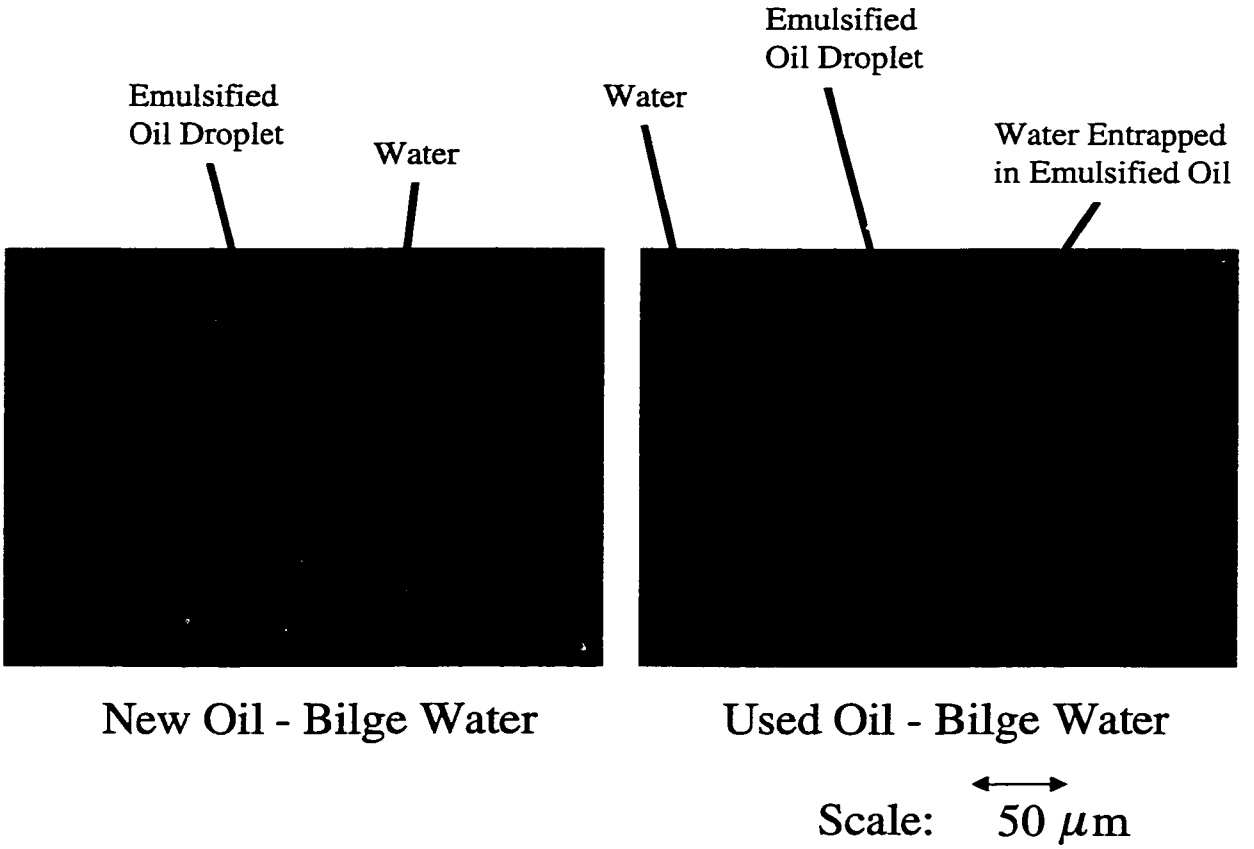

Figure 5.9: Microscopic Examination of Oil Emulsions Experienced in Bilge Water Composed of New and Used Diesel Engine Lubricating Oil

The scale identified in Figure 5.9 should not be interpreted as an indication of the size of oil emulsions that the membrane would experience because the bilge water sample was placed between two slides in order to view the emulsions. This likely resulted in a flattening of the entire bilge water sample, including the emulsions, and therefore

distorted the sizes of the objects being viewed. However, this does not have an impact on the conclusions noted as the purpose of these pictures is provided to highlight the difference in composition of these two oil emulsions, not provide an indication of emulsion size.

5.2 Pilot Scale Testing

The flat sheet tests described in section 5.1 provided an understanding of the effects of bilge water particulates on permeate flux. With this understanding of bilge water characteristics it was then appropriate to simulate shipborne conditions through the use of pilot scale testing. This allowed for operational parameters, such as backflushing, to be examined. Backflushing is expected to enhance membrane flux by reducing cake layer resistance and membrane fouling.

The following section presents and compares experimental results for the CERAMEM LMA membrane, having a pore radius of 0.0025 microns and the KOCH CM membrane, having a pore radius of 0.0082 microns.

The CERAMEM LMA membrane runs were conducted with cross-flow velocities ranging from 1.04 to 1.74 m/s, while those for the KOCH CM membrane were conducted with cross-flow velocities ranging from 3.12 to 3.75 m/s. The majority of the experimental runs were conducted with a transmembrane pressure of 207.6 KPa (30 psig). Runs treating bilge water, consisting of new diesel engine lubricating oil ("new bilge water"), using the CERAMEM LMA membrane and using a cross-flow velocity of 1.74 m/s were performed at 221.4 KPa (32 psig); this was the lowest pressure achievable using this cross-flow velocity. For all experimental runs the temperature normally started near 23°C and increased to 25°C due to the thermal energy imparted by the system's pump. In accordance with the ASTM standard D5090-90: Standardizing Ultrafiltration Permeate Flow Performance all of the experimental data presented in this section has been corrected to a transmembrane pressure of 207.6 KPa (30 psig) and a temperature of 25°C.

Examination of the various membrane modules, particularly following experimental runs with used bilge water, noted a slight build up of material at the entrance of the membrane flow channels. Accordingly, prior to the experimental runs with the KOCH CM

membrane and the treatment of bilge water made with used diesel engine lubricating oil ("used bilge water"), a pre-filter was added to the system. The purpose of this pre-filter was to safeguard against the possibility of plugging at the entrance of the membrane's hollow fibres. This pre-filter appears to have resulted in the adsorption and/or coalescence of oil within the bag filter. The impact of this pre-filter was only noted prior to the non-backflushed run (i.e., the last experimental run). For this run the pre-filter was not only removed, but the bilge water retentate was run through it in an attempt to re-introduce the oil back into the bilge water. Due to the different conditions that this series of experimental runs were conducted under they will be addressed separately.

5.2.1 Flux Decline Due to Irreversible Fouling

Prior to examination of the experimental data it is worthwhile to examine the effects of fouling on the membrane modules. Irreversible fouling results in the degradation of a membrane's flux capacity and therefore must be identified and corrected in order to properly compare experimental data.

Ideally the best method to evaluate the accumulation of irreversible fouling would be to clean and conduct pure water permeate runs after each experimental run. While the membranes were cleaned following each run, batches of synthetic bilge water were used for multiple runs. Due to the length of time required to make up synthetic bilge water, it was not possible to conduct a pure water permeate run until a batch of synthetic bilge water was discarded. Accordingly, pure water permeate runs were not conducted following each run. However, the extent of irreversible fouling could also be identified by the degree of flux decline from run to run.

The degree of irreversible fouling was assessed by examining the very early bilge water flux values of each experimental run (i.e., within the first 1-5 minutes) and determining the overall decline of these initial flux values, over a sequence of experimental runs. It is reasonable to expect that these values will closely approximate the decline in pure water

permeate flux because within the first few minutes of an experimental run a membrane will experience minimal fouling and the gel layer should still be relatively thin. Therefore the overall system resistance should be primarily comprised of the membrane resistance. Figures 5.10 and 5.11 show these initial flux rates for the CERAMEM LMA and KOCH CM membrane modules, respectively. These figures are comprised of data from both new and used bilge water runs and are presented versus the sequence (i.e., the chronological order) in which the experimental runs were conducted.

For the CERAMEM LMA membrane the pure water permeate flux value, before and after the sequence of runs, was approximately 97.1 L/m^2/hour and 64.7 L/m^2/hour, respectively. As revealed by Figure 5.10, the CERAMEM LMA membrane experienced a continual flux decline over the course of the experimental runs, caused by the inability of the cleaning regime to completely remove all the fouling which built up on the membrane surface during bilge water treatment. Accordingly, the CERAMEM LMA membrane flux results need to be corrected for this continual flux decline due to the increasing membrane resistance as the runs proceeded. Based upon the slope of the best fit for these bilge water values, identified in Figure 5.10, the CERAMEM LMA membrane experienced a flux decline of approximately 1.91 L/m^2/hour for each experimental run. Due to this irreversible fouling, experienced by the CERAMEM LMA membrane, the direct comparison of flux data from one experimental run to another does not solely represent the impact of the individual parameters examined. To account for the impact of the CERAMEM LMA membrane's fouling and therefore to properly compare the CERAMEM LMA membrane's experimental runs, flux ratios, rather than the fluxes, were examined. (The flux ratio values are presented in Appendix F.) The flux ratio is defined as;

$$\text{Flux Ratio} = \frac{\text{Bilge Water Flux}}{\text{Estimated PWP Flux for the given Bilge Water Run}}. \qquad (5.2)$$

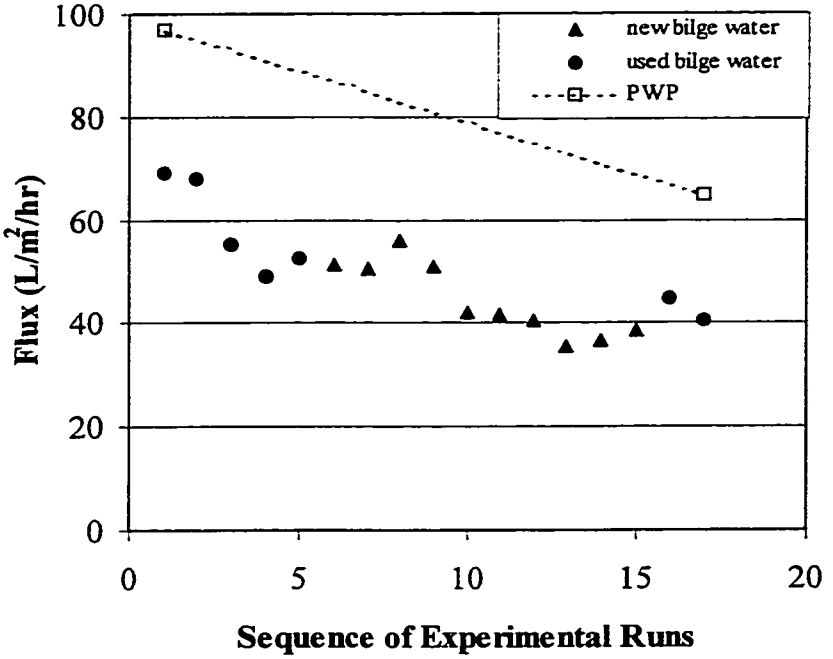

Figure 5.10: CERAMEM LMA Membrane Flux Decline

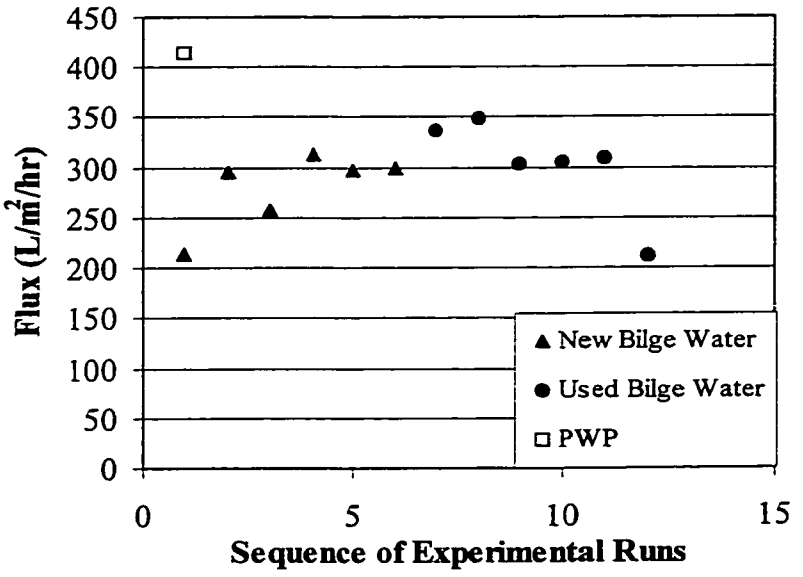

Figure 5.11: KOCH CM Membrane Flux Decline

For the KOCH CM membrane the pure water permeate flux rate for the virgin membrane was approximately 415 L/m^2/hour. As observed from Figure 5.11, except for the first and last experimental runs, the initial bilge water flux values appear to be reasonably consistent around a value of approximately 300 L/m^2/hour. Accordingly, it appears that the KOCH CM membranes did not experience any irreversible fouling. Therefore the flux values, from its various experimental runs, were compared directly for the KOCH CM membrane. Unfortunately, a post bilge water pure water permeate flux value was not obtained which could have confirmed this lack of irreversible fouling. (The KOCH CM membrane experienced a catastrophic failure at the end of its experimental runs; the membrane ruptured, witnessed by the presence of oil on the permeate side of the membrane. The KOCH CM membrane had a transparent plastic housing allowing for this observation.)

5.2.2 Pilot Scale Error

In order to properly assess the various experimental results it is necessary to determine if differences in observed flux rates are due to the changes in operational parameters or error. To assess the error it is necessary to review similar runs. However, due to the length of the experimental runs, their duration was 1 to 3 days, it was not possible to conduct many duplicate runs. Additionally, membrane fouling (particularly for the CERAMEM LMA membrane) made it very difficult to obtain duplicate runs.

However, the error associated with the experimental set-up and the data acquisition system can be assessed by reviewing the steady-state conditions. At the steady-state conditions the cake layer thickness is constant and therefore the membrane flux should stabilize. Thus the flux data, after this time, are essentially duplicate runs. The best runs to examine error are those that did not use any backflushing; as the reason for backflushing is to ensure that the cake layer does not reach its maximum thickness.

Accordingly, the experimental runs, for the CERAMEM LMA membrane, with no backflushing, were examined in order to determine the error, or precision, associated with the experimental runs. Various experimental runs, conducted with no backflushing were examined for the error associated with the flux, after the system had achieved steady-state conditions (i.e., the cake layer had achieved its steady-state thickness). All of the runs had very similar error associated with the steady-state flux. Figure 5.12 presents the flux data for the CERAMEM LMA membrane, with no backflushing, a transmembrane pressure of 220KPa gauge and a cross-flow velocity of 1.74m/s. As seen from Figure 5.12 the flux appears to achieve a steady state after approximately 31 hours of operation. (Appendix H presents all of these time versus flux data points.) The solid line is the average steady-state flux with the dashed lines representing the 95% confidence interval. The average steady-state flux for this particular experimental run was approximately 38.53 ± 0.24 L/m^2/hour, equating to approximately 0.62% error. As this run was representative of the various experimental runs this degree of error will be used throughout the analysis of the experimental data. (Appendix H provides details regarding the determination of the data presented in Figure 5.12)

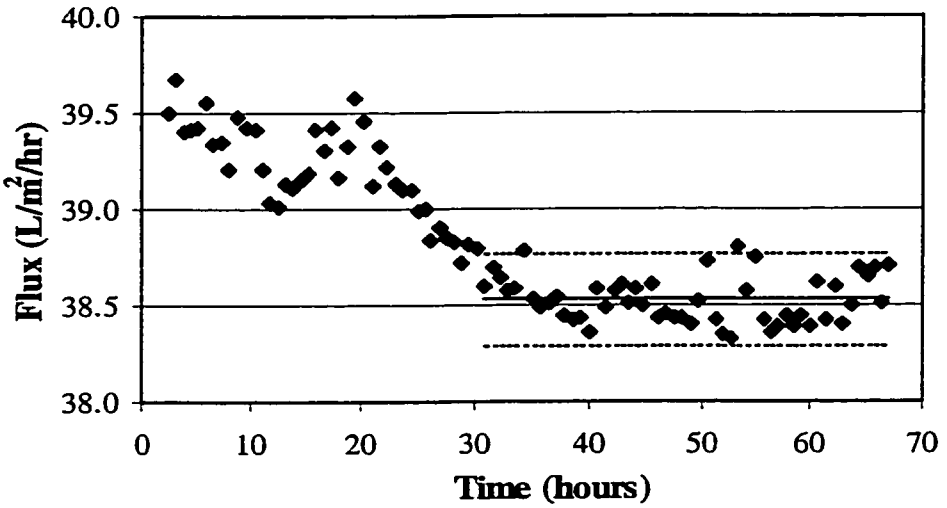

Figure 5.12: CERAMEM LMA Membrane, No Backflush, Operational Pressure of 220KPa, Cross-Flow Velocity of 1.74 m/s

Those experimental runs, which were examined through the use of the flux ratio, will have a greater error associated with them since the flux ratio (equation 5.2) has flux terms in both the numerator and the denominator. Accordingly, the percentage error associated with the use of flux ratio will be:

$$Flux\ Ratio = \frac{Flux \pm 0.62\%}{PWP\ Flux \pm 0.62\%}$$

equating to an error of ± 1.24%.

5.2.3 Effect of Bilge Water Composition

For the KOCH CM membrane, experimental runs conducted with used bilge water were performed with a membrane pre-filter, while experimental runs conducted with new bilge water did not have this pre-filter. Therefore these two sets of experimental runs cannot be compared. Therefore to identify the impact of new versus used bilge water on flux the various CERAMEM LMA membrane experimental runs are compared. Figures 5.13 through 5.15 are the experimental results for the CERAMEM LMA membranes, comparing new and used bilge water runs with comparable operational parameters (i.e., the same backflush and cross-flow velocity and using flux ratio to account for flux decline and any transmembrane pressure differences).

As shown in the previous section, the treatment of new or used bilge water appeared to be immaterial with respect to the irreversible fouling associated with the membranes. However, as seen with the flat sheet testing, new and used bilge water did result in different flux values, likely caused by a different cake layer formation (be it differing emulsion sizes within the cake layer or differing cake layer thickness). Figures 5.13 and 5.14 reveal a higher flux ratio (and therefore a higher flux) for new bilge water as compared to used bilge water, corroborating the flat sheet results. However, the magnitude of this difference, for the CERAMEM LMA membrane module, is not as great as that observed with the flat sheets. This is likely the result of the fact that the shear rate at the surface of the membrane in the stir cell was lower, resulting in a thicker cake and

therefore a greater cake layer resistance. A thicker cake layer would result in an increased flux decline, which could highlight the differences between new and used bilge water. Additionally, the experimental runs using flat sheet membranes were operated at higher transmembrane pressures and therefore they would experience a greater cake layer resistance than the pilot scale modules.

It should also be noted that the sequence of the runs presented in Figures 5.13 through 5.15 were all conducted in the same manner. That is, the used bilge water runs were conducted prior to the new bilge water runs. In fact, all of the used bilge water runs were conducted prior to the new bilge water runs. The order of the individual runs, for both the new and used bilge waters, was the following: the run using a backflush of 5 seconds was first, followed by the run using a backflush of 10 seconds and then the run using a backflush of 2.5 seconds. As seen from Figures 5.13 through 5.15 the order of the runs does not coincide with a sequential increase or decrease in flux ratios. The will be discussed further in section 5.2.4. Furthermore, as described earlier the use of flux ratios mitigates the impact of the CERAMEM LMA membrane fouling.

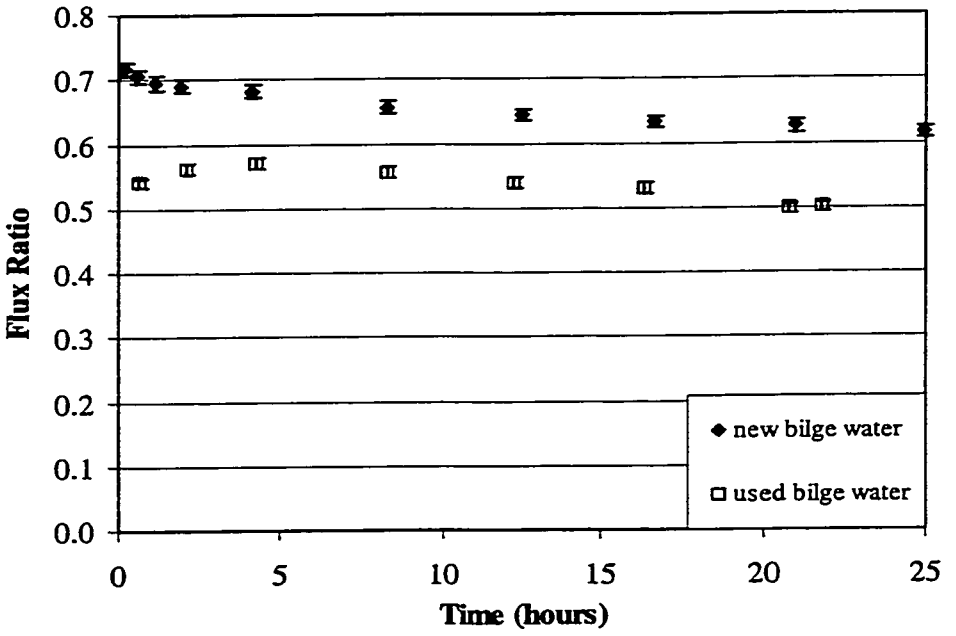

Figure 5.13: CERAMEM LMA Membrane –2.5 second Backflush per 120 second cycle

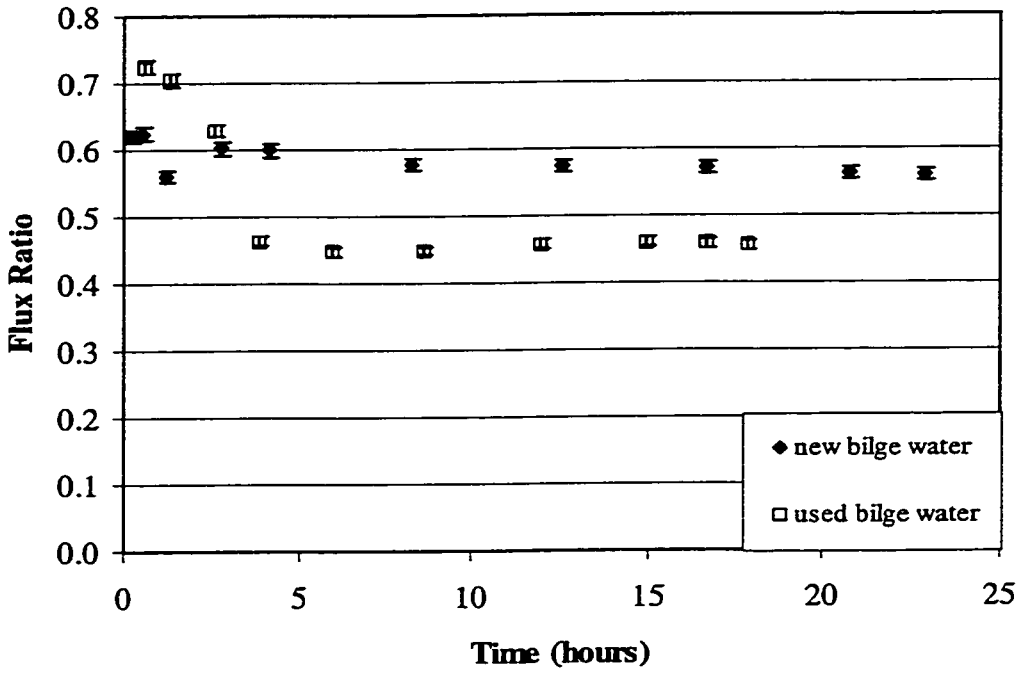

Figure 5.14: CERAMEM LMA Membrane –5 second Backflush per 120 second cycle

5.2.4 Effect of Backflushing

The following nomenclature is used to describe the degree of backflushing. The first number represents the duration of the backflushing and the second number represents the duration of the total cycle, including the backflushing and the normal membrane operation. For example, 2.5/120 represents a 2.5 second backflush followed by 117.5 seconds of normal membrane operation. The flux and flux ratios identified are the average fluxes and flux ratios for the total cycle. That is, they include the "lost time" associated with the backflushing.

While Figures 5.13 and 5.14 demonstrate the fact that used bilge water is more difficult to treat than new bilge water examination of the varying degree of backflushing shows that the difficulty associated with used bilge water can be mitigated. Figure 5.15, compares new and used bilge water runs, for the greatest degree of backflushing

conducted during experimental testing: a 10 second backflush in a 120 second total cycle time. It shows virtually no difference in flux for new and used bilge water runs. A closer review of Figures 5.13 and 5.14 shows that a lesser degree of backflushing, 2.5/120 versus 5/120, is accompanied by a greater difference between the new and used bilge water fluxes. For the 2.5/120 backflush (Figure 5.13) the difference in flux ratios between the new and used bilge water runs was approximately by 0.11, after approximately 24 hours of operation.

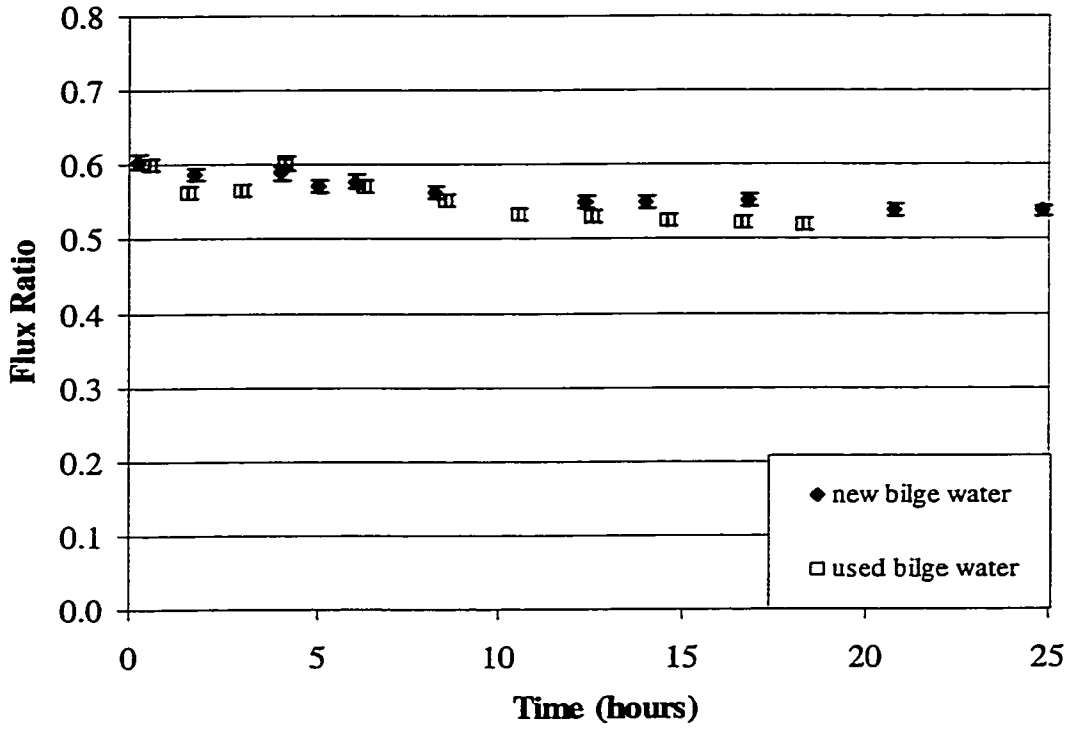

Figure 5.15: CERAMEM LMA Membrane –10 second Backflush per 120 second cycle

The 5/120 backflush (Figure 5.14) produced a difference in flux ratios, between the new and used bilge water runs, of approximately by 0.10, after approximately 24 hours of operation. As shown in Figure 5.15, when the backflush was increased to 10/120 the difference in flux ratios, between the new and used bilge water is essentially eliminated. Therefore it appears that increasing backflushing reduces the difficulty in treating used bilge water, as compared to new bilge water. Whether the negative impact of the used bilge water is due to better adhesion of the cake layer to the membrane or a thicker cake

layer or another factor, it seems that a greater backflush duration mitigates the higher cake layer resistance associated with used bilge water.

Additionally, examination of the flux ratio values reveals that for new bilge water the flux ratio drops as the backflush is increased. That is, the flux ratio is greatest for a backflush of 2.5/120 and least for a backflush of 10/120. For a backflush of 2.5/120 the flux ratio is approximately 0.61 and it drops to approximately 0.56 for a 5/120 backflush and is roughly 0.54 for the 10/120 backflush. (The flux ratio values quoted are after approximately 24 hours of operation.) However, for the used bilge water treatment such a defined trend does not exist. The flux ratios for the 2.5/120, 5/120 and 10/120 backflushes are approximately 0.50, 0.46 and 0.52, respectively (after approximately 24 hours of operation). Reviewing these flux ratio values reveals that the new bilge water has greater flux than used bilge water, which can be attributed to a lesser cake layer. Also, for new bilge water treatment the positive impact of backflushing is lost very early, that is, shorter backflushing durations seem satisfactory. However, for used bilge water treatment increasing backflushing seems to neither improve nor degrade flux. (It should be remembered that the flux ratio incorporates the backflush duration and therefore the lost permeation time.) What is uncertain with backflushing is how it impacts upon longer term fouling by its continual removal/lessening of the cake layer.

Figures 5.16 and 5.17 provide a comprehensive examination of the all the experimental runs conducted with varying degrees of backflushing, for the CERAMEM LMA and KOCH CM membranes respectively. (These figures show experimental runs conducted for the treatment of new bilge water.) From these figures the positive impact of backflushing, albeit small, can be noted. Figures 5.16a and 5.17a are provided to identify the error associated with the various experimental runs; in order to clearly show the error only selected data from Figures 5.16 are presented.

For the CERAMEM LMA membrane Figure 5.16 displays the experimental results in terms of flux ratio versus time, rather than flux versus time, due to the irreversible fouling

that it experienced. To categorically confirm the positive impact associated with backflushing, for the CERAMEM LMA, Figure 5.18 displays the flux versus time results.

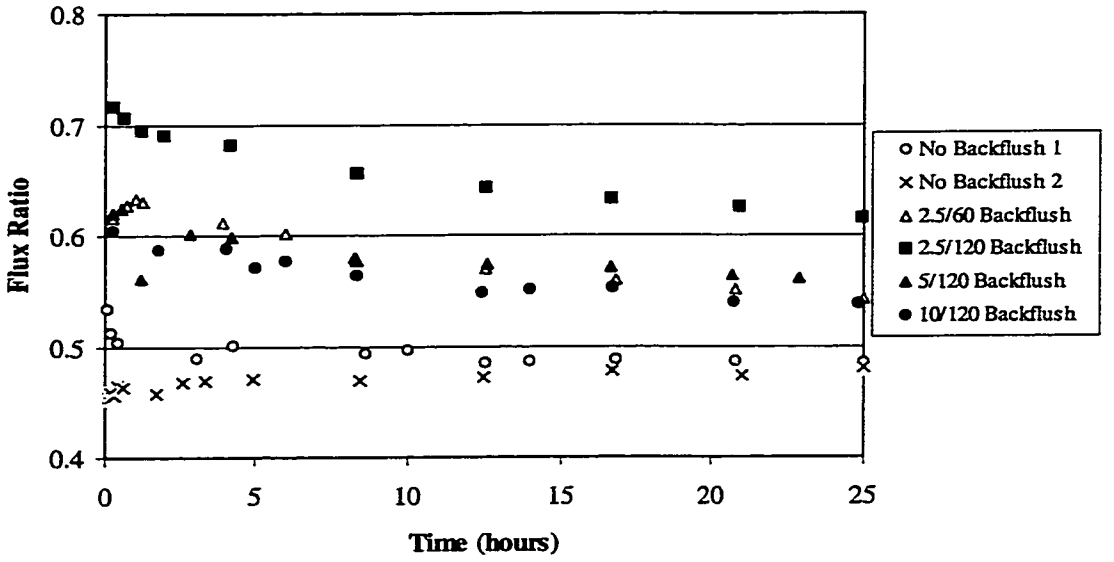

Figure 5.16: CERAMEM LMA Membrane Treating New Bilge Water with Varying Degrees of Backflushing – at 220 KPa

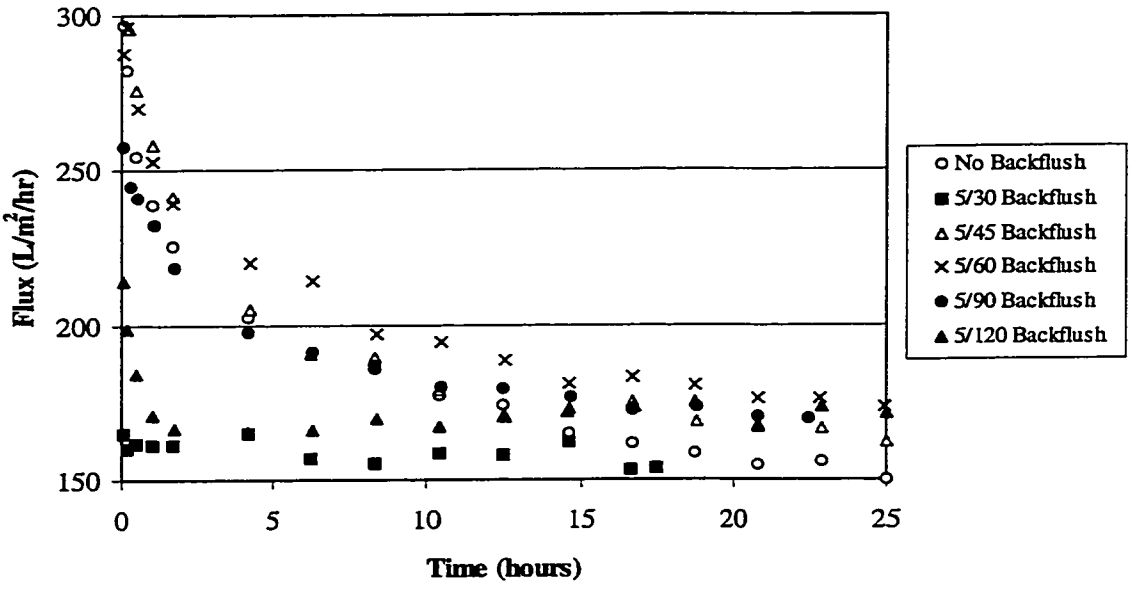

Figure 5.16a: CERAMEM LMA Membrane, selected runs including error bars, New Bilge Water Experimental Runs

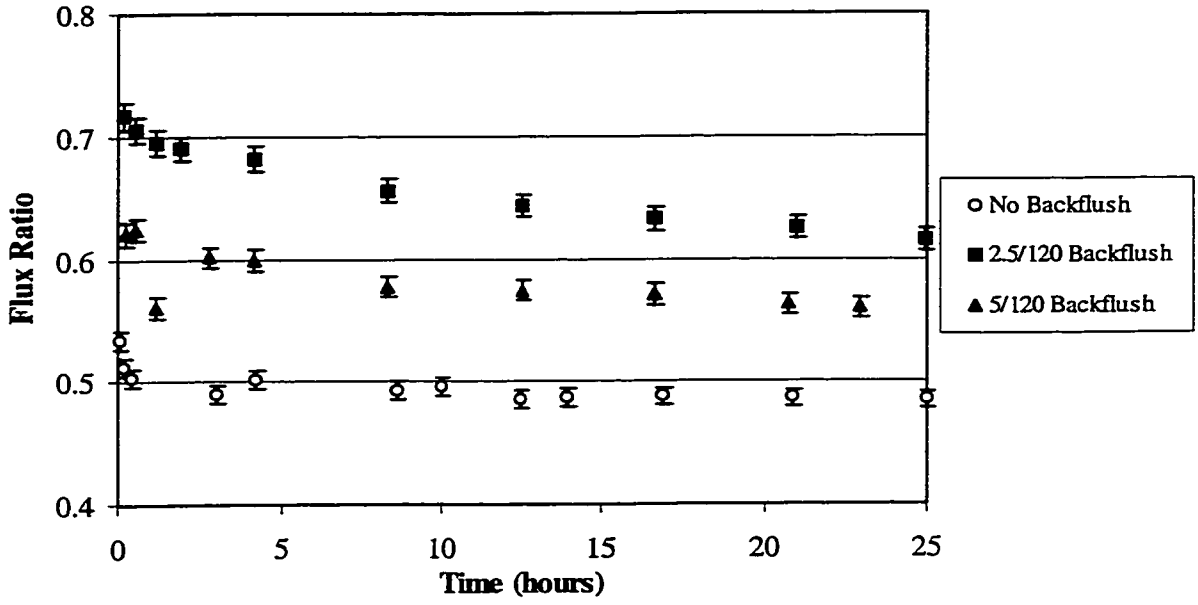

Figure 5.17: KOCH CM Membrane Treating New Bilge Water with Varying Degrees of Backflushing – at 206 KPa

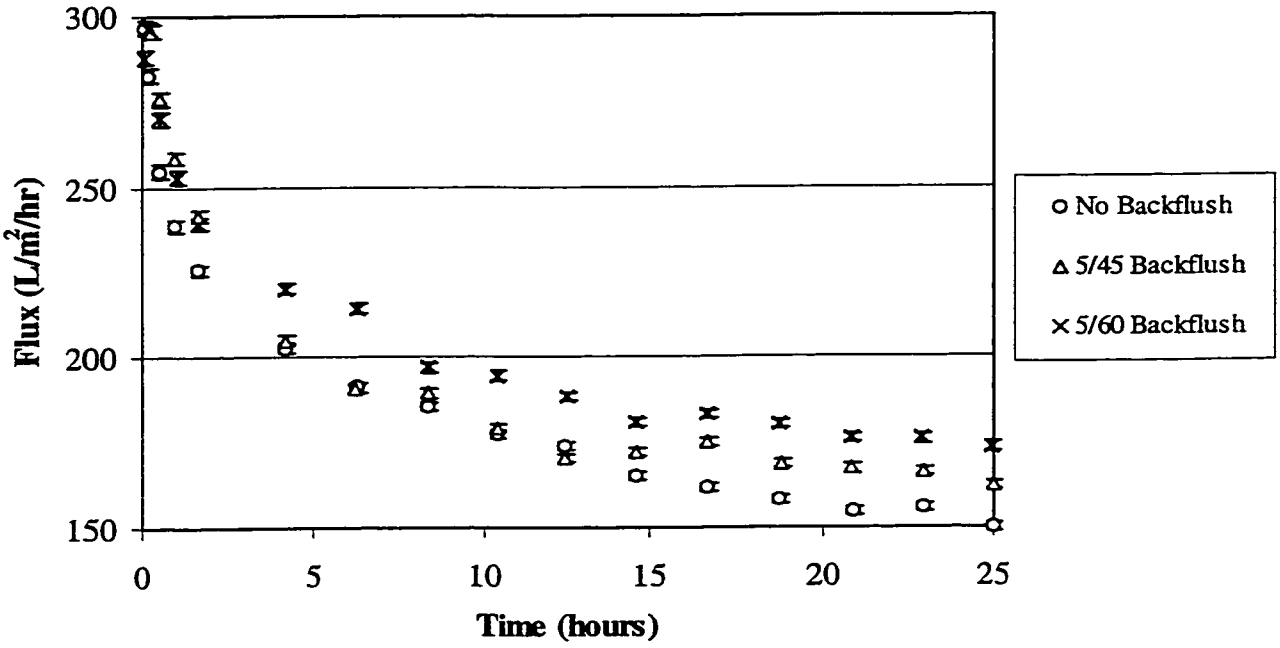

Figure 5.17a: KOCH CM Membrane, selected runs including error bars, New Bilge Water Experimental Runs

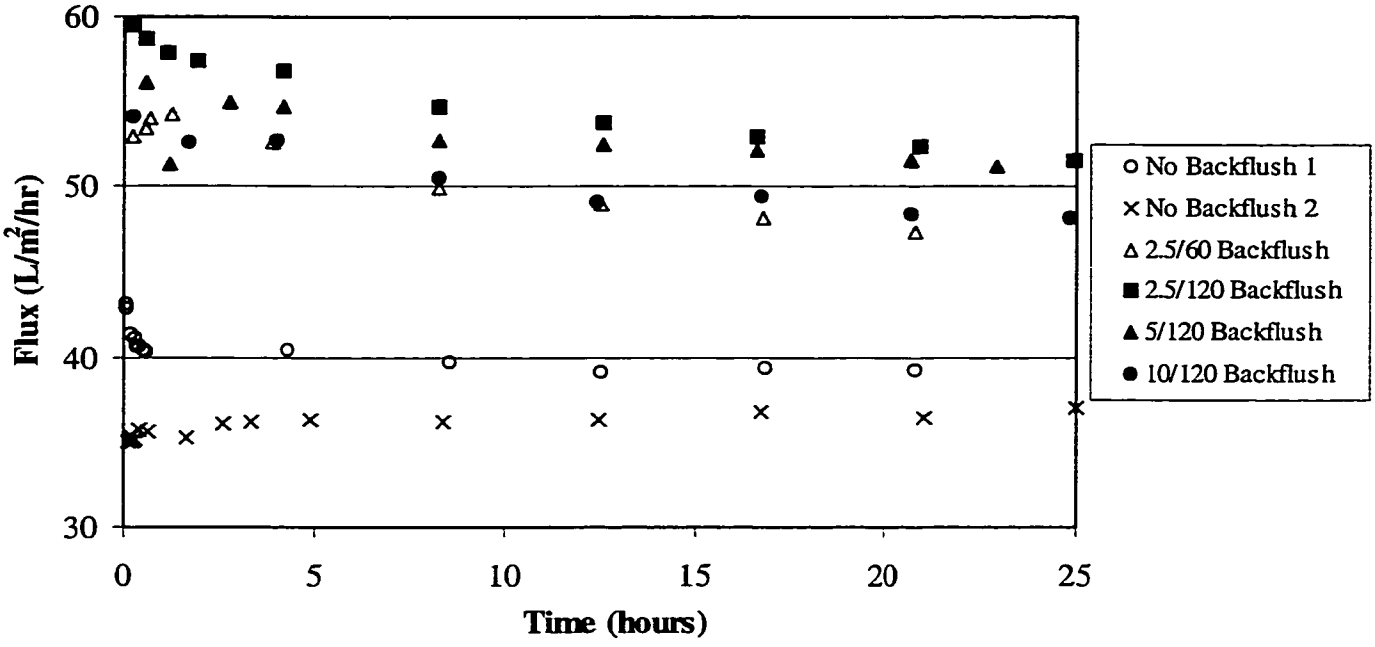

Figure: 5.18: CERAMEM LMA Membrane Treating New Bilge Water with Varying Degrees of Backflushing – at 220 KPa

For the CERAMEM LMA membrane backflushing improved the permeate flux ratio by up to 27%, based upon the flux at 24 hours. The actual permeate flux went from 39.12 L/m^2/hr for the run without backflushing to 54.03 L/m^2/hr for the run with the 2.5/120 backflush, which is an improvement of approximately 38%. The maximum observed flux enhancement resulted with a 2.5/120 backflush, the smallest backflush applied to the CERAMEM LMA membrane. The other degrees of backflushing all provided approximately the same amount of flux improvement, which was less than that provided by the 2.5/120 backflush. Therefore, for the CERAMEM LMA membrane treating new bilge water, it appears that the initial backflushing force provides the majority of benefits with any additional benefits being offset against the time lost when permeate is not produced.

While the impact of backflushing is not as apparent for the KOCH CM membrane, it still provides some minor flux enhancement, with the exception of the 5 second backflush in a

30 second total cycle time. This high frequency of backflushing may not have been effective because the lost flux, 5 seconds of a total time of 30 seconds, negated the benefits associated with the cake layer reduction.

To evaluate the effectiveness of backflushing it is necessary to review the non-backflushed runs in order to identify a benchmark to compare backflushed runs against. These runs will allow for an estimation of the time required for the cake layer to achieve its steady-state conditions. As described in section 3.5 the steady-state time can be determined through the use of equation 3.23. Therefore to solve for the steady-state time the membrane's pure water permeate flux, the steady-state flux when treating bilge water and the flux decline constant (τ_c) are required. The pure water permeate flux and the steady-state flux, when treating bilge water, are readily apparent from the experimental data. The value of the steady-state flux ($J(t_{ss})$) is taken as being the flux after 24 hours of operation. This value is used as it is very likely that the cake layer will have achieved steady-state conditions by this time.

As defined in equation 3.22 the flux decline constant (τ_c) is a function of the membrane resistance, maximum and bulk solute volume fractions, pure water permeate flux and specific cake layer resistance, of which only the specific cake layer resistance is not known. The specific cake layer resistance is determined through equation 3.12, which is dependent upon the maximum solute volume fraction and the critical solute size. For the CERAMEM LMA and KOCH CM membranes the critical solute particles radii are estimated as being 0.047 microns and 0.042 microns, respectively.

The steady-state cake layer thickness can be determined through equations 3.11 or 3.36. (If equation 3.11 is to be utilized the cake layer resistance can be determined from the experimental data.)

Therefore, for the treatment of new bilge water, the steady-state conditions for the CERAMEM LMA and KOCH CM membranes are estimated as:

	Steady-state time	Cake Layer Thickness
CERAMEM LMA membrane	6 hours	155 microns
KOCH CM membrane	20 minutes	36.8 microns

(The detailed calculations for the determination of these values are presented in Appendix I.)

The greater cake layer thickness associated with the CERAMEM LMA membrane explains why the CERAMEM LMA membrane is more affected by backflushing. Since the CERAMEM LMA membrane has an increased cake layer thickness it experiences greater cake layer resistance and therefore backflushing should provide more benefit.

Figure 5.19 details the accuracy of the theoretical fit for the CERAMEM LMA membrane, with no backflushing. Figure 5.20 reveals the accuracy of the theory, for the KOCH CM membrane, again without the use of backflushing. Reviewing these figures it is obvious that the theory does a poor job of predicting the actual flux decline. The theoretical fit is based upon equation 3.21 which reveals the dependence of flux to the pure water flux (i.e., pore size), operational time and the flux decline constant. Based upon the poor fit it would appear that the theory has omitted some operational parameters. For example, the theory does not account for fouling or cross-flow velocity.

The quicker steady-state time and thinner cake layer achieved by the KOCH CM membrane can be better understood when examining the impact of cross-flow velocity on both membranes. The CERAMEM LMA membrane was operated with a cross-flow velocity of 1.74 m/s, the maximum velocity allowing for a pressure of 30 or 32 psi. However, the KOCH CM membrane was operated with a cross-flow velocity of 3.75 m/s. This resulted in the CERAMEM LMA membrane being operated under laminar

conditions (a Reynolds number of approximately 1900) while the KOCH CM membrane was operated under turbulent conditions (a Reynolds number of approximately 4800). The difference between laminar and turbulent flow is known to have a significant impact upon the cake layer conditions as turbulent conditions are known to result in reduced cake layer thickness (Koltuniewicz et al., 1995). Similarly, Porter identified that the mass transfer co-efficient, and thus membrane flux, has a greater dependence on cross-flow velocity in turbulent flow as compared to laminar flow. In turbulent flow the mass transfer co-efficient is proportional to the cross-flow velocity raised to the power of 0.8 compared to the power of 0.33 in laminar flow (Porter, 1990).

From Figures 5.19 and 5.20 it can be observed that the theory overpredicts the (initial) flux for the CERAMEM LMA membrane and underpredicts flux for the KOCH CM membrane. An important limitation of the theory is that it does not incorporate fouling effects into its determination of flux. Therefore the overprediction for the CERAMEM LMA membrane suggests that the CERAMEM LMA membrane may experience fouling very early in its exposure to bilge water, whereas the KOCH CM membrane may be more resistant to the bilge water and fouls more gradually.

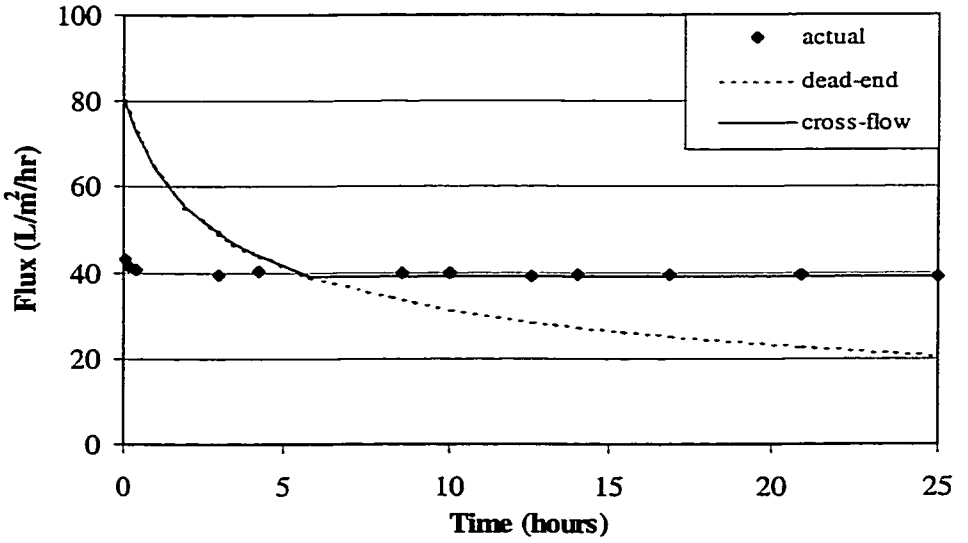

Figure 5.19: CERAMEM LMA Membrane Treating New Bilge Water at 220 KPa with No Backflush

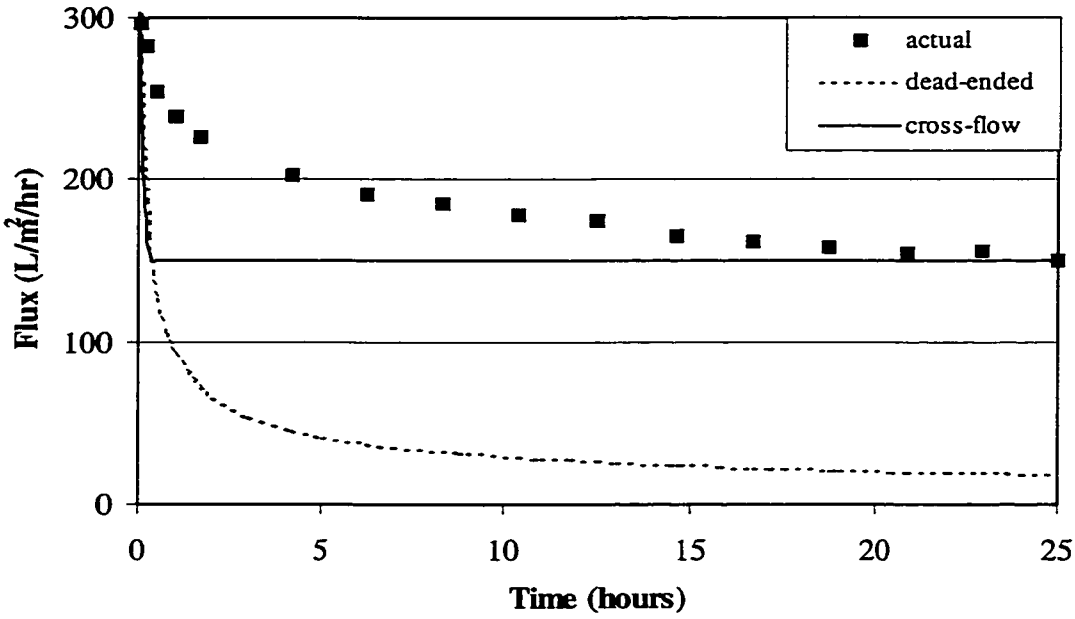

Figure 5.20: KOCH CM Membrane Treating New Bilge Water at 206KPa with No Backflush

To assess the impact of backflushing it is necessary to determine if the cake layer produced, during normal operation, is removed during backflushing. This can be examined by use of the equation 3.39, for cake layer removal, as developed in section 3.5. A limiting case for cake layer removal would exist when the backflush duration is very short in comparison with the normal operating cycle. In this situation a significant cake layer would accumulate, during the "long" operating cycle, and only a "short" backflushing time would exist to remove the cake layer. Accordingly, the limiting cases of cake layer removal conducted were;

a. for the CERAMEM LMA membrane, a 2.5 second backflush in a 120 second total cycle time, and

b. for the KOCH CM membranes, a 5 second backflush in a 120 second total cycle time.

For both membranes it is seen, from the theory, that the cake layer removal exceeds the cake layer buildup. (Appendix J provides sample calculations for the build up and removal of the gel layer. For example, for conditions of a 115 second operational cycle, followed by a 5 second backflush the following theoretical conditions would exist. For the CERAMEM LMA membrane a cake layer of approximately 1.06 microns would form and a cake layer as thick as 522 microns would be removed. For the KOCH CM membrane a cake layer of 4.16 microns would form and a cake layer as thick as 2,712 microns would be removed.)

To gain a better understanding of the impact of backflushing it is worthwhile to review the efficiency of backflushing, for varying degrees of backflushing, for the two membranes. Table 5.3 presents these results. Flux improvement is the ratio of the fluxes, for the various backflushed runs versus the non-backflushed run. For the CERAMEM LMA membrane this flux improvement was determined using the flux ratios in order to eliminate the impact of the continual irreversible membrane fouling. While for the KOCH CM membrane the flux improvement was determined using the fluxes from the various runs, since it did not experience irreversible fouling. These results are also presented graphically in Figures 5.21 and 5.22.

Table 5.3: Backflushing Flux Improvement

MEMBRANE	BACKFLUSH		FLUX IMPROVEMENT	
	Backflush Time per Cycle Time	Backflush Fraction $\left(\frac{backflush\ time}{cycle\ time}\right)$	Experimental	Theory
	(-)	(-)	(%)	(%)
CERAMEM LMA	0/120	0.000	0.0	0.0
	2.5/120	0.021	26.9 ± 3.1	100.0
	2.5/60	0.042	11.8 ± 1.4	96.3
	5/120	0.042	15.6 ± 1.8	95.7
	10/120	0.083	10.8 ± 1.3	87.2
KOCH CM	0/120	0.000	0.0	0.0
	5/120	0.042	14.3 ± 0.4	9.8
	5/90	0.056	13.0 ± 0.4	99.3
	5/60	0.083	15.7 ± 0.5	99.6
	5/45	0.111	8.0 ± 0.2	97.3
	5/30	0.167	2.3 ± 0.1	89.5

The obvious conclusion arrived at when reviewing Table 5.3 and Figures 5.21 and 5.22 is that the theory significantly overpredicts the impact that backflushing has upon membrane flux. The observed experimental results do not support the theory which predicts the complete removal of the cake layer. Therefore, the bilge water cake layer is not merely resting on the surface of the membranes, but is adhering to the membrane surface. Reviewing the theory (equations 3.29 and 3.30) shows that it does not incorporate membrane/cake layer interaction or backflushing pressure.

Additionally, it can be observed that the flux improvement drops off significantly faster, from the optimal degree of backflushing, than predicted. Therefore it would appear that

the positive impact of backflushing occurs very quickly, that a component of the cake layer is relatively easily removed. However, additional backflushing is less effective at removing the remaining cake layer. Therefore any additional positive benefits associated with backflushing are overtaken by the lost time for bilge water treatment. Figures 5.21 and 5.22 reveal the importance of keeping backflushing times as short as possible in order to maximize membrane operating time.

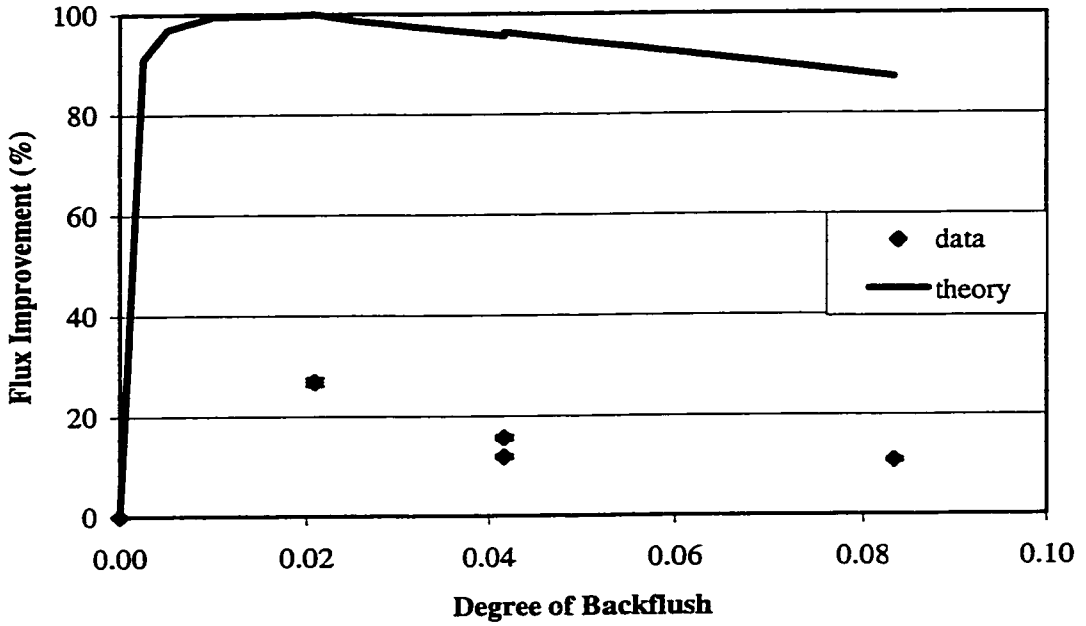

Figure 5.21: Flux Improvement versus Backflushing for CERAMEM LMA Membrane, New Bilge Water

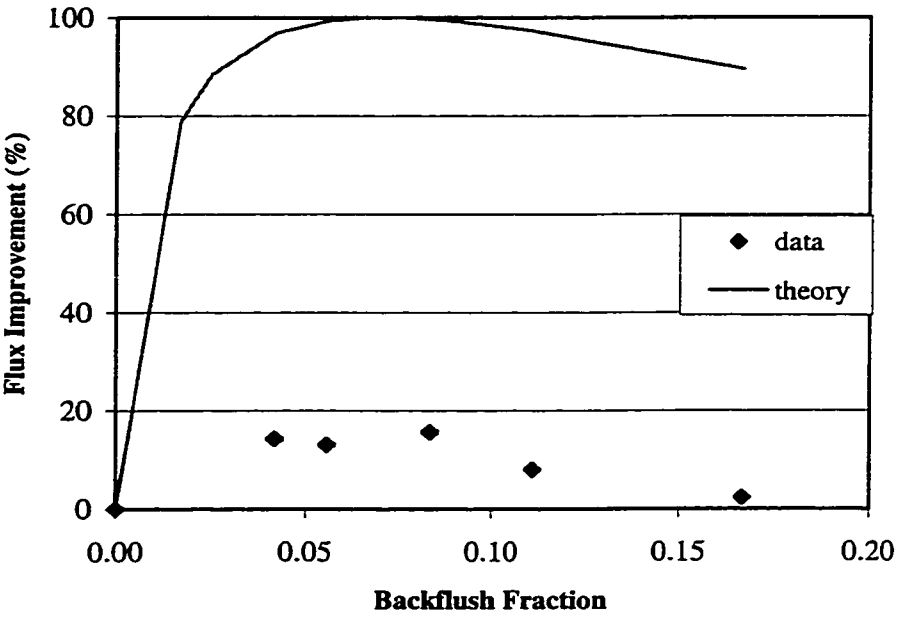

Figure 5.22: Flux Improvement versus Backflushing for KOCH CM Membrane, New Bilge Water

A better method to ensure the removal of the cake layer may be to increase the backflushing pressure. It should be noted that due to experimental setup the applied backflush differential pressure was quite low, no more than 5 psi (the backflush differential pressure being the backflush pressure less the transmembrane pressure).

The error associated with the experimental flux improvement values is due to the error carried throughout the calculations of these values. For the CERAMEM LMA membrane, due to the irreversible fouling it experienced, it utilized flux ratios to calculate its flux improvement. The percentage error associated with the flux ratios was approximately ± 1.24% therefore resulting in an error of ± 2.48% for the flux improvement values. Whereas the KOCH CM membrane used flux values to determine its flux improvement values and the error associated with these flux values was ± 0.62% and therefore the error associated with its flux improvement values was ± 1.24%.

5.2.5 Effect of Membrane Pre-Treatment

Reviewing the case of the used bilge water treatment with the KOCH CM membrane, Figure 5.23, it appears to disprove the above results as there does not appear to be any correlation between backflushing and flux. However, as stated earlier these experimental runs were conducted with a 100-micron pre-filter and this pre-filter appears to have performed some pre-treatment. In order to determine if the pre-filter provided any impact upon bilge water treatment Figure 5.24 shows the 24 hour flux values in the sequential order that the experimental runs were performed. As seen from this graph the flux rate continually increases, until the final run, for which the pre-filter was removed.

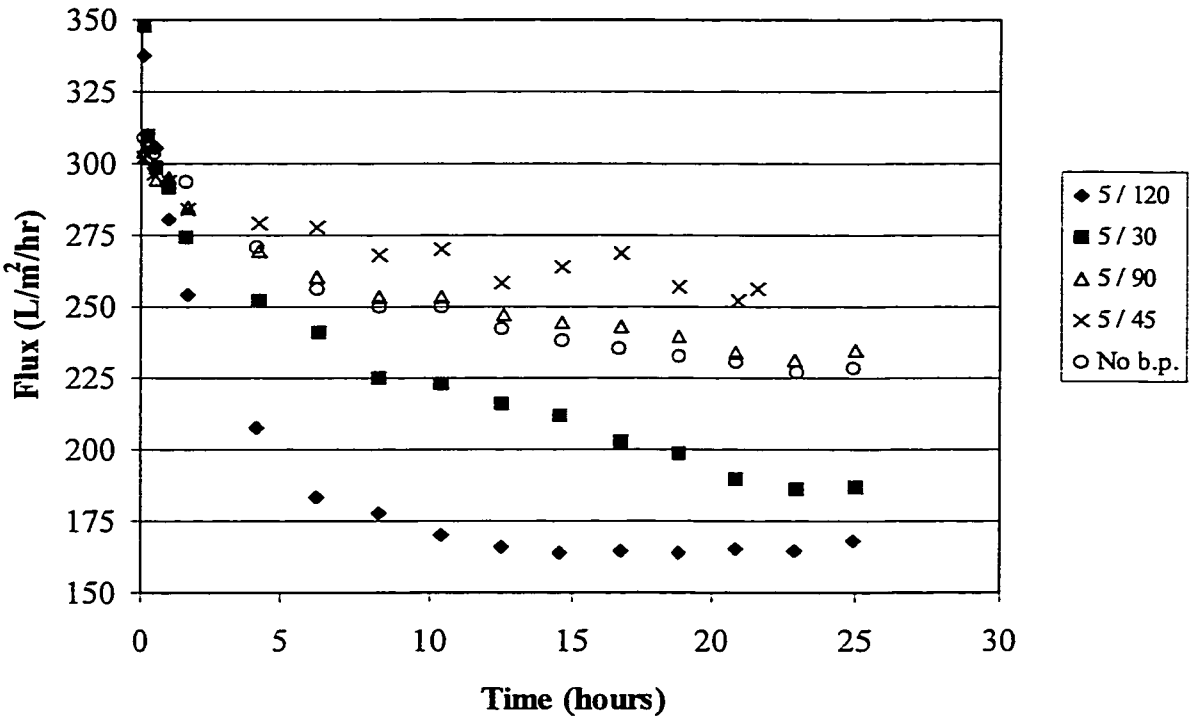

Figure 5.23: KOCH CM Membrane, Used Bilge Water, 206KPa, Varying Degrees of Backflushing

Additionally, the flux values are worth noting. The first experimental run, with used bilge water was the run using a 5/120 backflush. From Figure 5.23 it can be seen that this run produced a flux, after 24 hours of operation, of approximately 165 L/m^2/hour. This

compares to a flux value, after 24 hours of operation, of approximately 162 to 175 L/m^2/hour for various degrees of backflushing, for new bilge water. That is, this contradicts the results from the CERAMEM LMA membrane which showed a noticeable difference between new and used bilge water treatment using a 5/120 backflush (Figure 5.14).

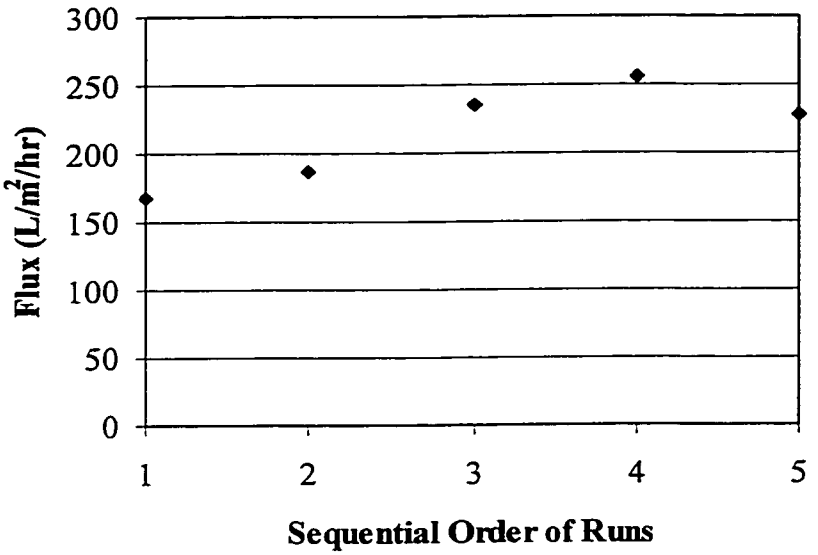

Figure 5.24: KOCH CM Membrane, 206KPa,
Sequential Order of Experimental Used Bilge Water Runs

However, Figure 5.24 reveals that the flux continues to increase from run to run; until the pre-filter was removed for the final run. After four experimental runs, approximately 100 hours of operation, the flux rate had risen from 165 L/m^2/hour to over 250 L/m^2/hour. Therefore it can be seen that the pre-filtration provided an extremely effective means of enhancing the membrane flux. With the exception of the backflushing none of the operational parameters were altered during these runs.

The results of a visual inspection of the pre-filter revealed that it was heavily fouled with oil and it was black in colour, in contrast to its initial white colour. Additionally, when

the pre-filter was drained it had collected free oil in its inner chamber; the bilge water flowed into the inside of the filter and then through the filter. Therefore, it appears that the pre-filter provided the oil emulsions with a coalescing medium, causing an increased membrane flux as the oil and particulate content of the bilge water were reduced.

5.2.6 Permeate Quality

Tables 5.4 and 5.5 provide the oil content values of the permeate, for the various experimental runs. As seen from these tables the permeate quality appears to be consistent and independent of the operational parameters and bilge water conditions that were altered, such as transmembrane pressure, degree of backflushing, other operational parameters or the treatment of bilge water containing either new or used lubricating oil.

Table 5.4: CERAMEM LMA Membrane Permeate Quality
(Pore Radius of 0.005 microns)

Pressure (KPa)	**Backflush - backflush per total cycle time (sec/sec)**	**Bilge Water**	**Oil Content (ppm)**
206	5/120	Used oil	19.8
206	10/120	Used oil	16.2
206	2.5/120	Used oil	46.0
206	5/120	Used oil	33.3
206	5/120	Used oil	1.7
220	5/120	New oil	33.5
220	10/120	New oil	29.7
220	2.5/120	New oil	14.4
220	2.5/60	New oil	23.7
220	5/120	New oil	4.3
206	5/120	New oil	23.1
220	No backflush	New oil	55.0
206	No backflush	New oil	9.8

Table 5.5: KOCH CM Membrane Permeate Quality (MWCO of 50,000 Daltons)

Pressure (KPa)	Backflush - backflush per total cycle time (sec/sec)	Bilge Water	Oil Content (ppm)
206	5/30	New oil	19.1
206	5/60	New oil	14.2
206	5/90	New oil	14.8
206	5/45	New oil	19.3
206	No backflush	New oil	14.1
206	5/120	New oil	8.9
186	5/120	New oil	12.9
206	5/30	Used oil	22.6
206	5/90	Used oil	28.7
206	5/45	Used oil	12.1
206	5/60	Used oil	19.4
206	No backflush	Used oil	8.8
206	No backflush	Used oil	19.8
206	5/120	Used oil	20.6

The average permeate oil content, for the CERAMEM LMA and KOCH CM membranes, were 23.9 ppm and 16.8 ppm, respectively.

Regarding the permeate oil content it is important to quantify the method used since "oils and greases" are defined by the method used for their determination (Greenberg et al., 1992). Unfortunately, the Canada Shipping Act does not provide a clear definition of "oil". Discussions with various Canadian naval authorities have confirmed that the new membrane based Oily Water Separator (OWS) System and the existing SAREX Coalescing OWS System have both successfully been certified by Transport Canada and International Maritime Organization. The new membrane based OWS being acquired by the Canadian Navy uses virtually the same membrane as the KOCH CM membrane that was tested; the same material, configuration and MWCO. (Appendix K provides details

of the Transport Canada certification for the new OWS – HYDROMEM - system being installed onboard Canadian Navy vessels.) In accordance with EPA Method 1664 the solid phase extraction method used provides a determination of hexane extractable compounds present and it is believed that oils, in the context of the Canada Shipping Act, are a subset of hexane extractable compounds. This is believed because oil emulsions are not expected to have a radius smaller than 0.0175 microns (Lipp et al., 1988) and the nominal pore sizes of the membranes (CERAMEM LMA – 0.005 microns; KOCH CM – 0.0058 microns) used are almost one complete order of magnitude smaller than the smallest possible oil emulsion.

6.0 CONCLUSIONS

The research conducted on the various flat sheet membranes and membrane modules provided insight into the impact of both the bilge water composition and system operational parameters on the membrane treatment of bilge water.

6.1 Effect of Bilge Water Composition

Membrane flux was lower when treating used bilge water as compared to treating new bilge water. The likely causes of this reduced flux were identified as the presence of fine solute particles, in addition to the oil emulsion, in used lubricating oil. Used lubricating oil was also found to produce a more complex and stable emulsion than new lubricating oil.

There appeared to be two critically sized particles in used bilge water, with the smaller particle being retained by membranes with a molecular weight cut-off no greater than 8,000 Daltons.

The quantity and type of surfactants present in the bilge water also have a substantial impact on a bilge water's oil concentration and its subsequent membrane treatment.

6.2 Oil Droplet Pore Plugging

Microfiltration membranes may be prone to oil droplet pore plugging due to the combination of transmembrane pressures utilized and pore sizes employed causing oil droplets to blind the pores of microfilters. However, due to the smaller pore sizes employed by ultrafiltration this phenomenon of oil droplet pore plugging should not be problematic for ultrafiltration membranes.

6.3 Flux Decline Due to Irreversible Fouling

In this work the ceramic membrane appeared to suffer from greater fouling than the polymeric membrane. The exact cause of this flux decline is uncertain. Among the possible causes are the membrane material/bilge water interaction or the cross-flow velocity employed. The ceramic membrane was used with a significantly lower cross-flow velocity.

6.4 Effect of Backflushing

Backflushing was significantly less effective than theoretically predicted, but it did provide a marginal improvement in membrane flux capacity. When utilizing backflushing it must be optimized such that the relative duration of the backflush, in comparison with the operating cycle, does not neutralize its effectiveness.

6.5 Effect of Membrane Pre-Treatment

Membrane pre-treatment, by means of a bag filter, provided a significant degree of flux improvement. The bag filter appeared to function as an adsorption and/or coalescence media for the oil and/or other bilge water contaminants.

6.6 Permeate Quality

The CERAMEM LMA and KOCH CM membranes produced permeate qualities averaging approximately 24-ppm and 17-ppm of oil. While this level of oil exceeds the 15-ppm requirement it must be noted that oil and grease is defined by the method used to determine oil and grease. The method employed was solid phase extraction, which is a modification to the EPA 1664 method and it is suspected that this method retains more oil than the hexane liquid extraction method.

7.0 RECOMMENDATIONS

A number of recommendations can be provided to enhance a shipborne system and a significant amount of follow on research could be conducted to enhance the system.

1. Whenever possible turbulent, rather than laminar, membrane cross-flow should be employed.

2. Pre-filtration should be employed as it provides a significant degree of flux enhancement. However, its necessity for frequent changes and therefore increased onboard stores is unknown. Further investigation could be undertaken to optimize the filtration size and media.

3. Further work into the characterization of bilge water and the impact that particular bilge water components have on membrane flux would also be useful. For example, the specific oil/membrane interaction could have significant impact on membrane fouling and subsequent in-situ flux enhancement techniques and/or cleaning regimes.

4. While backflushing was not as effective as theoretically predicted increasing its flux enhancement capability may be worth additional investigation. Specifically, the impact of increasing backflushing pressure should be investigated. Another aspect may be the optimization of the duration of the backflushing cycle.

8.0 REFERENCES

American Society for Testing and Materials, "1990: Annual Book of ASTM Standards, Section 11: Water and Environmental Technology", Volume 11.02, Standards D5090-90 and D1141-90 (1990).

Beney, P., Breuer, G., Jacobs, G., Larabee-Zierath, D., Mollenhauer, P., Norton, K. and Wichman, M., "Review, Evaluation, and Application of Solid Phase Extraction Methods", Hotline, Volume 35, Number 6, 1-5 (Dec. 1996).

Bil'dyukevich, A. and Dmitrieva, S., "Membrane Separation of Water-Oil Emulsions", Soviet Journal of Water Chemistry and Technology (Khimiya i Tekhnologiya Vody), Volume 11, Number 7, 641-643 (1989).

Bodzek, M. and Konieczny, K., "Treatment of Oil-Emulsion Wastewater with Ceramic Micro and Ultrafiltration Membranes:, Vom Wasser, Number 87, 207-221 (1996).

Cheryan, M., in "Ultrafiltration Handbook", Technomic Publishing Company, Lancaster, Pennsylvania, U.S.A. (1986), pp. 250-256.

Davis, R.., "Theory for Crossflow Mircofiltration" in "Membrane Handbook", W.S. Winston Ho and K.K. Sirkar, Eds., Van Nostrand Reinhold (1992), pp. 480-505.

Department of National Defence (DND), "Maritime Command Orders (MARCORDs)", MARCORD 43-1 Halifax, Canada (1999).

Department of National Defence (DND), "Technical Statement of Requirements for an Oily Water Separator System", Ottawa, Canada (July 1996).

Eykamp, W., "Mircofiltration and Ultrafiltration" in "Membrane Separation Technology. Principles and Applications", R.D. Noble and S.A. Stern, Eds., Elsevier Science B.V. (1995), pp. 1-43.

Ficheux, M., Bonakdar, L., Leal-Calderon, F. and Bibette, J., "Some Stability Criteria for Double Emulsions", Langmuir, Volume 14, 2702-2706 (1998).

Greenberg, A., Clesceri, L., Eaton, A., "18th Edition of Standard Methods For The Examination of Water and Wastewater", American Public Health Association (1992), pp. 5-24 to 5-29.

International Maritime Organization – United Nations, "International Convention for the Prevention of Pollution from Ships, 1973, as modified by the Protocol of 1978 relating thereto", IMO, London, England, 1999.

Koltuniewicz, A., Field, R. and Arnot, T., "Cross-Flow and Dead-End Microfiltration of Oily-Water Emulsion. Part I: Experimental Study and Analysis of Flux Decline", Journal of Membrane Science, Number 102, 193-207 (1995).

Lipp, P., Lee, C., Fane, A. and Fell, C., "A Fundamental Study of the Ultrafiltration of Oil-Water Emulsions", Journal of Membrane Science, Volume 36, 161-177 (1988).

Matsurra, T., "Synthetic Memranes and Membrane Separation Processes", CRC Press (1994), pp. 137-140.

Mulder, M., "Polarization Phenomena and Membrane Fouling" in "Membrane Separation Technology. Principles and Applications", R.D. Noble and S.A. Stern, Eds., Elsevier Science B.V. (1995), pp. 45-83.

NATO, "Proceedings from Special Working Group 12 Symposium on Oily Water and Membrane Technology", Brussels, Belgium (April 1994).

NATO, "Report of Special Working Group 12 Workshop on Oily Waste Water Treatment and Monitoring Systems", Hamilton, Canada (September 1999).

Nazzal, F. and Wiesner, M., "Microfiltration of Oil-in-Water Emulsions", Water Environ. Res., Number 68, 1187-1191 (November/December 1996).

Porter, M., "Handbook of Industrial Membrane Applications", Noyes Publications, Park Ridge, New Jersey, U.S.A. (1990).

Resera, A., "Oily Water Pollution Abatement Systems – Course Notes: EO 412.08", Naval Engineering Test Establishment (NETE), LaSalle, Canada (November 1992).

Resera, A., "Bilge Water Characterization Study and Bilge Fluid Production Estimates", NETE – Project Number IT1082, Report Number 14/95, LaSalle, Canada (June 1995).

Sawyer, C., McCarty, P. and Parkin, G., "Chemistry for Environmental Engineering – Fourth Edition", McGraw-Hill Incorporated, 1994, pages 241-245, 602-607.

Sethi, S. and Wiesner, M., "Performance and Cost Modelling of Ultrafiltration", Journal of Environmental Engineering, Volume 121, Number 12, 874-883 (1995).

Simms, K., "Oil and Suspended Solids Removal", in "Produced Water Treatment Design Manual", Wastewater Technology Centre, Burlington, Canada (1994), Chapter 3.

Stone, J., "EPA Method 1664: Waiting for Godot", Environmental Express (June 1995).

Transport Canada, "Canada Shipping Act", Ottawa, Canada, 1999.

Transport Canada, "Arctic Waters Pollution Prevention Act", Ottawa, Canada, 1999.

Tremblay, A., "Finely Porous Models and Radially Averaged Friction Factors", Journal of Applied Polymer Science, Volume 45, 159-166 (1992).

Anonymous, "Bilges of Discontent", Marine Engineering Review, 33-34 (May 1997).

APPENDIX A:

PARTICLE SIZE VERSUS CAKE LAYER DIFFUSIVITY

The following presents the calculations associated with the development of the data for Figure 3.2: Effect of Particle Size on Cake Layer Diffusivity.

In order to determine the data points, for this figure, equations 3.8 through 3.13 were utilized. These equations are:

$$D_{total} = D_{brn} + D_{shear}$$

$$D_{brn} = \frac{kT}{6\pi\mu a_p}$$

$$D_{shear} = \dot{\gamma} a_p^2 \kappa$$

$$\dot{\gamma} = \frac{\tau_w}{\mu\eta(\phi)}$$

$$\tau_w = \frac{4U\mu\eta(\phi_b)}{r_l - \delta}$$

$$\eta(\phi) = \left(1 + \frac{1.5\phi}{1 - \phi/0.58}\right)^2$$

$$\kappa = 0.33\phi^2\left(1 + 0.5e^{8.8\phi}\right)$$

where: $D_{total} = (Total)\ Diffusivity\ \left[m^2/s\right]$

$D_{brn} = Brownian\ Duffisivity\ \left[m^2/s\right]$

$D_{shear} = Shear\ Duffisivity\ \left[m^2/s\right]$

$k = Boltzmann\ Constant = 1.38 * 10^{-23}\left[kg * m^2/s^2/K\right]$

$T = Temperature\ [K]$

$\mu = viscosity\ [Pa * s]$

$a_p = solute\ particle\ radius\ [m]$

$\dot{\gamma} = local\ shear\ rate\ \left[s^{-1}\right]$

$\kappa = coefficient\ of\ induced\ diffusivity\ [-]$

$\tau_w = wall\ shear\ stress\ [Pa]$

$\eta(\phi) = relative\ viscosity\ [-]$

$\phi = solute\ volume\ fraction\ [-]$

$U = cross-flow\ velocity\ \left[m/s\right]$

$r_t = membrane\ channel\ radius\ [m]$

$\delta = cake\ layer\ thickness\ [m]$

Table A-1 provides the diffusivity results for a range of particle sizes, using the following assumptions (similar to the assumptions utilized by Sethi and Wiesner in their article "Performance and Cost Modelling of Ultrafiltration", 1995);

a. cross-flow velocity of 0.9 m/s,
b. membrane channel (hollow fibre or tube) radius of 0.001m,
c. cake layer thickness of 40 microns ($4*10^{-5}$ m),
d. temperature of 25°C,
e. bulk solute volume fraction of 200 ppm,
f. an average solute volume fraction of 0.29 at the membrane surface, and
g. bulk fluid viscosity of $8.91*10^{-4}$ Pa*s (i.e. viscosity of water at 25°C).

The following are a set of sample calculations, to determine the diffusivity for a particle having a radius of 0.65 microns, with the above mentioned conditions (assumptions).

$$Bulk\ relative\ viscosity = \eta(\phi_b) = \left(1 + \frac{1.5*(200/10^6)}{1-(200/10^6)/0.58}\right)^2 = 1.0006$$

$$\eta(\phi) = \left(1 + \frac{1.5*0.29}{1-0.29/0.58}\right)^2 = 3.50$$

$$\kappa = 0.33*0.29^2\left(1+0.5e^{8.8*0.29}\right) = 0.2058$$

$$\tau_w = \frac{4 * 0.90 * \left(8.91 * 10^{-4}\right) * 1.006}{0.0005 - 0.00004} = 6.98\ Pa$$

$$\dot{\gamma} = \frac{6.98}{\left(8.91 * 10^{-4}\right) * 3.50} = 2239\ s^{-1}$$

$$D_{shear} = 2239 * (0.65 * 10^{-6})^2 * 0.2058 = 1.95 * 10^{-12}\ m^2/s$$

$$D_{brn} = \frac{\left(1.38 * 10^{-23}\right) * 298}{6 * \pi * \left(8.91 * 10^{-4}\right) * \left(0.65 * 10^{-6}\right)} = 3.77 * 10^{-12}\ m^2/s$$

$$D_{total} = \left(1.95 * 10^{-12}\right) + \left(3.77 * 10^{-12}\right) = 5.72 * 10^{-12}\ m^2/s$$

Table A-1: Particle Radius versus Diffusivity

Particle Radius (microns)	rel. viscosity (-)	wall shear (Pa)	local shear rate (s^{-1})	Shear Diffusivity (m^2/s)	Browian Diffusivity (m^2/s)	**Total Diffusivity** (m^2/s)
0.001	3.50	6.98	2.24E+03	4.61E-16	2.45E-10	**2.45E-10**
0.005	3.50	6.98	2.24E+03	1.15E-14	4.90E-11	**4.90E-11**
0.010	3.50	6.98	2.24E+03	4.61E-14	2.45E-11	**2.45E-11**
0.020	3.50	6.98	2.24E+03	1.84E-13	1.22E-11	**1.24E-11**
0.030	3.50	6.98	2.24E+03	4.15E-13	8.17E-12	**8.58E-12**
0.040	3.50	6.98	2.24E+03	7.37E-13	6.12E-12	**6.86E-12**
0.050	3.50	6.98	2.24E+03	1.15E-12	4.90E-12	**6.05E-12**
0.060	3.50	6.98	2.24E+03	1.66E-12	4.08E-12	**5.74E-12**
0.065	3.50	6.98	2.24E+03	1.95E-12	3.77E-12	**5.72E-12**
0.070	3.50	6.98	2.24E+03	2.26E-12	3.50E-12	**5.76E-12**
0.080	3.50	6.98	2.24E+03	2.95E-12	3.06E-12	**6.01E-12**
0.090	3.50	6.98	2.24E+03	3.73E-12	2.72E-12	**6.46E-12**
0.100	3.50	6.98	2.24E+03	4.61E-12	2.45E-12	**7.06E-12**
0.120	3.50	6.98	2.24E+03	6.64E-12	2.04E-12	**8.68E-12**
0.140	3.50	6.98	2.24E+03	9.03E-12	1.75E-12	**1.08E-11**
0.160	3.50	6.98	2.24E+03	1.18E-11	1.53E-12	**1.33E-11**
0.180	3.50	6.98	2.24E+03	1.49E-11	1.36E-12	**1.63E-11**
0.200	3.50	6.98	2.24E+03	1.84E-11	1.22E-12	**1.97E-11**
0.225	3.50	6.98	2.24E+03	2.33E-11	1.09E-12	**2.44E-11**
0.250	3.50	6.98	2.24E+03	2.88E-11	9.80E-13	**2.98E-11**
0.300	3.50	6.98	2.24E+03	4.15E-11	8.17E-13	**4.23E-11**
0.400	3.50	6.98	2.24E+03	7.37E-11	6.12E-13	**7.44E-11**
0.500	3.50	6.98	2.24E+03	1.15E-10	4.90E-13	**1.16E-10**
1.000	3.50	6.98	2.24E+03	4.61E-10	2.45E-13	**4.61E-10**
5.000	3.50	6.98	2.24E+03	1.15E-08	4.90E-14	**1.15E-08**
10.000	3.50	6.98	2.24E+03	4.61E-08	2.45E-14	**4.61E-08**

APPENDIX B:

OIL DROPLET PORE PLUGGING ASSESSMENT

The following presents the calculations associated with the development of the data for Figure 3.4: Oil Droplet Pore Plugging.

In order to determine the data points, for this figure, equation 3.19 was utilized. This equation details the relationship between the critical system pressure required to force an oil droplet into a pore and the size of the oil droplet and is;

$$P_{crit} = \left(\frac{2\sigma\cos\theta}{r_{pore}}\right)\left[1 - \frac{2 + 3\cos\theta - \cos^3\theta}{4\left(\frac{r_{oil}}{r_{pore}}\right)^3\cos^3\theta} - \left(2 + 3\sin\theta - 3\sin^3\theta\right)\right]^{0.33},$$

where: P_{crit} = critical capillary pressure,

σ = oil-water interfacial tension,

θ = contact angle of the oil droplet to the membrane pore,

r_{oil} = oil droplet radius, and

r_{pore} = membrane pore radius.

It is assumed that the oil-water interfacial tension is 52 dynes/cm and the oil droplet/membrane pore contact angle is 25° (Nazzal and Wiesner, 1996). Additionally, as identified in section 2.3.2, the smallest size of oil emulsions that is expected to be present will have a radius of 0.0175 microns (Lipp et al, 1988).

$$\sigma = 52\frac{dyne}{cm} = 52\frac{dyne}{cm} * \frac{10^{-5}N}{1\,dyne} * \frac{100cm}{1m} = 0.052\frac{N}{m}$$

Therefore, based upon these variables, the data presented in Figure 3.4 is presented in Table B-1.

Table B-1: Membrane Pore Size vs. Critical Capillary Pressure

Membrane Pore Radius (microns)	Critical Pressure (Pa)	(atm)
0.001	8.83E+07	871.92
0.0025	3.18E+07	313.61
0.004	1.76E+07	173.95
0.006	9.73E+06	96.09
0.008	5.74E+06	56.69
0.01	3.28E+06	32.33
0.011	2.34E+06	23.08
0.012	1.52E+06	15.02
0.014	1.03E+05	1.02
0.0141	3.64E+04	0.36
0.01413	1.64E+04	0.16
0.01415	3.10E+03	0.03

The following are a set of sample calculations, for a membrane pore radius of 0.01 micron and the above stated assumptions.

$$\frac{2\sigma\cos\theta}{r_{pore}} = \frac{2(0.052)(\cos 25)}{10^{-8}}$$

$$= 9.43*10^{6}\ \text{Pa}$$

$$\left[1 - \frac{2 + 3\cos\theta - \cos^3\theta}{4\left(\frac{r_{oil}}{r_{pore}}\right)^3 \cos^3\theta} - \left(2 + 3\sin\theta - 3\sin^3\theta\right)\right]^{0.33} =$$

$$= \left[1 - \frac{2 + 3*\cos 25 - \cos^3 25}{4\left(\frac{1.75*10^{-8}}{10^{-8}}\right)^3 \cos^3 25} - \left(2 + 3*\sin 25 - 3*\sin^3 25\right)\right] = 0.3475$$

Therefore: $\mathbf{P_{crit}} = (9.43*10^{6}) * (0.3475) = 3.28*10^{6}\ \text{Pa} = \mathbf{32.33\ atm}$

APPENDIX C:

Detailed Derivation of the Average and Overall Flux Equations When Backflushing is Utilized

In section 3.5 equations, 3.27 through 3.30, identifying the overall (J_{bf}) and average (J_{avg}) flux, produced by a membrane module, when backflushing is used were identified. The following appendix provides the derivation of these equations.

As shown in sections 3.3 and 3.5 the following equations representing permeate flux, when backflushing is applied are applicable.

Flux as a function of time (with or without backflushing) is,

$$J(t) = \frac{J_{PWP}}{\left(1 + \frac{2t}{\tau_c}\right)^{0.5}}. \tag{3.21}$$

In the above equation the membrane flux decline constant (τ_c) and the pure water permeate flux (J_{PWP}) are independent of time.

The overall membrane flux (J_{bf}) is,

$$J_{bf} = J_{avg}\left(\frac{t_{op}}{t_{total}}\right), \tag{3.24}$$

where J_{avg} is the average flux during the operational cycle, not including the "lost" operational time associated with backflushing, t_{op} is the operational time and t_{total} is the operational time plus the backflushing time.

The average membrane flux during which the membrane treats bilge water is,

$$J_{avg} = \frac{1}{t_{total}} \int_0^{t_{total}} J(t)dt, \qquad \text{where } t_{op} < t_{ss}, \tag{3.25}$$

$$J_{avg} = \frac{1}{t_{total}}\left[\int_0^{t_{ss}} J(t)dt + (t_{total} - t_{ss})J(t_{ss})\right] \qquad \text{where } t_{op} > t_{ss}, \tag{3.26}$$

Where t_{ss} is the time at which the membrane's cake layer has achieved its steady state conditions.

Substituting these equations for the average membrane flux into the equation (3.24) for the overall flux provides,

$$J_{bf} = \left(\frac{t_{op}}{t_{total}^2}\right)\int_0^{t_{total}} J(t)dt, \qquad \text{where } t_{op} < t_{ss},$$

$$J_{bf} = \left(\frac{t_{op}}{t_{total}^2}\right)\left[\int_0^{t_{ss}} J(t)dt + (t_{total} - t_{ss})J(t_{ss})\right], \qquad \text{where } t_{op} > t_{ss}.$$

In all of the above equations for J_{avg} and J_{bf} the integral of $J(t)$ must be solved, which is,

$$\int J(t)dt = \int \frac{J_{PWP}}{\sqrt{1+\frac{2t}{\tau_c}}}dt = J_{PWP}\int \frac{dt}{\sqrt{1+\frac{2t}{\tau_c}}}.$$

As identified in the Handbook of Chemistry and Physics the solution for the above integral is,

$$\int \frac{dx}{\sqrt{a+bx}} = \frac{2\sqrt{a+bx}}{b}.$$

Therefore for the integral of $J(t)$, $a = 1$ and $b = \frac{2}{\tau_c}$ and the solution of this integral is,

$$\int J(t)dt = 2J_{PWP}\frac{\sqrt{1+\frac{2t}{\tau_c}}}{2/\tau_c} = J_{PWP}\tau_c\sqrt{1+\frac{2t}{\tau_c}}.$$

Substituting this value of the integral of *J(t)* into the expressions for the average and overall flux gives:

When the operational time is less than or equal to the time taken for the cake layer to achieve its steady state are,

$$J_{avg} = \left(\frac{1}{t_{total}}\right)\int_0^{t_{total}} J(t)dt$$

$$= \left(\frac{1}{t_{total}}\right)\left[J_{PWP}\tau_c\sqrt{1+\frac{2t_{total}}{\tau_c}} - J_{PWP}\tau_c\sqrt{1+\frac{2*0}{\tau_c}}\right]$$

$$J_{avg} = \left(\frac{J_{PWP}\tau_c}{t_{total}}\right)\left[\sqrt{1+\frac{2t_{total}}{\tau_c}} - 1\right] \qquad \text{where } t_{op} < t_{ss} \qquad (3.27)$$

$$J_{bf} = \left(\frac{t_{op}}{t_{total}^2}\right)\int_0^{t_{total}} J(t)dt$$

$$J_{bf} = \left(\frac{J_{PWP}\tau_c t_{op}}{t_{total}^2}\right)\left[\sqrt{1+\frac{2t_{total}}{\tau_c}} - 1\right] \qquad \text{where } t_{op} < t_{ss} \qquad (3.29)$$

When the operational time is greater than or equal to the time taken for the cake layer to achieve its steady state are,

$$J_{avg} = \left(\frac{1}{t_{total}}\right)\left[\int_0^{t_{ss}} J(t)dt + (t_{total} - t_{ss})J(t_{ss})\right]$$

$$= \left(\frac{1}{t_{total}}\right)\left[\left(J_{PWP}\tau_c\sqrt{1+\frac{2t_{ss}}{\tau_c}} - J_{PWP}\tau_c\sqrt{1+\frac{2*0}{\tau_c}}\right) + (t_{total} - t_{ss})J(t_{ss})\right]$$

$$J_{avg} = \left(\frac{1}{t_{total}}\right)\left[J_{PWP}\tau_C\left(\sqrt{1+\frac{2t_{ss}}{\tau_c}} - 1\right) + (t_{total} - t_{ss})J(t_{ss})\right] \qquad \text{where } t_{op} > t_{ss} \qquad (3.28)$$

$$J_{bf} = \left(\frac{t_{op}}{t_{total}^2}\right)\left[\int_0^{t_{ss}} J(t)dt + (t_{total} - t_{ss})J(t_{ss})\right]$$

$$J_{bf} = \left(\frac{t_{op}}{t_{total}^2}\right)\left[J_{PWP}\tau_c\left(\sqrt{1+\frac{2t_{ss}}{\tau_c}} - 1\right) + (t_{total} + t_{ss})J(t_{ss})\right] \qquad \text{where } t_{op} > t_{ss} \qquad (3.30)$$

APPENDIX D:

FLAT SHEET MEMBRANE RAW DATA

Flat Sheet Membrane Experimental Runs

The following is the raw data for the various flat sheet membrane experimental runs.

As described in section 4.1 the flat sheet membrane testing used an autosampler to collect permeate for a given time duration. Unfortunately, due to intermittent mechanical difficulties with the autosampler, some of the sampling containers experienced multiple samples and therefore had to be excluded from the tabulated data. All experimental runs were conducted for a total duration of 25 hours.

The raw data collected from the various membrane flat sheet experimental runs was the volume of permeate collected over a given sample time in a known time interval, from the start of the experimental run. To determine a temperature corrected flux and volumetric reduction the volume of permeate collected was converted to a flux by dividing the collected volume by the sampling time and the membrane (i.e. stir cell) area. For the flat sheet testing two stir cells were used. They had the following dimensions:

Small Stir Cell:

Inside Diameter = 0.0338m

Cross Sectional Area = $8.97*10^{-4}$ m^2

Height = 0.080m

Volume = $71.8*10^{-6}$ m^3 = 71.8mL

Large Stir Cell:

Inside Diameter = 0.07025m

Cross Sectional Area = $3.88*10^{-3}$ m^2

Height = 0.115m

Volume = $445.7*10^{-6}$ m^3 = 445.7mL

To standardize all the flux they were corrected to 25°C in accordance with ASTM standard D5090-90: Standardizing Ultrafiltration Permeate Flow Performance. The temperature correction is:

$$Flux\ at\ 25^{\circ}C = (Flux\ @\ Temp.)* \left[1 + 0.03(25^{\circ}C - Temp.)\right]$$

The volumetric reduction was determined as the ratio of the total permeate volume per the total amount of bilge water treated in the stir cell, at a given time. As described in section 4 the stir cell was fed with bilge water, but no bilge water left the stir cell as the operational pressure did not exceed the pressure relief valve setting. Accordingly, once the stir cell filled with bilge water, the input of additional bilge water equaled the membrane's permeate flux. Therefore, volumetric reduction can be defined as (equation 5.1):

$$VR = \frac{Total\ Permeate\ Volume\ at\ a\ Given\ Time}{Stir\ Cell\ Volume + Total\ Permeate\ Volume\ at\ a\ Given\ Time}$$

1. OSMONICS GN Membrane MWCO = 10,000 Daltons

Solution: Bilge Water, prepared in accordance with the method described in section 4.3. For this experimental run the bilge water was prepared using used diesel engine lubricating oil, rather than new diesel engine lubricating oil.

Pressure: 345 KPa (50 psig)

Stir Cell: Small

Sample Time: 59 minutes

Date: 27 April 1998

Temperature: Starting – 23.2°C

Ending – 23.2°C

Table D-1: OSMONICS GN Experimental Data, dated 27 April 1998

Time (start - end of sample) (hour)	Permeate (mL)	Flux ($L/m^2/hr$)	Estimated Temperature (°C)	Flux (at 25°C) ($L/m^2/hr$)	Volumetric Reduction (-)
0 – 1	6.493	7.36	23.2	7.76	0.084
1 – 2	4.752	5.39	23.2	5.68	0.185
3 – 4	3.349	3.80	23.2	4.00	0.215
4 – 5	3.001	3.40	23.2	3.58	0.240
5 – 7	2.794	3.17	23.2	3.34	0.283
7 – 9	2.002	2.27	23.2	2.39	0.311
9 – 11	2.292	2.60	23.2	2.74	0.341
11 – 13	1.979	2.24	23.2	2.36	0.364
13 – 15	1.903	2.16	23.2	2.27	0.385
15 – 17	1.867	2.12	23.2	2.23	0.405
17 – 19	1.916	2.17	23.2	2.29	0.423
19 – 21	1.835	2.08	23.2	2.19	0.440
21 – 23	1.808	2.05	23.2	2.16	0.456
23 – 25	1.750	1.98	23.2	2.09	0.470

Sample Calculations:

The following sample calculations are representative for all of the flat sheet membrane data and are provided here to identify how the flat sheet membrane data, in section 5.1, was obtained. For all of the flat sheet membrane experimental results the true raw data was the sample time and permeate volume, as provided in the above table. From this raw data the flux, corrected to 25°C, and the volumetric reduction were determined.

The following is a sample calculation for the first data point (i.e. data associated with the 0-1 hour sample) of the above tabulated data.

Flux

$$\text{Flux} = \frac{\textit{permeate volume}}{\textit{membrane (stir cell) area / sample time}}$$

This experimental run was conducted with the small stir cell; i.e. the membrane area associated with the small stir cell is $8.97*10^{-4}$ m^2.

$$= \frac{6.493mL}{8.97*10^{-4}\ m^2 \Big/ \left[59\ \text{min}*\left(\frac{1\ hr}{60\ \text{min}}\right)\right]}$$

$$= 7.36\ \text{L/m}^2\text{/hr} \quad \text{at } 23.2^\circ\text{C}$$

The temperature for the first data point, in the 0 –1 hour time interval, was determined by:

$$= \textit{starting temp.} + \frac{\textit{time from the start of the run}}{\textit{total run time}} * \textit{temp. gain}$$

$$= 23.2^\circ C + \frac{0.5\ \textit{hours}}{25\ \textit{hours}} * (23.2 - 23.2)^\circ C$$

$$= 23.2^\circ C$$

The standardized flux, corrected to 25°C, was determined in accordance with ASTM standard D5090-90:

$$\text{Flux, corrected to } 25°C = 7.36\ L/m^2/hr * (1 + 0.03(25.0°C - 23.2°C))$$
$$= 7.76\ L/m^2/hr$$

Volumetric Reduction

In accordance with equation 5.1 volumetric reduction (VR) is:

$$VR = \frac{Total\ Permeate\ volume\ at\ a\ given\ time}{Stir\ Cell\ Volume + Total\ Permeate\ volume\ at\ a\ given\ time}$$

Total Permeate Volume at a given time =

$$Permeate\ Throughput * Collection\ Time + Previous\ amount\ of\ permeate\ collected$$
$$= \frac{6.493\ mL}{59\ minutes} * 60\ minutes + 0mL$$
$$= 6.603mL$$

$$VR = \frac{6.603mL}{71.8mL + 6.603mL}$$

$$VR = 0.0842$$

Solution: Bilge Water, prepared in accordance with the method described in section 4.3. For this experimental run the bilge water was prepared using used diesel engine lubricating oil, rather than new diesel engine lubricating oil.

Pressure: 345 KPa (50 psig)

Stir Cell: Large

Sample Time: 30 minutes

Date: 05 June 1998

Temperature: Starting – 24.5°C

Ending – 26.2°C

Table D-2: OSMONICS GN Experimental Data, dated 05 June 1998

Time (start - end of sample) (hour)	Permeate (mL)	Flux ($L/m^2/hr$)	Estimated Temperature (°C)	Flux (at 25°C) ($L/m^2/hr$)	Volumetric Reduction (-)
0 – 1	21.409	11.05	24.5	11.21	0.088
1 – 2	33.006	17.03	24.6	17.24	0.196
2 – 3	33.362	17.21	24.7	17.39	0.283
3 – 4	32.850	16.95	24.7	17.09	0.351
4 – 5	32.483	16.76	24.8	16.87	0.407
5 – 7	32.212	16.62	24.9	16.69	0.494
7 – 9	31.082	16.04	25.0	16.04	0.557
9 – 11	30.328	15.65	25.1	15.59	0.604
11 – 13	29.731	15.34	25.3	15.22	0.642
13 – 15	29.050	14.99	25.4	14.81	0.673
15 – 17	28.341	14.62	25.5	14.39	0.698
17 – 19	28.184	14.54	25.7	14.25	0.719
19 – 21	27.778	14.33	25.8	13.99	0.738
23 – 25	27.124	14.00	26.1	13.54	0.753

Solution: Distilled Water
Pressure: 345 KPa (50 psig)
Stir Cell: Large
Sample Time: 10 minutes
Date: 08 June 1998
Temperature: Starting – 24.1°C
Ending – 25.0°C

Table D-3: OSMONICS GN Experimental Data, dated 08 June 1998

Time (start - end of sample) (hour)	Permeate (mL)	Flux ($L/m^2/hr$)	Estimated Temperature (°C)	Flux (at 25°C) ($L/m^2/hr$)
0 – 1	28.387	43.94	24.1	45.13
1 – 2	25.378	39.28	24.1	40.30
2 – 3	24.484	37.90	24.2	38.84
3 – 4	24.555	38.01	24.2	38.91
4 – 5	24.024	37.19	24.2	38.03
5 – 7	23.606	36.54	24.3	37.33
7 – 9	23.528	36.42	24.4	37.13
9 – 11	23.469	36.33	24.4	36.95
11 – 13	23.095	35.75	24.5	36.29
13 – 15	22.769	35.25	24.6	35.70
15 – 17	23.307	36.08	24.6	36.47
17 – 19	23.214	35.94	24.7	36.24
19 – 21	23.179	35.88	24.8	36.11

2. OSMONICS GH Membrane MWCO = 2,500 Daltons

Solution: Bilge Water, prepared in accordance with the method described in section 4.3. For this experimental run the bilge water was prepared using used diesel engine lubricating oil, rather than new diesel engine lubricating oil.

Pressure: 345 KPa (50 psig)

Stir Cell: Small

Sample Time: 59 minutes

Date: 28 April 1998

Temperature: Starting – 23.8°C

Ending – 23.8°C

Table D-4: OSMONICS GH Experimental Data, dated 28 April 1998

Time (start - end of sample) (hour)	Permeate (mL)	Flux ($L/m^2/hr$)	Estimated Temperature (°C)	Flux (at 25°C) ($L/m^2/hr$)	Volumetric Reduction (-)
0 – 1	2.885	3.27	23.8	3.39	0.039
1 – 2	2.592	2.94	23.8	3.04	0.072
2 – 3	3.328	3.77	23.8	3.91	0.111
3 – 4	3.641	4.13	23.8	4.28	0.150
4 – 5	4.009	4.54	23.8	4.71	0.189
5 – 7	3.996	4.53	23.8	4.69	0.257
7 – 9	3.555	4.03	23.8	4.17	0.309
9 – 11	4.015	4.55	23.8	4.71	0.359
11 – 13	3.887	4.41	23.8	4.56	0.401
13 – 15	4.000	4.53	23.8	4.70	0.439
15 – 17	4.044	4.58	23.8	4.75	0.473
17 – 19	3.788	4.29	23.8	4.45	0.501
19 – 21	3.667	4.16	23.8	4.31	0.526
21 – 23	3.470	3.93	23.8	4.07	0.547
23 – 25	3.724	4.22	23.8	4.37	0.568

Solution: Distilled Water
Pressure: 345 KPa (50 psig)
Stir Cell: Small
Sample Time: 59 minutes
Date: 27 April 1998
Temperature: Starting – 23.0°C
Ending – 24.4°C

Table D-5: OSMONICS GH Experimental Data, dated 27 April 1998

Time (start - end of sample) (hour)	Permeate (mL)	Flux ($L/m^2/hr$)	Estimated Temperature (°C)	Flux (at 25°C) ($L/m^2/hr$)
0 – 1	0.132	0.15	23.0	0.16
1 – 2	5.131	5.82	23.1	6.15
2 – 3	4.938	5.60	23.1	5.91
3 – 4	4.766	5.40	23.2	5.69
4 – 5	5.030	5.70	23.3	6.00
7 – 9	4.830	5.47	23.4	5.73
9 – 11	5.193	5.89	23.5	6.14
11 – 13	5.090	5.77	23.6	6.00
13 – 15	5.137	5.82	23.8	6.04
15 – 17	5.180	5.87	23.9	6.07
17 – 19	5.343	6.06	24.0	6.24
19 – 21	5.315	6.02	24.1	6.19
21 – 23	5.440	6.17	24.2	6.31

3. OSMONICS GK Membrane MWCO = 3,500 Daltons

Solution: Bilge Water, prepared in accordance with the method described in section 4.3. For this experimental run the bilge water was prepared using used diesel engine lubricating oil, rather than new diesel engine lubricating oil.

Pressure: 345 KPa (50 psig)

Stir Cell: Small

Sample Time: 59 minutes

Date: 03 May 1998

Temperature: Starting – 23.6°C

Ending – 25.5°C

Table D-6: OSMONICS GK Experimental Data, dated 03 May 1998

Time (start - end of sample) (hour)	Permeate (mL)	Flux ($L/m^2/hr$)	Estimated Temperature (°C)	Flux (at 25°C) ($L/m^2/hr$)	Volumetric Reduction (-)
0 – 1	0.793	0.90	23.6	0.94	0.011
1 – 2	8.112	9.19	23.7	9.55	0.320
5 – 7	4.479	5.08	24.0	5.23	0.374
7 – 9	4.156	4.71	24.2	4.83	0.454
11 – 13	4.178	4.74	24.5	4.81	0.488
13 – 15	4.108	4.66	24.6	4.71	0.516
15 – 17	4.242	4.81	24.8	4.84	0.543
17 – 19	4.198	4.76	24.9	4.77	0.567
19 – 21	4.014	4.55	25.1	4.54	0.587
21 – 23	4.063	4.60	25.2	4.57	0.606

Solution: Distilled Water
Pressure: 345 KPa (50 psig)
Stir Cell: Small
Sample Time: 50 minutes
Date: 01 May 1998
Temperature: Starting – 24.4°C
Ending – 24.7°C

Table D-7: OSMONICS GK Experimental Data, dated 01 May 1998

Time (start - end of sample) (hour)	Permeate (mL)	Flux ($L/m^2/hr$)	Estimated Temperature (°C)	Flux (at 25°C) ($L/m^2/hr$)
0 – 1	24.318	32.52	24.4	33.10
2 – 3	10.188	13.63	24.4	13.86
3 – 4	12.489	16.70	24.4	16.98
5 – 7	12.887	17.23	24.5	17.51
9 – 11	13.193	17.64	24.5	17.90
11 – 13	13.392	17.91	24.5	18.16
13 – 15	13.644	18.25	24.6	18.49
15 – 17	14.690	19.65	24.6	19.89
17 – 19	15.139	20.25	24.6	20.48
19 – 21	15.067	20.15	24.6	20.37
21 – 23	14.612	19.54	24.7	19.74
23 – 25	15.300	20.46	24.7	20.66

4. OSMONICS GM Membrane MWCO = 8,000 Daltons

Solution: Bilge Water, prepared in accordance with the method described in section 4.3. For this experimental run the bilge water was prepared using used diesel engine lubricating oil, rather than new diesel engine lubricating oil.

Pressure: 345 KPa (50 psig)

Stir Cell: Small

Sample Time: 40 minutes

Date: 13 April 1998

Temperature: Starting – 24.0°C

Ending – 25.2°C

Table D-8: OSMONICS GM Experimental Data, dated 13 April 1998

Time (start - end of sample) (hour)	Permeate (mL)	Flux ($L/m^2/hr$)	Estimated Temperature (°C)	Flux (at 25°C) ($L/m^2/hr$)	Volumetric Reduction (-)
0 – 1	2.362	3.95	24.0	4.07	0.047
1 – 2	2.800	4.68	24.1	4.81	0.097
2 – 3	2.097	3.51	24.1	3.60	0.132
3 – 4	2.417	4.04	24.2	4.14	0.168
4 – 5	2.567	4.29	24.2	4.39	0.204
5 – 7	2.647	4.43	24.3	4.52	0.268
7 – 9	2.158	3.61	24.4	3.68	0.313
9 – 11	2.673	4.47	24.4	4.54	0.362
11 – 13	2.125	3.35	24.5	3.60	0.397
13 – 15	2.020	3.38	24.6	3.41	0.426
15 – 17	2.345	3.92	24.7	3.95	0.456
17 – 19	2.545	4.25	24.8	4.28	0.486
19 – 21	2.476	4.14	24.9	4.15	0.512

Solution: Bilge Water, prepared in accordance with the method described in section 4.3. For this experimental run the bilge water was prepared using used diesel engine lubricating oil, rather than new diesel engine lubricating oil.

Pressure: 345 KPa (50 psig)

Stir Cell: Small

Sample Time: 55 minutes

Date: 10 April 1998

Temperature: Starting – 24.4°C

Ending – 24.4°C

Table D-9: OSMONICS GM Experimental Data, dated 10 April 1998

Time (start - end of sample) (hour)	Permeate (mL)	Flux ($L/m^2/hr$)	Estimated Temperature (°C)	Flux (at 25°C) ($L/m^2/hr$)	Volumetric Reduction (-)
0 – 1	2.227	2.71	24.4	2.76	0.033
1 – 2	2.886	3.51	24.4	3.57	0.072
2 – 3	0.847	1.03	24.4	1.05	0.083
3 – 4	0.509	0.62	24.4	0.63	0.089
4 – 5	0.248	0.30	24.4	0.31	0.093
5 – 7	0.781	0.95	24.4	0.97	0.130
9 – 11	0.537	0.65	24.4	0.66	0.166
15 – 17	0.502	0.61	24.4	0.62	0.176
17 – 19	0.755	0.92	24.4	0.93	0.191
19 – 21	0.782	0.95	24.4	0.97	0.207
21 – 23	0.564	0.69	24.4	0.70	0.217
23 – 25	0.450	0.55	24.4	0.56	0.234

Solution: Distilled Water
Pressure: 345 KPa (50 psig)
Stir Cell: Small
Sample Time: 20 minutes
Date: 12 April 1998
Temperature: Starting – 24.3°C
Ending – 24.3°C

Table D-10: OSMONICS GM Experimental Data, dated 12 April 1998

Time (start - end of sample) (hour)	Permeate (mL)	Flux ($L/m^2/hr$)	Estimated Temperature (°C)	Flux (at 25°C) ($L/m^2/hr$)
0 – 1	11.708	39.15	24.3	39.97
1 – 2	15.876	53.08	24.3	54.20
2 – 3	14.501	48.48	24.3	49.50
3 – 4	14.248	47.64	24.3	48.64
4 – 5	13.575	45.39	24.3	46.34
5 – 7	13.016	43.52	24.3	44.43
7 – 9	12.278	41.05	24.3	41.91

5. OSMONICS QW Membrane MWCO = 30,000 Daltons

Solution: Bilge Water, prepared in accordance with the method described in section 4.3. For this experimental run the bilge water was prepared using used diesel engine lubricating oil, rather than new diesel engine lubricating oil and SEACLEAN surfactant rather than CLEANBREAK.

Pressure: 345 KPa (50 psig)

Stir Cell: Small Sample Time: 55 minutes

Date: 25 April 1998

Temperature: Starting – 24.2°C; Ending – 24.2°C

Table D-11: OSMONICS QW Experimental Data, dated 25 April 1998

Time (start - end of sample) (hour)	Permeate (mL)	Flux ($L/m^2/hr$)	Estimated Temperature (°C)	Flux (at 25°C) ($L/m^2/hr$)	Volumetric Reduction (-)
0 – 1	1.082	1.32	24.2	1.35	0.016
1 – 2	4.584	5.57	24.2	5.71	0.079
2 – 3	4.069	4.95	24.2	5.07	0.129
3 – 4	4.442	5.40	24.2	5.53	0.177
4 – 5	4.375	5.32	24.2	5.45	0.220
5 – 7	4.111	5.00	24.2	5.12	0.289
7 – 9	3.939	4.79	24.2	4.90	0.345
9 – 11	4.375	5.32	24.2	5.45	0.397
11 – 13	4.315	5.25	24.2	5.37	0.442
13 – 15	4.336	5.27	24.2	5.40	0.480
15 – 17	4.093	4.98	24.2	5.10	0.511
17 – 19	4.437	5.39	24.2	5.52	0.542
19 – 21	4.145	5.04	24.2	5.16	0.567
21 – 23	3.976	4.83	24.2	4.95	0.588
23 – 25	3.813	4.64	24.2	4.75	0.607

Solution: Bilge Water, prepared in accordance with the method described in section 4.3. For this experimental run the bilge water was prepared using used diesel engine lubricating oil, rather than new diesel engine lubricating oil and SEACLEAN surfactant rather than CLEANBREAK.

Pressure: 345 KPa (50 psig)

Stir Cell: Large

Sample Time: 20 minutes

Date: 11 June 1998

Temperature: Starting – 25.6°C

Ending – 27.0°C

Table D-12: OSMONICS QW Experimental Data, dated 11 June 1998

Time (start - end of sample) (hour)	Permeate (mL)	Flux ($L/m^2/hr$)	Estimated Temperature (°C)	Flux (at 25°C) ($L/m^2/hr$)	Volumetric Reduction (-)
0 – 1	25.210	19.51	25.6	19.16	0.145
1 – 2	24.725	19.14	25.7	18.76	0.252
2 – 3	24.121	18.67	25.7	18.27	0.333
3 – 4	23.518	18.20	25.8	17.78	0.396
4 – 5	22.787	17.69	25.8	17.20	0.448
5 – 7	21.864	16.92	25.9	16.47	0.525
7 – 9	19.190	14.85	26.0	14.41	0.577
9 – 11	18.862	14.60	26.1	14.11	0.618
11 – 13	18.211	14.10	26.2	13.58	0.651
13 – 15	17.727	13.72	26.3	13.17	0.677
15 – 17	17.011	13.17	26.4	12.59	0.700
17 – 19	16.783	12.99	26.6	12.38	0.719
19 – 21	16.649	12.89	26.7	12.24	0.735
21 – 23	16.677	12.91	26.8	12.22	0.750
23 – 25	16.555	12.81	26.9	12.08	0.763

Solution: Distilled Water
Pressure: 345 KPa (50 psig)
Stir Cell: Small
Sample Time: 5 minutes
Date: 21 April 1998
Temperature: Starting – 23.5°C
Ending – 23.5°C

Table D-13: OSMONICS QW Experimental Data, dated 21 April 1998

Time (start - end of sample) (hour)	Permeate (mL)	Flux ($L/m^2/hr$)	Estimated Temperature (°C)	Flux (at 25°C) ($L/m^2/hr$)
0 – 1	14.820	198.20	23.5	207.12
1 – 2	5.016	67.08	23.5	70.10
2 – 3	3.822	51.12	23.5	53.42
3 – 4	4.337	58.00	23.5	60.61
4 – 5	4.208	56.28	23.5	58.81
5 – 7	4.277	57.20	23.5	59.77
7 – 9	4.180	55.90	23.5	58.42
9 – 11	4.728	63.23	23.5	66.08
11 – 13	4.606	61.60	23.5	64.37
13 – 15	4.561	61.00	23.5	63.74
15 – 17	4.837	64.69	23.5	67.60
17 – 19	4.741	63.41	23.5	66.26

6. OSMONICS QX Membrane Pore Size Range: 0.01 – 0.1 microns

Solution: Bilge Water, prepared in accordance with the method described in section 4.3. For this experimental run the bilge water was prepared using used diesel engine lubricating oil, rather than new diesel engine lubricating oil and SEACLEAN surfactant rather than CLEANBREAK.

Pressure: 345 KPa (50 psig)

Stir Cell: Small

Sample Time: 50 minutes

Date: 20 April 1998

Temperature: Starting – 25.1°C

Ending – 24.5°C

Table D-14: OSMONICS QX Experimental Data, dated 20 April 1998

Time (start - end of sample) (hour)	Permeate (mL)	Flux ($L/m^2/hr$)	Estimated Temperature (°C)	Flux (at 25°C) ($L/m^2/hr$)	Volumetric Reduction (-)
0 – 1	23.750	31.76	25.1	31.68	0.284
1 – 2	23.326	31.20	25.1	31.13	0.440
2 – 3	22.919	30.65	25.0	30.65	0.539
3 – 4	23.670	31.66	25.0	31.66	0.662
5 – 7	23.380	31.27	25.0	31.27	0.733
7 – 9	23.829	31.87	24.9	31.94	0.780
9 – 11	23.966	32.05	24.9	32.17	0.813
11 – 13	22.970	30.72	24.8	30.88	0.836
13 – 15	23.971	32.06	24.8	32.27	0.855
15 – 17	22.770	30.45	24.7	30.70	0.870
17 – 19	22.500	30.09	24.7	30.38	0.881
19 – 21	21.891	29.28	24.6	29.60	0.891
21 – 23	21.804	29.16	24.6	29.52	0.899

Solution: Bilge Water, prepared in accordance with the method described in section 4.3. For this experimental run the bilge water was prepared using used diesel engine lubricating oil, rather than new diesel engine lubricating oil.

Pressure: 345 KPa (50 psig)

Stir Cell: Large

Sample Time: 20 minutes

Date: 27 June 1998

Temperature: Starting – 23.7°C

Ending – 27.7°C

Table D-15: OSMONICS QX Experimental Data, dated 27 June 1998

Time (start - end of sample) (hour)	Permeate (mL)	Flux ($L/m^2/hr$)	Estimated Temperature (°C)	Flux (at 25°C) ($L/m^2/hr$)	Volumetric Reduction (-)
0 – 1	42.538	32.92	23.7	34.18	0.223
1 – 2	37.202	28.79	23.9	29.76	0.349
2 – 3	35.775	27.69	24.0	28.48	0.437
3 – 4	34.859	26.98	24.2	27.62	0.503
4 – 5	34.466	26.68	24.4	27.18	0.554
5 – 7	33.544	25.96	24.5	26.33	0.629
7 – 9	32.263	24.97	24.8	25.09	0.681
9 – 11	31.457	24.35	25.2	24.23	0.719
11 – 13	30.187	23.36	25.5	23.02	0.747
13 – 15	13.255	10.26	25.8	10.01	0.758
15 – 17	13.633	10.55	26.1	10.20	0.769
17 – 19	15.733	12.18	26.4	11.65	0.779
19 – 21	11.734	9.08	26.8	8.60	0.787
21 – 23	12.383	9.58	27.1	8.98	0.794
23 – 25	11.844	9.17	27.4	8.51	0.801

Solution: Distilled Water
Pressure: 345 KPa (50 psig)
Stir Cell: Small
Sample Time: 4 minutes
Date: 18 April 1998
Temperature: Starting – 23.2°C
Ending – 24.0°C

Table D-16: OSMONICS QX Experimental Data, dated 18 April 1998

Time (start - end of sample) (hour)	Permeate (mL)	Flux ($L/m^2/hr$)	Estimated Temperature (°C)	Flux (at 25°C) ($L/m^2/hr$)
0 – 1	24.895	416.18	23.2	438.64
1 – 2	10.946	182.99	23.2	192.69
2 – 3	8.240	137.75	23.3	144.92
3 – 4	7.525	125.80	23.3	132.22
4 – 5	6.466	108.09	23.3	113.51
5 – 7	5.962	99.67	23.4	104.57
7 – 9	4.649	77.72	23.4	81.39
9 – 11	4.290	71.72	23.5	74.97
11 – 13	3.818	63.83	23.6	66.60
13 – 15	3.540	59.18	23.6	61.63
15 – 17	3.493	58.39	23.7	60.70
17 – 19	3.380	56.50	23.7	58.63
19 – 21	3.274	54.73	23.8	56.69
21 – 23	3.123	52.21	23.9	53.97
23 – 25	3.036	50.75	23.9	52.37

Solution: Distilled Water
Stir Cell: Large
Date: 22 June 1998

Pressure: 345 KPa (50 psig)
Sample Time: 1 minutes
Temperature: Starting – 23.7°C
Ending – 23.7°C

Table D-17: OSMONICS QX Experimental Data, dated 22 June 1998

Time (start - end of sample) (hour)	Permeate (mL)	Flux ($L/m^2/hr$)	Estimated Temperature (°C)	Flux (at 25°C) ($L/m^2/hr$)
0 – 1	17.559	271.81	23.7	282.41
1 – 2	13.363	206.86	23.7	214.93
2 – 3	12.312	190.59	23.7	198.02

Solution: Distilled Water
Stir Cell: Large
Date: 02 July 1998

Pressure: 345 KPa (50 psig)
Sample Time: 1 minutes
Temperature: Starting – 24.2°C
Ending – 24.7°C

Table D-18: OSMONICS QX Experimental Data, dated 02 July 1998

Time (start - end of sample) (hour)	Permeate (mL)	Flux ($L/m^2/hr$)	Estimated Temperature (°C)	Flux (at 25°C) ($L/m^2/hr$)
0 – 1	23.804	368.48	377.32	24.2
1 – 2	14.892	230.53	235.71	24.3
2 – 3	12.977	200.88	205.10	24.3
3 – 4	12.519	193.79	197.57	24.4
4 – 5	11.843	183.33	186.63	24.4
5 – 7	11.805	182.74	185.75	24.5
7 - 9	10.961	169.68	171.96	24.6

7. KOCH M100 Membrane MWCO = 20,000 Daltons

Solution: Bilge Water, prepared in accordance with the method described in section 4.3. For this experimental run the bilge water was prepared using used diesel engine lubricating oil, rather than new diesel engine lubricating oil.

Pressure: 345 KPa (50 psig)

Stir Cell: Large

Sample Time: 6 minutes

Date: 10 July 1998

Temperature: Starting – 24.7°C

Ending – 25.7°C

Table D-19: KOCH M100 Experimental Data, dated 10 July 1998

Time (start - end of sample) (hour)	Permeate (mL)	Flux ($L/m^2/hr$)	Estimated Temperature (°C)	Flux (at 25°C) ($L/m^2/hr$)	Volumetric Reduction (-)
0 – 1	9.465	24.42	24.7	24.64	0.175
1 – 2	7.005	18.07	24.7	18.21	0.270
2 – 3	6.505	16.78	24.8	16.89	0.340
3 – 4	6.444	16.63	24.8	16.71	0.398
4 – 5	6.365	16.42	24.9	16.49	0.445
5 – 7	6.301	16.26	24.9	16.30	0.521
7 – 9	5.833	15.05	25.0	15.06	0.574
9 – 11	6.222	16.05	25.1	16.02	0.619
11 – 13	6.201	16.00	25.1	15.93	0.656
13 – 15	6.408	16.53	25.2	16.42	0.687
15 – 17	6.480	16.72	25.3	16.57	0.713
17 – 19	6.813	17.58	25.4	17.38	0.736
19 – 21	6.916	17.84	25.5	17.60	0.756
21 – 23	7.005	18.07	25.5	17.78	0.773
23 - 25	7.029	18.13	25.6	17.80	0.789

Solution: Bilge Water, prepared in accordance with the method described in section 4.3. For this experimental run new diesel engine lubricating oil and CLEANBREAK detergent were used.

Pressure: 345 KPa (50 psig)

Stir Cell: Large

Sample Time: 20 minutes

Date: 07 July 1998

Temperature: Starting – 24.8°C

Ending – 24.2°C

Table D-20: KOCH M100 Experimental Data, dated 07 July 1998

Time (start - end of sample) (hour)	Permeate (mL)	Flux ($L/m^2/hr$)	Estimated Temperature (°C)	Flux (at 25°C) ($L/m^2/hr$)	Volumetric Reduction (-)
0 – 1	56.076	43.40	24.8	43.67	0.274
1 – 2	41.543	32.15	24.8	32.37	0.397
2 – 3	38.120	29.50	24.7	29.73	0.477
3 – 4	36.886	28.55	24.7	28.79	0.537
4 – 5	38.882	30.09	24.7	30.37	0.587
5 – 7	39.167	30.32	24.7	30.61	0.661
7 – 9	37.473	29.00	24.6	29.33	0.711
9 – 11	36.904	28.56	24.6	28.92	0.747
11 – 13	35.648	27.59	24.5	27.98	0.774
13 – 15	34.650	26.82	24.5	27.23	0.796
15 – 17	33.454	25.89	24.4	26.33	0.813
17 – 19	32.907	25.47	24.4	25.94	0.827
19 – 21	32.659	25.28	24.3	25.78	0.840

Solution: Bilge Water, prepared in accordance with the method described in section 4.3. For this experimental run the bilge water was prepared using used diesel engine lubricating oil, rather than new diesel engine lubricating oil. and SEACLEAN, rather than CLEANBREAK detergent.

Pressure: 345 KPa (50 psig)

Stir Cell: Small

Sample Time: 59 minutes

Date: 14 May 1998

Temperature: Starting – 24.4°C

Ending – 23.4°C

Table D-21: KOCH M100 Experimental Data, dated 14 May 1998

Time (start - end of sample) (hour)	Permeate (mL)	Flux ($L/m^2/hr$)	Estimated Temperature (°C)	Flux (at 25°C) ($L/m^2/hr$)	Volumetric Reduction (-)
0 – 1	29.291	33.20	24.4	33.82	0.293
1 – 2	28.652	32.47	24.3	33.12	0.451
2 – 3	25.799	29.24	24.3	29.85	0.543
5 – 7	23.600	26.75	24.2	27.41	0.716
7 – 9	21.876	24.79	24.1	25.46	0.759
9 – 11	21.724	24.62	24.0	25.35	0.790
15 – 17	19.195	21.76	23.8	22.55	0.843
17 – 19	18.739	21.24	23.7	22.07	0.855
19 – 21	18.549	21.02	23.6	21.89	0.866
23 - 25	17.673	20.03	23.5	20.96	0.882

Solution: Bilge Water, prepared in accordance with the method described in section 4.3. For this experimental run the bilge water was prepared using used diesel engine lubricating oil, rather than new diesel engine lubricating oil.

Pressure: 345 KPa (50 psig)

Stir Cell: Large

Sample Time: 10 minutes

Date: 19 October 1998

Temperature: Starting – 24.7°C

Ending – 24.7°C

Table D-22: KOCH M100 Experimental Data, dated 19 October 1998

Time (start - end of sample) (hour)	Permeate (mL)	Flux ($L/m^2/hr$)	Estimated Temperature (°C)	Flux (at 25°C) ($L/m^2/hr$)	Volumetric Reduction (-)
0 – 1	18.438	28.54	24.7	28.80	0.199
1 – 2	13.357	20.68	24.7	20.86	0.300
2 – 3	9.952	15.41	24.7	15.54	0.360
3 – 4	9.109	14.10	24.7	14.23	0.406
9 – 11	6.415	9.93	24.7	10.02	0.563
11 – 13	3.776	5.85	24.7	5.90	0.582
13 – 15	4.474	6.93	24.7	6.99	0.602
15 – 17	5.100	7.89	24.7	7.97	0.622
17 – 19	4.172	6.46	24.7	6.52	0.638
19 – 21	4.084	6.32	24.7	6.38	0.652
21 – 23	4.330	6.70	24.7	6.76	0.655
23 - 25	3.643	5.64	24.7	5.69	0.676

Solution: Distilled Water
Pressure: 345 KPa (50 psig)
Stir Cell: Small
Sample Time: 20 minutes
Date: 13 May 1998
Temperature: Starting – 23.5°C
Ending – 25.0°C

Table D-23: KOCH M100 Experimental Data, dated 13 May 1998

Time (start - end of sample) (hour)	Permeate (mL)	Flux ($L/m^2/hr$)	Estimated Temperature (°C)	Flux (at 25°C) ($L/m^2/hr$)
1 – 2	28.510	95.32	23.6	99.41
2 – 3	26.036	87.05	23.6	90.63
3 – 4	24.757	82.77	23.7	86.03
4 – 5	22.558	75.42	23.8	78.25
7 – 9	15.917	53.22	23.9	54.93
9 – 11	15.692	52.47	24.1	53.96
11 – 13	15.302	51.16	24.2	52.44
13 – 15	15.255	51.00	24.3	52.09
17 – 19	15.934	53.27	24.5	54.03

Solution: Distilled Water
Pressure: 345 KPa (50 psig)
Stir Cell: Large
Sample Time: 1 minutes
Date: 6 July 1998
Temperature: Starting – 24.0°C
Ending – 24.0°C

Table D-24: KOCH M100 Experimental Data, dated 6 July 1998

Time (start - end of sample) (hour)	Permeate (mL)	Flux ($L/m^2/hr$)	Estimated Temperature (°C)	Flux (at 25°C) ($L/m^2/hr$)
0 – 1	13.629	210.98	24.0	217.31
1 – 2	8.054	124.68	24.0	128.42
2 – 3	7.255	112.31	24.0	115.68
3 – 4	6.955	107.66	24.0	110.89
4 – 5	6.209	96.11	24.0	99.00
5 – 7	6.281	97.23	24.0	100.15
7 – 9	5.318	82.32	24.0	84.79
9 – 11	5.125	79.33	24.0	81.71

Solution: Distilled Water
Pressure: 345 KPa (50 psig)
Stir Cell: Large
Sample Time: 2 minutes
Date: 8 July 1998
Temperature: Starting – 23.8°C
Ending – 24.5°C

Table D-25: KOCH M100 Experimental Data, dated 8 July 1998

Time (start - end of sample) (hour)	Permeate (mL)	Flux ($L/m^2/hr$)	Estimated Temperature (°C)	Flux (at 25°C) ($L/m^2/hr$)
0 – 1	16.919	130.95	23.8	135.66
1 – 2	7.242	56.05	23.8	58.02
2 – 3	5.978	46.27	23.9	47.86
3 – 4	5.480	42.41	23.9	43.83
4 – 5	5.119	39.62	23.9	40.91
5 – 7	4.940	38.24	23.9	39.45
7 – 9	4.396	34.02	24.0	35.05
9 – 11	4.472	34.61	24.1	35.60
11 – 13	3.951	30.58	24.1	31.40
13 – 15	3.635	28.13	24.2	28.84
15 – 17	3.486	26.98	24.2	27.61
17 – 19	3.080	23.84	24.3	24.36
19 – 21	2.668	20.65	24.3	21.06

8. KOCH M180 Membrane MWCO = 50,000 Daltons

Solution: Bilge Water, prepared in accordance with the method described in section 4.3. For this experimental run the bilge water was prepared using used diesel engine lubricating oil, rather than new diesel engine lubricating oil.

Pressure: 345 KPa (50 psig)

Stir Cell: Large

Sample Time: 59 minutes

Date: 11 May 1998

Temperature: Starting – 23.8°C

Ending – 26.4°C

Table D-26: KOCH M180 Experimental Data, dated 11 May 1998

Time (start - end of sample) (hour)	Permeate (mL)	Flux ($L/m^2/hr$)	Estimated Temperature (°C)	Flux (at 25°C) ($L/m^2/hr$)	Volumetric Reduction (-)
1 – 2	22.567	25.58	23.8	26.52	0.471
5 – 7	24.288	27.53	24.2	28.16	0.699
11 – 13	19.170	21.73	24.9	21.77	0.776
13 – 15	18.272	20.71	25.2	20.61	0.820
15 – 17	18.159	20.58	25.4	20.34	0.849
17 – 19	17.966	20.36	25.6	19.98	0.870
19 – 21	17.049	19.32	25.9	18.82	0.885
21 – 23	16.142	18.30	26.1	17.70	0.896
23 - 25	15.694	17.79	26.3	17.08	0.905

Solution: Distilled Water
Pressure: 345 KPa (50 psig)
Stir Cell: Small
Sample Time: 30 minutes
Date: 6 May 1998
Temperature: Starting – 23.6°C
Ending – 25.2°C

Table D-27: KOCH M180 Experimental Data, dated 06 May 1998

Time (start - end of sample) (hour)	Permeate (mL)	Flux ($L/m^2/hr$)	Estimated Temperature (°C)	Flux (at 25°C) ($L/m^2/hr$)
1 – 2	11.760	26.21	23.7	27.25
2 – 3	15.877	35.39	23.7	36.72
5 – 7	7.817	17.42	23.9	17.98
7 – 9	7.173	15.99	24.1	16.44
9 – 11	7.290	16.25	24.2	16.64
17 – 19	7.287	16.24	24.7	16.39
19 – 21	7.228	16.11	24.8	16.19
23 – 25	7.368	16.42	25.1	16.38

9. KOCH P707 Membrane **MWCO = 150,000 Daltons**

Solution: Bilge Water, prepared in accordance with the method described in section 4.3. For this experimental run the bilge water was prepared using used diesel engine lubricating oil, rather than new diesel engine lubricating oil.

Pressure: 345 KPa (50 psig)

Stir Cell: Large

Sample Time: 50 minutes

Date: 15 May 1998

Temperature: Starting – 22.8°C; Ending – 23.3°C

Table D-28: KOCH P707 Experimental Data, dated 15 May 1998

Time (start - end of sample) (hour)	Permeate (mL)	Flux ($L/m^2/hr$)	Estimated Temperature (°C)	Flux (at 25°C) ($L/m^2/hr$)	Volumetric Reduction (-)
0 – 1	26.240	35.09	22.8	37.39	0.234
1 – 2	24.442	32.69	22.8	34.81	0.371
2 – 3	23.068	30.85	22.9	32.84	0.462
3 – 4	22.449	30.02	22.9	31.94	0.528
4 – 5	21.487	28.74	22.9	30.55	0.578
5 – 7	20.866	27.91	22.9	29.65	0.650
7 – 9	19.270	25.77	23.0	27.35	0.697
9 – 11	18.950	25.34	23.0	26.87	0.733
11 – 13	18.063	24.16	23.0	25.58	0.760
13 – 15	17.600	23.54	23.1	24.90	0.781
15 – 17	17.016	22.76	23.1	24.04	0.799
17 – 19	16.430	21.97	23.2	23.19	0.813
19 – 21	15.592	20.85	23.2	21.98	0.825
21 – 23	15.115	20.21	23.2	21.28	0.835
23 – 25	14.605	19.53	23.3	20.54	0.844

Solution: Distilled Water
Pressure: 345 KPa (50 psig)
Stir Cell: Small
Sample Time: 5 minutes
Date: 14 May 1998
Temperature: Starting – 23.4°C
Ending – 23.0°C

Table D-29: KOCH P707 Experimental Data, dated 14 May 1998

Time (start - end of sample) (hour)	Permeate (mL)	Flux ($L/m^2/hr$)	Estimated Temperature (°C)	Flux (at 25°C) ($L/m^2/hr$)
0 - 1	35.496	474.72	23.4	497.59
1 – 2	22.985	307.40	23.3	323.50
2 – 3	18.560	248.22	23.1	262.26
3 - 4	16.370	218.93	23.0	232.24

APPENDIX E:

FLAT SHEET DETAILED DATA AND PRESENTATION

The flat sheet raw data, presented in Appendix D, was examined to determine how to most accurately present it. A simple means of presenting the data was to plot membrane flux, at the completion of a 24 hour experimental run, against the various membrane's molecular weight cut-off; this was presented in Figure 5.1. The data points presented in Figure 5.1 were:

Table E-1: Summary of Flat Sheet Flux Data, after 24 hours, Used Bilge Water

Membrane	**Flux** **(at the end of a 24 hour experimental run, corrected to 25°C)** ($L/m^2/hr$)	**Date**
OSMONICS GH	4.37	28 April 1998
OSMONICS GK	4.57	03 May 1998
OSMONICS GM	4.15 0.56	13 April 1998 10 April 1998
OSMONICS GN	2.09 13.54	27 April 1998 05 June 1998
KOCH M100	17.80	10 July 1998
KOCH M180	17.08	11 May 1998
OSMONICS QW	4.75	25 April 1998
KOCH P707	20.54	15 May 1998
OSMONICS QX	23.02	27 June 1998

It should be noted that in certain instances a number of experimental runs were conducted. In these instances, the above flux values selected, were those deemed to provide the best representation for the individual membrane performance. For example, for the OSMONICS QX membrane the flux value presented was that after 12 hours (11 – 13 hour sample interval) rather than after 24 hours (23 – 25 hour sample interval) of operation. This earlier flux value was used, as a review of the raw data (Table D-15)

reveals that catastrophic fouling occurred beyond the 13th hour of this experimental run; detailed in section 5.1.3 and Figure 5.8 as oil droplet pore plugging.

The next segment of flat sheet data presented was Table 5.1. As alluded to in the above discussion of the selection of the presented results for the OSMONICS QX membrane examining the 24 hour flux results did not necessarily present a true picture of the efficiency of the membranes, due to various factors, such as membrane fouling. In order to mitigate the factors and examine the membrane flux of unfouled membranes it was determined to review the flux values after one hour of operation. It was felt that the flux at this stage of the experimental runs would well represent unfouled membranes, due to their limited exposure to bilge water. Additionally, it was assumed that after one hur of operation a steady state cake layer would be formed. Based upon these assumptions the membrane flux would be defined by the membrane and cake layer resistive components.

To determine the membrane and cake layer resistive components the Pure Water Permeate (PWP) flux was required in addition to the bilge water flux. These PWP fluxes were determined from the maximum flux values obtained from the various PWP runs (the maximum flux values were generally, but not always, the initial ones). The maximum flux values were used because PWP flux values, by definition, are the fluxes associated with pure water; i.e. water free of impurities. Due to the fact that PWP flux runs were conducted with the same experimental apparatus as the bilge water runs all impurities could not be removed from the experimental apparatus, despite the best efforts of flushing and cleaning the equipment. Accordingly the flux values and their associated resistive components were identified in Table 5.1, which is re-presented below.

Table 5.1: Resistive Component Values for Flat Sheet Membranes

Membrane			PWP Flux at 345 KPa	Flux at 1hour and 345 KPa	Resistive Component	
Name	MWCO (Daltons)	Pore Radius[1] (microns)	($L/m^2/hr$)	($L/m^2/hr$)	Membrane (10^{14} m^{-1})	Cake Layer (10^{14} m^{-1})
GH	2,500	0.0018	6.15	4.75	2.264	0.667
GK	3,500	0.0022	33.10	5.23	0.421	2.241
GM	8,000	0.0033	54.20	3.57	0.257	3.643
GN	10,000	0.0037	105.27	17.39	0.132	0.668
M100	20,000	0.0052	217.31	24.64	0.064	0.501
QW	30,000	0.0064	207.12	19.16	0.067	0.659
M180	50,000	0.0082	245.40	28.16	0.065	0.438
P707	150,000	0.0143	323.50	37.39	0.043	0.329
QX	3,600,000[2]	0.05[2]	438.64	34.18	0.032	0.376

[1] Pore Radius was obtained using equation 4.1 and the fact that MWCO represents 90% separation.

[2] Estimated – Membrane was a microfiltration membrane and was characterized by a pore size range of 0.01 – 0.1 microns, rather than MWCO.

The following are a set of sample calculations used to determine the membrane and cake layer resistive components. These sample calculations are presented for the OSMONICS GH membrane.

The membrane and cake layer resistive components are determined through the application of equations 3.1 and 3.2 (see section 3 – THEORY).

OSMONICS GH Membrane Resistive Component:

The membrane resistive component is determined through the examination of the PWP flux values. Since it is a PWP run it assumed that the cake layer and fouling resistive components are negligible and therefore equation 3.2 reduces to:

$$R_{total} = R_{mem}$$

Accordingly equation 3.1 becomes:

$$J = \frac{\Delta P}{\mu R_{mem}}$$

As identified in Table 5.1 the PWP flux for the OSMONICS GH membrane is 6.15 L/m^2/hr.

$$J = 6.15 \; {}^{L}/_{m^2/hr} * \left(\frac{0.001\, m^3}{1\, L}\right) * \left(\frac{1\, hr}{3600\, s}\right) = 1.708 * 10^{-6} \; {}^{m^3}/_{m^2/s}$$

All the flat sheet membrane experimental runs were conducted at 50 psi, which is equal to 344,558 Pa. The dynamic viscosity of water is equal to 0.000891 Pa*s. Therefore the membrane resistance associated with the OSMONICS GH membrane is:

$$R_{mem} = \frac{\Delta P}{\mu J}$$

$$= \frac{344558\ Pa}{(0.000891\ Pa*s)\left(1.708*10^{-6}\ {}^{m}/_{s}\right)}$$

$$= 2.264*10^{14}\ m^{-1}$$

To determine the cake layer resistance the flux associated with the bilge water run needs to be examined. Again, since the flux was taken after only 1 hour of operation it is assumed that membrane fouling is negligible. Therefore, for the bilge water run, equation 3.1 simplifies to:

$$R_{total} = R_{mem} + R_{cake}$$

or $$R_{cake} = R_{total} - R_{mem}$$

As identified in Table 5.1 the bilge water flux for the OSMONICS GH membrane is 4.75 L/m^2/hr.

$$J = 4.75 \; {}^{L}/_{m^2/hr} * \left(\frac{0.001\, m^3}{1\, L}\right) * \left(\frac{1\, hr}{3600\, s}\right) = 1.319 * 10^{-6} \; {}^{m^3}/_{m^2/s}$$

Therefore the total resistance associated with the bilge water experimental run was:

$$R_{total} = \frac{\Delta P}{\mu J}$$

$$= \frac{344558\ Pa}{(0.000891\ Pa*s)\left(1.319*10^{-6}\ m/s\right)}$$

$$= 2.931*10^{14}\ m^{-1}$$

Therefore the cake layer resistance for the OSMONICS GH membrane is:

$$R_{cake} = \left(2.931*10^{14}\right) - \left(2.264*10^{14}\right) m^{-1}$$

$$= 0.667*10^{14}\ m^{-1}$$

Figure 5.2: Cake Layer Resistance vs. Membrane MWCO

Figure 5.2 presents the experimental cake layer resistive values as presented in Table 5.1 and the theoretically determined cake layer resistive values. The theoretical cake layer resistances were determined using equations 3.11, 3.12 and 3.36.

$$R_{cake} = \hat{R}_{cake}\delta \tag{3.11}$$

$$\hat{R}_{cake} = \frac{37.5\phi_{\max}^2}{a_p^2(1-\phi_{\max})^2} \tag{3.12}$$

$$\delta_{ss} = \frac{\left(R_{mem}^2 + 2C\hat{R}_{cake}t_{ss}\right)^{0.5} - R_{mem}}{\hat{R}_{cake}} \tag{3.36}$$

Based upon review of Table 5.1 and the plot of experimental R_{cake} values in Figure 5.2 it was speculated that there is more than one sized particle in the bilge water.

For the various flat sheet membranes, at a particular pore size the membrane pores become large enough to allow the smaller particulates to pass through them. This is determined by using a particle to pore size ratio; if the ratio is less than one then all the particles pass through the membrane. It should be noted that particles which are

marginally smaller than the membrane may be partially retained by the membrane. Accordingly the membrane pore radius was divided by a factor of 0.707 to compensate for this effect. (Sethi and Wiesner, 1995)

If the particle to pore size ratio was less than one then the membrane cake layer would only be comprised of the larger particles. Conversely, if the particle to pore size ratio was greater than one then the membrane cake layer was comprised of both the small and large particles.

Using an EXCEL spreadsheet the theoretical and experimental cake layers were determined for given (large and small) particulate sizes. The particulate sizes were determined, for all of the membranes, by optimizing the size of the two critically sized particles to select the critically sized particles which provided the best fit to the experimentally determined cake layer resistive values. The best fit between the theoretical and cake layer resistive values was determined by obtaining the smallest value of the sum of the square of the differences between all of the theoretical and experimental values. This was accomplished through an iterative process. The sizes of the small and large critically sized particles were found to be 0.0034 microns and 0.0241 microns, respectively. The theoretical and experimental results are presented in Tables E-2 and E-3. As a sample of the calculations performed in the spreadsheet the determination of the cake layer is shown for the OSMONICS QW membrane.

In solving for the cake layer resistive components the following system parameters and assumptions were used in the calculations;

a. it was assumed that the steady state cake Layer formed in 1 hour (3,600 seconds),
b. since bilge water fluxes after only 1 hour were examined it was assumed that fouling was negligible,
c. the maximum solute (oil) concentration at the membrane surface is assumed to be 0.58 (58%),
d. the bulk solute (oil) concentration is assumed to be 0.002 (2000 ppm), and

e. the transmembrane pressure was 344,588 Pa (50psi).

Theoretical Cake Layer Resistive Component (Table E-2):

1. Membrane Resistance

$J_{PWP-QX} = 203.61$ L/m^2/hr $= 5.66 * 10^{-5}$ m^3/m^2/s

$$R_{mem} = \frac{\Delta P}{\mu J_{PWP}} = \frac{344558\ Pa}{(0.000891\ Pa*s)\left(5.66*10^{-5}\ m/s\right)}$$

$$= 6.83 * 10^{12}\ m^{-1}$$

2. Cake Layer Thickness

As shown in section 3 – Theory the steady state cake layer thickness can be equated as;

$$\delta_{ss} = \frac{\left(R_{mem}^2 + 2C\hat{R}_{cake}t_{ss}\right)^{0.5} - R_{mem}}{\hat{R}_{cake}}, \tag{3.36}$$

where: C = constant $= \frac{\Delta P \phi_b}{\mu(\phi_{max} - \phi_b)}$, and (3.33)

$$\hat{R}_{cake} = \frac{37.5\phi_{max}^2}{a_p^2(1-\phi_{max})^3}. \tag{3.12}$$

As detailed in section 5.1.1 the large particles were determine to be approximately 24.1nm and the small particles were approximately 3.4nm in radius. Therefore for the large and small particles the theoretical steady state cake layer is:

2a. Large Particle:

$$\hat{R}_{cake} = \frac{37.5*0.58^2}{(24.1*10^{-9})^2(1-0.58)^3} = 2.93*10^{17}\ m^{-2}$$

$$C = \frac{(344558)0.58}{(0.000891)(0.58-0.002)} = 1.34*10^6$$

$$\delta = \frac{\left((6.83*10^{12})^2 + 2(1.34*10^6)(2.93*10^{17})3600\right)^{0.5} - (6.83*10^{12})}{2.93*10^{17}}$$

= 159 microns

2b. Small Particle:

$$\hat{R}_{cake} = \frac{37.5 * 0.58^2}{\left(3.4 * 10^{-9}\right)^2 (1 - 0.58)^3} = 1.47 * 10^{19}\ m^{-2}$$

$$C = \frac{(344558)0.58}{(0.000891)(0.58 - 0.00135)} = 9.02 * 10^5$$

$$\delta = \frac{\left((6.83 * 10^{12})^2 + 2(9.02 * 10^5)(1.47 * 10^{19})3600\right)^{0.5} - (6.83 * 10^{12})}{1.47 * 10^{19}}$$

$= 20.5$ microns

3. Determination if the small particle is retained by the membrane:

For membranes, which have pores that are either much smaller or larger than a particle, the question of particulate retention is straight forward. However, for particles which are comparable in size to a membranes pores the retention of the particle is not as apparent. Particles of the same size as a membrane's pores would not be expected to pass through the membrane; in fact it is reasonable to expect that a membrane's pores would have to be somewhat larger than the particle for the particle to pass through. Accordingly, a factor of $1/\sqrt{2}$ was applied to the membrane pore, when determining the particle to pore size ratio.

QX membrane has a pore size approximately equal to 0.0064 microns.

$$\frac{Particle}{Membrane\ Pore} = \frac{0.0034}{0.0064/\sqrt{2}} = 0.530$$

Since the particle to membrane pore ratio is less than 1 the small particle will not be retained by the membrane and therefore the cake layer, associated with the QX membrane, will be comprised solely of the larger particulates.

4. Cake Layer Resistive Component:

$$R_{cake} = R_{cake-large} + R_{cake-small}$$

$$= \hat{R}_{cake-large}\delta_{large} + 0$$

$$= (2.93 * 10^{17})(159 * 10^{-6})$$

$4.67*10^{14}\ m^{-1}$

Experimental Cake Layer Resistive Component (Table E-3):

From the experimental runs, with the QX membrane, the PWP flux was found to be 203.61L/m^2/hr and the bilge water flux, after 1 hour of operation, was found to be 19.16L/m^2/hr. Therefore the membrane, total and cake layer resistances are:

$$R_{mem} = \frac{\Delta P}{\mu J_{PWP}}$$

$$= \frac{344558}{(0.000891)\left(203.61/1000/3600\right)} = 6.72*10^{12}\ m^{-1}$$

$$R_{total} = \frac{\Delta P}{\mu J_{bilge\ water}}$$

$$\frac{344558}{(0.000891)\left(19.16/1000/3600\right)} = 7.26*10^{13}\ m^{-1}$$

$$R_{cake} = R_{total} - R_{mem}$$

$$= (7.26*10^{13}) - (6.72*10^{12}) = 6.59*10^{13}\ m^{-1}$$

Table E-2: Theoretically Determined Cake Layer Resistive Component for the Flat Sheet Membranes

Membrane				Cake Layer Thickness			Cake Layer Resistance		
Name	MWCO (Daltons)	Pure Water Flux ($m^3/m^2/s$)	Membrane Resistance (m^{-1})	Large Particles (m)	Small Particles (m)	Particle Size : Membrane Pore Ratio (-)	Large Particles (m^{-1})	Small Particles (m^{-1})	Total (m^{-1})
GH	2,500	$8.33*10^{-8}$	$4.64*10^{15}$	$1.04*10^{-6}$	$7.00*10^{-7}$	1.83	$3.04*10^{11}$	$1.03*10^{13}$	$1.06*10^{13}$
GK	3,500	$7.73*10^{-6}$	$5.00*10^{13}$	$7.83*10^{-5}$	$1.79*10^{-5}$	1.55	$2.29*10^{13}$	$2.63*10^{14}$	$2.86*10^{14}$
GM	8,000	$2.65*10^{-5}$	$1.46*10^{13}$	$1.38*10^{-4}$	$2.00*10^{-5}$	1.03	$4.05*10^{13}$	$2.95*10^{14}$	$3.36*10^{14}$
GN	10,000	$3.16*10^{-5}$	$1.22*10^{13}$	$1.44*10^{-4}$	$2.02*10^{-5}$	0.92	$4.22*10^{13}$	-	$4.22*10^{13}$
M100	20,000	$4.73*10^{-5}$	$8.16*10^{12}$	$1.69*10^{-4}$	$2.05*10^{-5}$	0.65	$4.55*10^{13}$	-	$4.55*10^{13}$
QW	30,000	$5.66*10^{-5}$	$6.83*10^{12}$	$1.59*10^{-4}$	$2.05*10^{-5}$	0.53	$4.67*10^{13}$	-	$4.67*10^{13}$
M180	50,000	$6.82*10^{-5}$	$5.67*10^{12}$	$1.63*10^{-4}$	$2.06*10^{-5}$	0.41	$4.77*10^{13}$	-	$4.77*10^{13}$
P707	150,000	$9.31*10^{-5}$	$4.15*10^{12}$	$1.68*10^{-4}$	$2.07*10^{-5}$	0.24	$4.91*10^{13}$	-	$4.91*10^{13}$
QX	3,600,000	$1.65*10^{-4}$	$2.34*10^{12}$	$1.74*10^{-4}$	$2.08*10^{-5}$	0.05	$5.08*10^{13}$	-	$5.08*10^{13}$

Table E-3: Experimentally Determined Cake Layer Resistive Component for the Flat Sheet Membranes

Membrane		Pure Water Flux	Membrane Resistance	Bilge Water Flux	Total Resistance	Cake Layer Resistance
Name	MWCO (Daltons)	($m^3/m^2/s$)	(m^{-1})	($m^3/m^2/s$)	(m^{-1})	(m^{-1})
GH	2,500	6.15	$2.26*10^{14}$	4.75	$2.93*10^{14}$	$6.67*10^{13}$
GK	3,500	33.10	$4.20*10^{13}$	5.23	$2.66*10^{14}$	$2.24*10^{14}$
GM	8,000	54.20	$2.57*10^{13}$	3.57	$3.90*10^{14}$	$3.64*10^{14}$
GN	10,000	105.27	$1.32*10^{13}$	17.39	$7.99*10^{13}$	$6.68*10^{13}$
M100	20,000	217.31	$6.40*10^{12}$	24.64	$5.65*10^{13}$	$5.01*10^{13}$
QW	30,000	207.12	$6.72*10^{12}$	19.16	$7.26*10^{13}$	$6.59*10^{13}$
M180	50,000	245.40	$5.67*10^{12}$	28.16	$4.94*10^{13}$	$4.38*10^{13}$
P707	150,000	323.50	$4.30*10^{12}$	37.39	$3.72*10^{13}$	$3.29*10^{13}$
QX	3,600,000	438.64	$3.17*10^{12}$	34.18	$4.07*10^{13}$	$3.76*10^{13}$

As stated earlier to determine the optimal sizes for the small and large particulates were determined by minimizing the sum of the squares of the difference between the theoretical and experimental cake layer resistive components. Table E-4 reveals how the sum of the squares, for the optimal particle sizes, was determined.

Table E-4: Sample Calculation of the Sum of the Squares of the Theoretical and Experimental Cake Layer Resistive Components

Membrane	Theoretical Cake Layer Resistance (m^{-1})	Experimental Cake Layer Resistance (m^{-1})	Difference (Th. – Exp.) (m^{-1})	Difference^2 (m^{-2})
GH	$1.06*10^{13}$	$6.67*10^{13}$	$-5.61*10^{13}$	$3.14*10^{27}$
GK	$2.86*10^{14}$	$2.24*10^{14}$	$6.24*10^{13}$	$3.89*10^{27}$
GM	$3.36*10^{14}$	$3.64*10^{14}$	$-2.84*10^{13}$	$8.04*10^{26}$
GN	$4.22*10^{13}$	$6.67*10^{13}$	$-2.45*10^{13}$	$5.99*10^{26}$
M100	$4.55*10^{13}$	$5.00*10^{13}$	$-4.50*10^{12}$	$2.03*10^{25}$
QW	$4.67*10^{13}$	$6.59*10^{13}$	$-1.92*10^{13}$	$3.68*10^{26}$
M180	$4.77*10^{13}$	$4.37*10^{13}$	$3.99*10^{12}$	$1.59*10^{25}$
P707	$4.91*10^{13}$	$3.29*10^{13}$	$1.62*10^{13}$	$2.62*10^{26}$
QX	$5.08*10^{13}$	$3.75*10^{13}$	$1.33*10^{13}$	$1.76*10^{26}$
	TOTAL			**$9.28*10^{27}$**

Steady State Cake Layer Conditions

Table 5.2 presents the steady state cake layer thickness and the time required to achieve this steady state cake layer, as determined by the experimental results. Table 5.2 is re-presented below.

Table 5.2: Flat Sheet Steady State Cake Layer Conditions

Membrane			Steady State Cake Layer Conditions	
Name	**MWCO (Daltons)**	**Pore Radius (microns)**	**Thickness (microns)**	**Time (seconds)**
GH	2,500	0.0018	4.5	879
GK	3,500	0.0022	15.2	1753
GM	8,000	0.0033	24.7	3841
GN	10,000	0.0037	228.0	7946
M100	20,000	0.0052	170.9	4017
QW	30,000	0.0064	224.9	6672
M180	50,000	0.0082	149.3	3074
P707	150,000	0.0082	112.3	1743
QX	3,600,000	0.05	128.1	2102

These values were determined through the use of the experimental pure water permeate and bilge water flux values, plus the determined values of the critically sized particles (the small particle having a radius of 0.0034 microns and the large particle having a radius of 0.0241 microns). The particle size was used to determine the specific cake layer resistance, which allowed for the determination of the steady state cake layer thickness, in accordance with equation 3.11. For those membranes which retained both the small and large particles (GH, GK and GM) the smaller particulate was used to determine the specific cake layer resistance as it is the smaller particle which defines the cake layer resistance. The steady state time for the formation of the cake layer was determined in accordance with 3.21 or 3.23, which provided the relationship between the steady state time, pure water permeate flux and the bilge water flux.

Table E-5 provides a summary of the values obtained in the determination of the time required to achieve the steady state cake layer and its thickness. Following Table E-5 is a sample calculation, using the M100 membrane.

Table E-5: Determination of Steady State Cake Layer Thickness for Flat Sheet Membranes

Membrane	J_{PWP}		R_{mem}	$J_{bilge\ water}$		R_{total}	R_{cake}	Specific Cake Layer Resistance	Cake Layer Thickness	Flux Decline Constant	Steady State Time
	($L/m^2/hr$)	($m^3/m^2/s$)	(m^{-1})	($L/m^2/hr$)	($m^3/m^2/s$)	(m^{-1})	(m^{-1})	(m^{-2})	(m)	(-)	(s)
GH	6.15	$1.71*10^{-6}$	$2.26*10^{14}$	4.75	$1.32*10^{-6}$	$2.93*10^{14}$	$6.67*10^{13}$	$1.47*10^{19}$	$4.53*10^{-6}$	2599.89	879.2
GK	33.10	$9.19*10^{-6}$	$4.20*10^{13}$	5.23	$1.45*10^{-6}$	$2.66*10^{14}$	$2.24*10^{14}$	$1.47*10^{19}$	$1.52*10^{-5}$	89.75	1752.6
GM	54.20	$1.51*10^{-5}$	$2.57*10^{13}$	3.57	$9.92*10^{-7}$	$3.90*10^{14}$	$3.64*10^{14}$	$1.47*10^{19}$	$2.47*10^{-5}$	33.47	3841.1
GN	105.27	$2.92*10^{-5}$	$1.32*10^{13}$	17.39	$4.83*10^{-6}$	$7.99*10^{13}$	$6.68*10^{13}$	$2.93*10^{17}$	$2.28*10^{-4}$	445.83	7945.8
M100	217.31	$6.04*10^{-5}$	$6.40*10^{12}$	24.64	$6.84*10^{-6}$	$5.65*10^{13}$	$5.01*10^{13}$	$2.93*10^{17}$	$1.71*10^{-4}$	104.62	4016.5
QW	207.12	$5.75*10^{-5}$	$6.72*10^{12}$	19.16	$5.32*10^{-6}$	$7.26*10^{13}$	$6.59*10^{13}$	$2.93*10^{17}$	$2.25*10^{-4}$	115.17	6671.6
M180	245.40	$6.82*10^{-5}$	$5.67*10^{12}$	28.16	$7.82*10^{-6}$	$4.94*10^{13}$	$4.38*10^{13}$	$2.93*10^{17}$	$1.49*10^{-4}$	82.04	3074.2
P707	323.50	$8.99*10^{-5}$	$4.30*10^{12}$	37.39	$1.04*10^{-5}$	$3.72*10^{13}$	$3.29*10^{13}$	$2.93*10^{17}$	$1.12*10^{-4}$	47.21	1743.4
QX	438.64	$1.22*10^{-4}$	$3.17*10^{12}$	34.18	$9.49*10^{-6}$	$4.07*10^{13}$	$3.76*10^{13}$	$2.93*10^{17}$	$1.28*10^{-4}$	25.68	2101.7

Sample Calculation (using the data for the M100 membrane)

The steady state cake layer thickness is determined through equation 3.11 and the time required to achieve steady state conditions is determined through equation 3.23.

To utilize equation 3.11 first the specific cake layer resistance $(\hat{R}_{cake})$must be determined. In accordance with equation 3.12 the specific cake layer resistance is defined as;

$$\hat{R}_{cake} = \frac{37.5\,\phi_{\max}^2}{a_p^2(1-\phi_{\max})^3}.$$

The pores of the M100 membrane are larger than the smaller particulate, therefore its cake layer will be comprised of the larger particles. Therefore its specific cake layer resistance will be:

$$\hat{R}_{cake} = \frac{37.5*0.58^2}{(24.1*10^{-8}\ m)^2(1-0.58)^3}$$
$$= 2.93*10^{17}\ \mathrm{m}^2$$

The cake layer thickness is then determined by equation 3.11; i.e. the cake layer resistance divided by the specific cake layer resistance. The cake layer resistance is determined as shown in the sample calculation for the GH membrane (pages E-4 to E-6). Therefore, for the M100 membrane the steady state cake layer thickness is;

$$\delta_{ss} = \frac{R_{cake}}{\hat{R}_{cake}}$$
$$= \frac{5.10*10^{13}\ m^{-1}}{2.93*10^{17}\ m^{-2}} = 170.9\ microns.$$

The time required to achieve the steady state conditions is the product of the flux decline constant $(\tau_c)$and the square of the ratio of the pure water permeate and bilge water fluxes, as define d by equation 3.23.

The flux decline constant is determined in accordance with equation 3.22. For the M100 membrane it is equal to:

$$\tau_c = \frac{R_{mem}(\phi_{max} - \phi_b)}{J_{PWP}\hat{R}_{cake}\phi_b}$$

$$= \frac{(6.41*10^{12}\ m^{-1})(0.58 - 0.002)}{(6.04*10^{-5}\ m/s)(2.93*10^{17}\ m^{-2})0.002}$$

$$= 104.62$$

Therefore, for the M100 membrane, the steady state time is equal to:

$$t_{ss} = \left(\frac{\tau_c}{2}\right)\left[\left(\frac{J_{PWP}}{J(t_{ss})}\right)^2 - 1\right]$$

$$= \left(\frac{104.62}{2}\right)\left[\left(\frac{6.034*10^{-5}}{6.84*10^{-6}}\right)^2 - 1\right]$$

$$= 4016.5 \text{ seconds}$$

APPENDIX F:

CERAMEM LMA MEMBRANE RAW DATA

CERAMEM LMA Membrane Experimental Results

The following is the data for the various experimental runs conducted with the CERAMEM LMA membrane. Presented first are time versus flux (corrected to 25°C) data for the various experimental runs. Presented after these tables is an example of how these data sets were determined from the raw data.

NEW BILGE WATER RESULTS

That is, the following series of experimental data were conducted with Bilge Water prepared in accordance with the method described in section 4.3.

Date: 19 February 1999

Pressure: 221.4 KPa (32 psig)

Degree of Backflush: A 5 second backflush in a total operational cycle of 120 seconds.

Table F-1: CERAMEM LMA Experimental Data, dated 19 February 1999

Time (hours)	Flux corrected to 25°C ($L/m^2/hr$)	Flux Ratio (-)
0.55	56.14	0.624
1.17	51.27	0.561
2.78	54.98	0.602
4.15	54.73	0.599
8.27	52.79	0.578
12.58	52.54	0.575
16.63	52.20	0.571
20.73	51.53	0.564
22.91	51.26	0.561

Date: 20 February 1999

Pressure: 221.4 KPa (32 psig)

Degree of Backflush: A 10 second backflush in a total operational cycle of 120 seconds.

Table F-2: CERAMEM LMA Experimental Data, dated 20 February 1999

Time (hours)	Flux corrected to 25°C ($L/m^2/hr$)	Flux Ratio (-)
0.21	54.15	0.604
1.72	52.63	0.587
3.98	52.76	0.589
8.28	50.51	0.564
12.39	49.14	0.548
16.73	49.47	0.550
20.74	48.36	0.552
24.82	48.17	0.540
28.93	47.65	0.538

Date: 22 February 1999

Pressure: 221.4 KPa (32 psig)

Degree of Backflush: A 2.5 second backflush in a total operational cycle of 120 seconds.

Table F-3: CERAMEM LMA Experimental Data, dated 22 February 1999

Time (hours)	Flux corrected to 25°C ($L/m^2/hr$)	Flux Ratio (-)
0.21	59.56	0.712
0.56	58.72	0.702
1.15	57.87	0.692
1.93	57.48	0.687
4.14	56.84	0.679
8.28	54.75	0.654
12.55	53.79	0.643
16.62	52.93	0.632
20.93	52.38	0.626
24.94	51.52	0.616
29.28	51.12	0.611

Date: 24 February 1999

Pressure: 221.4 KPa (32 psig)

Degree of Backflush: A 2.5 second backflush in a total operational cycle of 60 seconds.

Table F-4: CERAMEM LMA Experimental Data, dated 24 February 1999

Time (hours)	Flux corrected to 25°C ($L/m^2/hr$)	Flux Ratio (-)
0.23	52.98	0.616
0.55	53.42	0.627
0.68	53.97	0.632
1.22	54.25	0.631
3.89	52.59	0.611
8.25	49.92	0.602
12.52	48.98	0.580
16.80	48.18	0.569
20.83	47.36	0.560
25.12	46.66	0.550
29.14	46.47	0.542

Date: 01 March 1999

Pressure: 207.6 KPa (30 psig)

Degree of Backflush: A 5 second backflush in a total operational cycle of 120 seconds.

Table F-5: CERAMEM LMA Experimental Data, dated 01 March 1999

Time (hours)	Flux corrected to 25°C ($L/m^2/hr$)	Flux Ratio (-)
0.18	41.82	0.532
0.65	40.29	0.512
1.68	36.98	0.470
3.98	39.62	0.504
8.28	38.81	0.493
12.58	38.66	0.492
16.55	37.85	0.481
20.86	37.38	0.475
25.15	37.10	0.472
29.20	36.76	0.467

Date: 03 March 1999

Pressure: 221.4 KPa (32 psig)

Degree of Backflush: None.

Table F-6: CERAMEM LMA Experimental Data, dated 03 March 1999

Time (hours)	Flux corrected to 25°C ($L/m^2/hr$)	Flux Ratio (-)
0.05	43.10	0.534
0.17	41.35	0.513
0.41	40.63	0.504
4.26	40.44	0.501
8.57	39.78	0.493
12.53	39.16	0.485
16.83	39.36	0.488
20.83	39.25	0.487
25.10	39.12	0.485

Date: 06 March 1999

Pressure: 207.6 KPa (30 psig)

Degree of Backflush: None.

Table F-7: CERAMEM LMA Experimental Data, dated 06 March 1999

Time (hours)	Flux corrected to 25°C ($L/m^2/hr$)	Flux Ratio (-)
0.13	35.95	0.477
0.23	36.70	0.487
0.52	36.00	0.478
0.63	35.58	0.473
0.85	36.39	0.483
1.28	35.93	0.477
1.64	30.32	0.403
2.12	30.70	0.408
2.51	30.89	0.410
2.93	36.58	0.486
3.72	36.53	0.485

USED BILGE WATER RESULTS

That is, the following series of experimental data were conducted with Bilge Water prepared in accordance with the method described in section 4.3, except that used diesel engine lubricating oil, rather than new diesel engine lubricating oil, was used.

Date: 01 February 1999

Pressure: 207.6 KPa (30 psig)

Degree of Backflush: A 5 second backflush in a total operational cycle of 120 seconds.

Table F-8: CERAMEM LMA Experimental Data, dated 01 February 1999

Time (hours)	Flux corrected to 25°C ($L/m^2/hr$)	Flux Ratio (-)
0.60	67.90	0.724
1.33	66.12	0.705
2.58	58.89	0.628
3.83	43.46	0.464
5.98	41.99	0.448
8.63	42.05	0.449
11.95	42.95	0.458
14.93	43.24	0.461
16.60	43.00	0.459
17.84	42.80	0.457

Date: 03 February 1999

Pressure: 207.6 KPa (30 psig)

Degree of Backflush: A 10 second backflush in a total operational cycle of 120 seconds.

Table F-9: CERAMEM LMA Experimental Data, dated 03 February 1999

Time (hours)	Flux corrected to 25°C ($L/m^2/hr$)	Flux Ratio (-)
0.53	55.34	0.601
1.55	51.87	0.563
2.95	52.01	0.565
4.13	55.42	0.602
6.23	52.57	0.571
8.56	50.78	0.551
10.55	49.18	0.534
12.57	48.85	0.531
14.56	48.40	0.526
16.54	48.15	0.523
18.21	47.87	0.520

Date: 07 February 1999

Pressure: 207.6 KPa (30 psig)

Degree of Backflush: A 2.5 second backflush in a total operational cycle of 120 seconds.

Table F-10: CERAMEM LMA Experimental Data, dated 07 February 1999

Time (hours)	Flux corrected to 25°C ($L/m^2/hr$)	Flux Ratio (-)
0.62	48.90	0.541
2.16	50.80	0.562
4.25	51.56	0.570
8.27	50.25	0.556
12.26	48.78	0.540
16.28	48.00	0.531
18.50	39.26	0.434
20.72	45.06	0.499
21.72	45.34	0.502

Date: 10 February 1999

Pressure: 221.4 KPa (32 psig)

Degree of Backflush: A 5 second backflush in a total operational cycle of 120 seconds.

Table F-11: CERAMEM LMA Experimental Data, dated 10 February 1999

Time (hours)	Flux corrected to 25°C ($L/m^2/hr$)	Flux Ratio (-)
0.34	55.97	0.601
0.66	54.28	0.582
1.09	47.01	0.504
2.25	50.49	0.542
3.98	48.95	0.525
8.63	47.81	0.513
11.29	47.46	0.509
13.96	47.59	0.511
16.94	47.82	0.513
18.38	47.33	0.508
20.47	45.40	0.487
25.37	47.71	0.512
29.36	47.78	0.513

Date: 15 April 1999

Pressure: 207.6 KPa (30 psig)

Degree of Backflush: A 5 second backflush in a total operational cycle of 120 seconds.

Table F-12: CERAMEM LMA Experimental Data, dated 15 April 1999

Time (hours)	Flux corrected to 25°C ($L/m^2/hr$)	Flux Ratio (-)
0.05	40.05	0.57
0.13	44.96	0.64
0.25	44.52	0.63
0.48	44.56	0.63
0.99	43.79	0.62
1.68	42.63	0.61
4.13	33.82	0.48
8.23	34.01	0.48
12.43	33.62	0.48
16.63	33.52	0.48
18.77	27.56	0.39

Date: 19 April 1999

Pressure: 207.6 KPa (30 psig)

Degree of Backflush: A 5 second backflush in a total operational cycle of 120 seconds.

Table F-13: CERAMEM LMA Experimental Data, dated 19 April 1999

Time (hours)	Flux corrected to 25°C ($L/m^2/hr$)	Flux Ratio (-)
0.09	36.83	0.537
0.17	40.53	0.591
0.25	36.47	0.532
0.51	37.73	0.550
1.00	37.20	0.542
1.79	36.10	0.524
4.15	35.20	0.513
8.33	33.36	0.486
12.49	32.90	0.480
16.98	30.93	0.451
20.86	28.65	0.418
22.09	28.68	0.418

Sample Calculations

The following describes how the pilot scale experimental data, presented in the above tables, was obtained.

During the experimental runs the following raw data was captured with the LABVIEW software program;

a. time,
b. level in the permeate tank (the hydrostatic head in the tank was sensed, which was then converted into a water level in the tank),
c. transmembrane pressure, and
d. temperature of the bilge water.

The permeate tank's pressure transducer continually fed a signal to the personal computer. At a set point, associated with the high tank level, the permeate tank's discharge valve opened thereby dumping the collected permeate back into the bilge water tank. Similarly at a lower set point, associated with the low tank level, the discharge valve was closed, allowing for the permeate tank to fill. In this manner it was possible to determine the volume of permeate collected over a given time interval.

Flux Value – Sample Calculation

The following sample calculations are based upon the raw data for the CERAMEM LMA experimental run of 19 April 1999. Table F-14 presents a sample of the raw data for an interval representing the filling of the permeate tank. (The automated data acquisition program collected approximately 600 data points for every filling of the permeate tank. Therefore, Table F-14 is an abbreviated data set. It is presented only to demonstrate the raw data recorded by the data acquisition program.)

The procedure described below was applied for a number of the permeate tank filling intervals in order to obtain the data tables.

Table F-14: CERAMEM LMA Experimental Raw Data, dated 19 April 1999

Time (minutes)		Permeate Tank Level (cm)		Pressure (psig)	Temp. (°C)
91.34		9.01		29.94	25.01
92.54		9.61		30.11	24.99
93.62		10.12		29.91	24.99
94.76		10.72		30.06	24.99
95.99		11.28		29.95	25.01
97.08		11.84		30.03	24.99
98.15		12.36		29.95	24.99
99.23		12.86		30.06	24.99
100.38		13.45		29.99	25.04
101.53		13.98		29.96	25.01
102.63		14.54		30.02	25.01
103.77		15.09		30.01	24.96
104.91		15.65		30.00	24.99
106.05		16.23		29.98	24.99
107.25		16.77		29.91	24.99
108.34		17.32		29.91	25.01
109.61		17.93		29.96	24.99
110.72		18.47		30.03	24.99
111.85		19.04		30.10	24.99
113.01		19.62		30.06	24.99
114.16		20.15		30.00	25.01
115.37		20.74		29.98	24.96
116.48		21.31		30.05	25.01
117.78		21.93		30.01	25.01
118.90		22.52		29.98	25.01
120.10		23.08		29.96	24.96
121.25		23.63		29.93	24.99
122.37		24.21		29.97	24.93
123.45		24.72		30.03	25.01
124.05		25.03		29.96	25.01

From Table F-14 it can be seen that the level in the permeate tank increased by 16.02cm (25.03-9.01) over a time interval of 32.71 minutes (124.05-91.34). The permeate low and high levels were actually slightly beyond the 9.01cm and 25.03cm levels, but these levels were used to determine the flux value in order to eliminate errors in the pressure transducer associated with the tank emptying.

As seen from Table F-14 the temperature of the permeate is within 0.1°C of 25°C. This is because this particular example was well into an experimental run and at this point the bilge water was maintained at 25°C by the cooling system. However, at the start of an experimental run the temperature may have been as low as 23°C. All the experimental data was corrected to 25°C in accordance with ASTM standard D5090-90: Standardizing Ultrafiltration Permeate Flow Performance. This temperature correction is demonstrated for the initial data set presented in Table F-14:

$$Tank\ Level\ @\ 25^{o}C = \frac{Uncorrected\ Tank\ Level}{100\% + 3(Temp - 25^{o}C)\%}$$

$$Tank\ Level\ @\ 25^{o}C\ @\ 91.34\,\text{min}utes = \frac{9.01cm}{1 + 0.03(25.01 - 25)}$$

$$= 9.01cm$$

The tank level, corrected to 25°C, at 125.04 minutes was 25.02cm.

The flowrate through the membrane was determined by:

$$Flowrate = \frac{\Delta Tank\ Volume}{\Delta Time}$$

$$Flowrate = \frac{\Delta Tank\ Level * Tank\ Area}{\Delta Time} = \frac{\Delta Tank\ Level * \pi(\text{tank radius})^2}{\Delta Time}$$

Where the radius of the permeate tank is 0.074m.

$$Flowrate\ \ @\ 25^{o}C = \frac{(0.2502 - 0.0901)\,m * (\pi * 0.074^2)\,m^2}{(125.04 - 91.34)/60}$$

$$= \frac{0.002756\ m^3}{0.5452\ hr}$$

$$= 0.005054\ {}^{m^3}/_{hr} = 5.054\ {}^{L}/_{hr}$$

The membrane flux is the flowrate divided by the membrane surface area, which for the CERAMEM LMA membrane is 0.14 m^2 (1.5ft^2). Therefore the flux, over the time interval, was:

$$Flux @ 25^{\circ}C = \frac{Flowrate\ 25^{\circ}C}{Membrane\ Surface\ Area}$$

$$= \frac{5.054\ L/hr}{0.14 m^2}$$

$$= 36.10\ L/m^2 * hr$$

Flux Ratio – Sample Calculation

As identified in equation 5.2 (page 73) the flux ratio is;

$$\text{Flux Ratio} = \frac{\text{Bilge Water Flux}}{\text{Estimated PWP Flux for the given Bilge Water Run}}.$$

The following sample calculation will use the data from the CERAMEM LMA experimental run, dated 22 February 1999.

As identified in section 5.2.1 the new CERAMEM LMA membrane had a PWP flux of 97.1 L/m^2/hour and after the series of experimental runs the PWP flux had decreased to 64.7 L/m^2/hour as a result of fouling. A total of 17 experimental runs were conducted with the CERAMEM LMA membrane and assuming that the flux decline was constant with each experimental run then the decline in PWP flux per experimental run is;

$$= \frac{\text{Overall PWP Decline}}{\text{Number of Experimental Runs}}$$

$$= \frac{97.1 - 64.7}{17}\ L/(m^2 * hr)/Experimental\ Run$$

$$= 1.91\ L/(m^2 * hr)/Experimental\ Run$$

The CERAMEM LMA experimental run dated 20 February 1999 was the eighth experimental run conducted with the CERAMEM LMA membrane. Therefore the estimated PWP flux for the CERAMEM LMA membrane, for this experimental run, is;

$$= Virgin\ PWP\ FluxValue - PWP\ Decline$$

$$= 97.1 - 1.91 * 8$$

$$= 83.73\ L/(m^2 * hr)$$

Therefore the flux ratio is the observed bilge water flux divided by this estimated PWP flux. Using the data point at approximately 4.14 hours as an example the flux ratio is;

$$= \frac{56.84\ L/(m^2 * hr)}{83.73\ L/(m^2 * hr)}$$

$$= 0.679$$

APPENDIX G:

KOCH CM MEMBRANE RAW DATA

KOCH CM Membrane Experimental Results

The following is the data for the various experimental runs conducted with the KOCH CM membrane. Presented are the time versus flux (corrected to 25°C) data for the various experimental runs. These data sets were obtained in the same manner as those for the CERAMEM LMA membrane; of which sample calculations were presented in Appendix F.

As done with the CERAMEM LMA experimental runs all of the KOCH CM runs, conducted with "New Bilge Water" were conducted without a pre-membrane bag filter. However, some of the KOCH CM experimental runs, conducted with "Used Bilge Water" had a pre-membrane bag filter in place, while others din not.

NEW BILGE WATER RESULTS

That is, the following series of experimental data were conducted with Bilge Water prepared in accordance with the method described in section 4.3.

Date: 09 August 1999

Pressure: 207.6 KPa (30 psig)

Degree of Backflush: A 5 second backflush in a total operational cycle of 120 seconds.

Table G-1: KOCH CM Experimental Data, dated 09 August 1999

Time (hours)	Flux corrected to 25°C ($L/m^2/hr$)
0.07	214.45
0.20	198.78
0.50	184.30
1.03	170.80
1.71	166.55
4.18	165.78
6.27	165.88
8.37	169.94
10.38	166.93
12.53	170.15
14.62	172.90
16.72	173.41
18.73	175.30
20.83	167.51
22.93	173.68
25.02	171.48

Date: 10 August 1999

Pressure: 207.6 KPa (30 psig)

Degree of Backflush: A 5 second backflush in a total operational cycle of 30 seconds.

Table G-2: KOCH CM Experimental Data, dated 10 August 1999

Time (hours)	Flux corrected to 25°C ($L/m^2/hr$)
0.05	164.78
0.20	160.38
0.50	161.89
1.03	161.05
1.68	161.23
4.15	165.04
6.24	156.71
8.34	155.34
10.42	158.46
12.46	157.94
14.58	162.34
16.65	153.08
17.48	153.52

Date: 11 August 1999

Pressure: 207.6 KPa (30 psig)

Degree of Backflush: A 5 second backflush in a total operational cycle of 60 seconds.

Table G-3: KOCH CM Experimental Data, dated 11 August 1999

Time (hours)	Flux corrected to 25°C ($L/m^2/hr$)
0.07	287.91
0.18	296.36
0.53	270.05
1.02	252.96
1.68	239.55
4.20	220.24
6.28	214.34
8.36	197.04
10.43	194.52
12.51	188.49
14.58	180.91
16.66	183.15
18.73	180.45
20.82	176.38
22.89	176.00
24.97	173.58

Date: 13 August 1999

Pressure: 207.6 KPa (30 psig)

Degree of Backflush: A 5 second backflush in a total operational cycle of 90 seconds.

Table G-4: KOCH CM Experimental Data, dated 13 August 1999

Time (hours)	Flux corrected to 25°C ($L/m^2/hr$)
0.08	257.64
0.30	244.74
0.55	240.98
1.04	232.29
1.73	218.49
4.17	197.64
6.28	191.10
8.33	187.17
10.43	180.01
12.48	179.72
14.64	177.00
16.70	172.52
18.77	173.45
20.83	170.33
22.52	169.62

Date: 14 August 1999

Pressure: 207.6 KPa (30 psig)

Degree of Backflush: A 5 second backflush in a total operational cycle of 45 seconds.

Table G-5: KOCH CM Experimental Data, dated 14 August 1999

Time (hours)	Flux corrected to 25°C ($L/m^2/hr$)
0.08	312.50
0.24	295.51
0.48	276.03
0.99	258.42
1.67	241.45
4.19	204.95
6.24	190.80
8.33	189.53
10.39	179.14
12.48	170.52
14.58	172.02
16.68	175.01
18.78	168.59
20.83	167.24
22.93	166.52
25.03	162.09

Date: 16 August 1999

Pressure: 207.6 KPa (30 psig)

Degree of Backflush: None.

Table G-6: KOCH CM Experimental Data, dated 16 August 1999

Time (hours)	Flux corrected to 25°C ($L/m^2/hr$)
0.07	296.75
0.20	282.54
0.50	254.69
0.98	238.79
1.65	225.68
4.17	202.66
6.27	191.22
8.33	185.70
10.38	177.57
12.48	174.11
14.58	165.01
16.67	161.61
18.73	158.41
20.87	154.65
22.92	156.04
25.02	150.08

Date: 18 August 1999

Pressure: 193.0 KPa (28 psig)

Degree of Backflush: A 5 second backflush in a total operational cycle of 120 seconds.

Table G-7: KOCH CM Experimental Data, dated 18 August 1999

Time (hours)	Flux corrected to 25°C ($L/m^2/hr$)
0.08	278.94
0.24	273.90
0.53	263.55
1.04	251.36
1.68	240.75
4.23	220.35
6.26	212.73
8.34	199.85
10.41	193.17
12.52	186.69
14.59	183.52
16.68	184.50
18.79	175.67
20.86	175.65
22.93	176.27
25.05	170.96

USED BILGE WATER RESULTS

That is, the following series of experimental data were conducted with Bilge Water prepared in accordance with the method described in section 4.3, except that used diesel engine lubricating oil, rather than new diesel engine lubricating oil, was used.

Date: 01 September 1999

Pressure: 207.6 KPa (30 psig)

Degree of Backflush: A 5 second backflush in a total operational cycle of 120 seconds.

Note: The pre-membrane bag filter was in place for this experimental run.

Table G-8: KOCH CM Experimental Data, dated 01 September 1999

Time (hours)	Flux corrected to 25°C ($L/m^2/hr$)
0.06	337.79
0.50	305.63
0.96	280.56
1.65	253.87
4.13	207.41
6.23	183.00
8.34	177.53
10.41	170.09
12.49	166.16
14.56	164.05
16.66	164.84
18.73	163.60
20.83	165.06
22.88	164.83
24.98	167.95

Date: 04 September 1999

Pressure: 207.6 KPa (30 psig)

Degree of Backflush: A 5 second backflush in a total operational cycle of 30 seconds.

Note: The pre-membrane bag filter was in place for this experimental run.

Table G-9: KOCH CM Experimental Data, dated 04 September 1999

Time (hours)	Flux corrected to 25°C ($L/m^2/hr$)
0.08	348.21
0.23	309.96
0.53	298.55
1.01	291.94
1.64	274.55
4.18	252.37
6.25	241.26
8.33	224.80
10.43	222.90
12.51	216.04
14.58	211.97
16.70	202.49
18.73	198.31
20.85	189.82
22.96	186.08
24.99	186.91

Date: 05 September 1999

Pressure: 207.6 KPa (30 psig)

Degree of Backflush: A 5 second backflush in a total operational cycle of 90 seconds.

Note: The pre-membrane bag filter was in place for this experimental run.

Table G-10: KOCH CM Experimental Data, dated 05 September 1999

Time (hours)	Flux corrected to 25°C ($L/m^2/hr$)
0.08	304.20
0.25	301.94
0.53	294.60
0.98	295.00
1.71	285.00
4.20	269.51
6.22	260.54
8.33	253.75
10.40	253.77
12.53	247.27
14.59	244.54
16.67	242.78
18.73	239.85
20.85	234.07
22.91	231.38
25.03	234.79

Date: 07 September 1999

Pressure: 207.6 KPa (30 psig)

Degree of Backflush: A 5 second backflush in a total operational cycle of 45 seconds.

Note: The pre-membrane bag filter was in place for this experimental run.

Table G-11: KOCH CM Experimental Data, dated 07 September 1999

Time (hours)	Flux corrected to 25°C ($L/m^2/hr$)
0.08	302.10
0.23	305.82
0.48	296.82
0.99	293.77
1.68	283.79
4.20	279.07
6.23	277.99
8.33	268.12
10.39	270.08
12.49	258.47
14.61	264.12
16.66	268.48
18.74	256.63
20.86	251.98
21.58	256.10

Date: 11 September 1999

Pressure: 207.6 KPa (30 psig)

Degree of Backflush: None.

Note: The pre-membrane bag filter was not in place for this experimental run.

Table G-12: KOCH CM Experimental Data, dated 11 September 1999

Time (hours)	Flux corrected to 25°C ($L/m^2/hr$)
0.08	309.19
0.24	305.72
0.48	303.64
0.98	293.11
1.64	293.92
4.16	270.92
6.21	256.13
8.34	249.76
10.39	249.72
12.49	242.41
14.58	238.51
16.63	235.52
18.76	232.53
20.80	230.66
22.94	226.93
24.98	228.19

Date: 28 September 1999

Pressure: 207.6 KPa (30 psig)

Degree of Backflush: A 5 second backflush in a total operational cycle of 120 seconds.

Note: The pre-membrane bag filter was not in place for this experimental run.

Table G-13: KOCH CM Experimental Data, dated 28 September 1999

Time (hours)	Flux corrected to 25°C ($L/m^2/hr$)
0.07	212.83
0.23	208.01
0.51	201.35
0.98	199.72
1.68	199.17
4.13	189.11
6.28	192.25
8.32	189.48
10.45	185.23
12.48	181.71
14.59	184.16
16.66	181.35
18.73	178.08
20.80	179.89
22.92	177.54
24.99	178.28

APPENDIX H:
DETMINATION OF PILOT SCALE TESTING ERROR

As identified in section 5.2.2 the error associated with the pilot scale testing was determined through a comparison of the flux values, after the experimental runs achieved steady-state conditions. This is due to the fact that once steady-state conditions are achieved the flux values should remain constant, assuming that no membrane fouling occurs beyond this point in the experimental run.

The following will present the determination of error for the experimental run using the CERAMEM LMA membrane conducted on March 3rd, 1999, under the following operational conditions;

a. no backflushing,
b. a cross-flow velocity of 1.74 m/s,
c. using new bilge water, and
d. a transmembrane pressure of 220 KPa.

The error associated with this run was found to quite adequately portray the error associated with all the conducted experimental runs. In fact, this experimental run provided a (relatively) high degree of flux variability and thus provides a worse case for the error.

The determination of the flux values was conducted in the same manner as for the raw data. Sample calculations for the determination of flux values can be found in Appendix F – CERAMEM LMA Membrane Raw Data.

A three-phase process was required to determine the error associated with the pilot scale testing. First, average flux values throughout an experimental run had to be determined from the raw data. Second, the onset of steady-state conditions had to be determined. Third, the error, associated with the steady-state flux values had to be determined.

Table H-1 presents the flux values throughout the experimental run. From Table H-1 it can be seen that steady state occurs at approximately 30.84 hours and continues until the end of the experimental run, a time of 66.92 hours.

Therefore the average steady-state flux is equal to:

$$= \frac{\sum_{time=30.84 hours}^{time=66.92 hours} fluxes}{number\ of\ flux\ data\ values}$$

$$= \frac{2003.35}{52}$$

$$= 38.53 \text{ L/m}^2\text{/hr}$$

The standard deviation of the average steady-state flux value (from 30.84 to 66.92 hours) is:

$$= \sqrt{\frac{n\sum x^2 - \left(\sum x\right)^2}{n(n-1)}}$$

$$= \sqrt{\frac{52 * 77182 - 4{,}013{,}423}{52 * (52-1)}}$$

$$= 0.1213 \text{ L/m}^2\text{/hr}$$

The error associated with a 95% confidence interval is:

$$= \pm 1.96(\text{standard deviation})$$

$$= \pm 1.96(0.1213) = \pm 0.238\ L/m^2 * hr$$

Therefore, in this case, the steady-state flux is 38.53 ± 0.24 L/m^2*hr, or in percentage terms $38.53\ L/m^2 * hr \pm 0.62\%$.

Table H-1: Average Flux Values for the CERAMEM LMA Experimental Run, dated 03 March 1999

Time (hours)	Permeate Flux (L/m2/hr)	Time (hours)	Permeate Flux (L/m2/hr)	Time (hours)	Permeate Flux (L/m2/hr)
0.40	40.96	22.96	39.13	44.81	38.50
1.13	36.75	23.65	39.10	45.55	38.60
1.85	36.09	24.33	39.10	46.25	38.43
2.52	39.50	24.95	38.99	46.88	38.46
3.17	39.67	25.57	39.00	47.55	38.44
3.83	39.41	26.17	38.84	48.26	38.44
4.55	39.41	26.80	38.91	48.99	38.40
5.20	39.43	27.43	38.85	49.75	38.52
5.89	39.56	28.10	38.82	50.55	38.72
6.64	39.33	28.76	38.71	51.29	38.42
7.37	39.35	29.41	38.81	51.97	38.35
8.07	39.21	30.10	38.79	52.67	38.33
8.83	39.47	30.84	38.59	53.42	38.80
9.62	39.42	31.53	38.69	54.20	38.57
10.37	39.41	32.16	38.64	55.00	38.75
11.08	39.21	32.84	38.57	55.76	38.42
11.79	39.03	33.53	38.59	56.46	38.36
12.46	39.02	34.28	38.78	57.16	38.39
13.12	39.13	35.04	38.53	57.88	38.44
13.82	39.11	35.77	38.49	58.56	38.39
14.52	39.15	36.48	38.51	59.21	38.45
15.18	39.18	37.13	38.54	59.89	38.39
15.89	39.41	37.82	38.44	60.66	38.62
16.61	39.31	38.54	38.43	61.42	38.42
17.27	39.43	39.25	38.43	62.18	38.60
17.95	39.16	39.96	38.36	62.88	38.40
18.66	39.32	40.70	38.59	63.56	38.50
19.39	39.57	41.47	38.49	64.30	38.70
20.15	39.45	42.19	38.58	65.00	38.66
20.86	39.12	42.87	38.61	65.66	38.70
21.54	39.33	43.53	38.51	66.30	38.51
22.25	39.22	44.14	38.59	66.92	38.70

APPENDIX I:

DETERMINATION OF MEMBRANE MODULE STEADY STATE CONDITIONS AND COMPARISON WITH THE FLUX VERSUS TIME THEORY

The determination of the steady state conditions, that is the time required to achieve the steady state cake layer and its thickness, are presented below. Additionally, the comparison of the membrane experimental conditions with the time dependent flux theory, detailed by equation 3.21, is also presented.

The following sample calculations are conducted using the experimental data for the KOCH CM membrane.

Steady State Conditions

As shown in Figure 5.11 the PWP flux for the KOCH CM membrane was approximately 415 $L/m^2/hr$, which equates to $1.15*10^{-4}$ $m^3/m^2/s$.

Table G-6 details the experimental data for the KOCH CM membrane, when no backflushing was utilized. As seen from this table the flux after approximately 24 hours, which should reasonably portray steady state conditions, was 150.08 $L/m^2/hr$, which equates to $4.17*10^{-5}$ $m^3/m^2/s$. (It is assumed that the irreversible fouling after the formation of the steady state conditions and 24 hours is negligible.) This experimental run was conducted at a transmembrane pressure of 206,735 Pa.

The dynamic viscosity of water is 0.000891 Pa*s.

Using equation 3.3 the membrane resistance can be determined:

$$R_{mem} = \frac{\Delta P}{\mu J_{PWP}} = \frac{206735}{0.000891*\left(1.15*10^{-4}\right)}$$

$$= 2.01*10^{12}\ m^{-1}$$

Using equation 3.23 the time required for the steady state cake layer to be formed can be determined. The only unknown in this equation is the time constant associated with flux decline (τ_c), which can be determined by equation 3.22.

As shown by Sethi and Wiesner the maximum solute (oil) concentration, at the cake layer, is approximately 0.58 and the bulk solute concentration has been assumed as 200 ppm.

The specific cake layer resistance ($\hat{R}_{cake}$) is determined in accordance with equation 3.12. The only unknown variable in this equation is the critical particle size (a_p), which is determined through the diffusivity versus particle size method (as done in Appendix A). Figure I-1 presents diffusivity versus particle size for the KOCH CM membrane. From this figure it can be seen that the critical particle size for the KOCH CM membrane is approximately 0.042 microns.

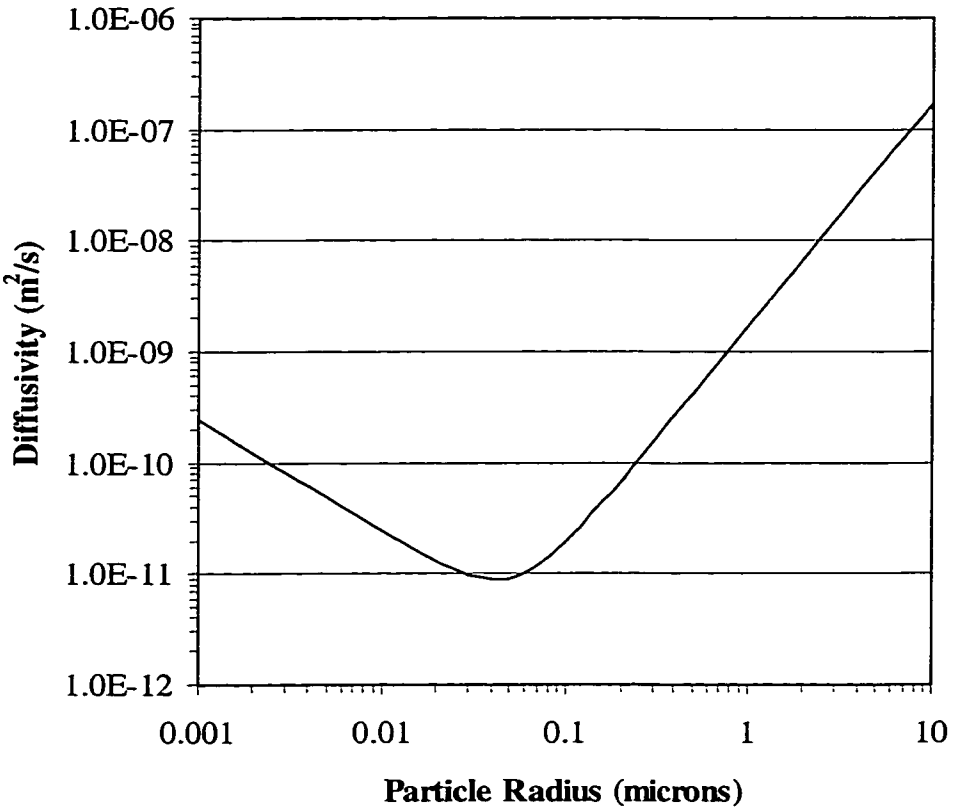

Figure I-1: Effect of Particle Size on Cake Layer Diffusivity, for the KOCH CM Membrane

Therefore the specific cake layer resistance is equal to:

$$\hat{R}_{cake} = \frac{37.5\phi_{max}^2}{a_p^2(1-\phi_{max})^3}$$

$$= \frac{37.5*0.58^2}{(4.2*10^{-8})^2(1-0.58)^3}$$

$$= 9.65*10^{16}\ m^{-2}$$

Therefore the time constant associated with flux decline is:

$$\tau_c = \frac{R_{mem}(\phi_{max}-\phi_b)}{J_{PWP}\hat{R}_{cake}\phi_b}$$

$$= \frac{(2.01*10^{12})(0.58-0.0002)}{(1.15*10^{-4})(9.65*10^{16})0.0002}$$

$$= 456.74$$

Using equation 3.23 the time required for the cake layer to achieve its steady state condition is:

$$t_{ss} = \left(\frac{\tau_c}{2}\right)\left[\left(\frac{J_{PWP}}{J(t_{ss})}\right)^2 - 1\right]$$

$$= \left(\frac{456.74}{2}\right)\left[\left(\frac{1.15*10^{-4}}{4.17*10^{-5}}\right)^2 - 1\right]$$

$$= 1515.7 \text{ seconds} = 25.3 \text{ minutes}$$

The cake layer thickness is determined in accordance with equation 3.36:

$$\delta_{ss} = \frac{(R_{mem}^2 + 2C\hat{R}_{cake}t_{ss})^{0.5} - R_{mem}}{\hat{R}_{cake}}$$

where the constant in equation 3.36 is defined as:

$$C = \frac{\Delta P \phi_b}{\mu(\phi_{max} - \phi_b)}$$

$$= \frac{206375 * 0.0002}{0.000891(0.58 - 0.0002)}$$

$$= 92{,}000$$

Thus the cake layer thickness is:

$$\delta_{ss} = \frac{\left((2.01*10^{12})^2 + 2*92000*(9.65*10^{16})*1515.7\right)^{0.5} - 2.01*10^{12}}{9.65*10^{16}}$$

$$= 36.80 \text{ microns}$$

Experimental Data vs. Time Dependent Flux

Figures 5.19 and 5.20 are created by plotting the experimental data (for no backflushing) against the theoretically determined flux values, for both cross-flow and dead-ended membrane flows. The cross-flow and dead-ended flow are determined in accordance the above time dependent flux theory; specifically equation 3.21. The theoretical cross-flow membrane flow was determined in precisely the same manner as the dead-ended flow, except that after the cake layer has achieved its steady state condition the flux no longer declines. Conversely, in dead-ended filtration the cake layer will continually grow.

As detailed above the pure water permeate flux (J_{PWP}) is $1.15*10^{-4}$ $m^3/m^2/s$, the membrane resistance (R_{mem}) is $2.01*10^{12}$ m^{-1} and the time constant associated with flux decline (τ_c) is 456.74. The theoretical flux at a given time is determined in accordance with equation 3.16 and the experimental values (for no backflushing) are as detailed in Table G-6. Table I-1 shows the theoretical cross-flow and dead-ended values compared to the experimental flux values; plotted gives Figure 5.19.

Table I-1: Experimental vs. Theoretical Flux Values, for the KOCH CM Membrane, No Backflushing, New Bilge Water

Time		Theoretical Flux		Experimental Flux
		Dead-Ended	Cross-Flow	
(hours)		(L/m2/hr)	(L/m2/hr)	(L/m2/hr)
0.01		385.48	385.48	
0.07		289.61	289.61	296.75
0.10		258.39	258.39	
0.20		203.53	203.53	282.54
0.30		173.28	173.28	
0.42		150.08	150.08	
0.50		139.17	150.08	254.69
0.75		115.82	150.08	
0.98		102.10	150.08	238.79
1.65		79.80	150.08	225.68
2.00		72.72	150.08	
3.00		59.68	150.08	
4.17		50.79	150.08	202.66
5.00		46.42	150.08	
6.27		41.52	150.08	191.22
7.00		39.31	150.08	
8.33		36.05	150.08	185.70
9.00		34.70	150.08	
10.38		32.32	150.08	177.57
11.00		31.41	150.08	
12.48		29.49	150.08	174.11
13.00		28.90	150.08	
14.58		27.30	150.08	165.01
15.00		26.91	150.08	
16.67		25.54	150.08	161.61
17.50		24.93	150.08	
18.73		24.09	150.08	158.41
19.00		23.93	150.08	
20.87		22.83	150.08	154.65
22.00		22.24	150.08	
22.92		21.79	150.08	156.04
24.00		21.29	150.08	
25.02		20.87	150.08	150.08

As an example of how the theoretical flux values were determined the following sample calculation is conducted at a time of 0.20 hours.

$$J(0.20hours) = \frac{J_{PWP}}{\left(1+\frac{2t}{\tau_c}\right)^{0.5}}$$

$$= \frac{1.15*10^{-4}}{\left(1+\frac{2*(0.20*3600)}{456.74}\right)^{0.5}}$$

$$= 5.65*10^{-5}\ m^3/m^2/s = 203.53\ L/m^2/hr$$

APPENDIX J:

THEORETICAL CAKE LAYER FORMATION AND REMOVAL

During the treatment of any fluid the flux at a given time is defined by equation 3.21, which is,

$$J(t)=\frac{J_{PWP}}{\left(1+\frac{2t}{\tau_c}\right)^{0.5}}.$$

Thus, when utilizing backflushing the flux at conclusion of the operating cycle, i.e. when the backflushing is conducted, is determined by,

$$J(t_{op})=\frac{J_{PWP}}{\left(1+\frac{2t_{op}}{\tau_c}\right)^{0.5}}.$$

Therefore the total system resistance can be determined by applying equations 3.1 and 3.2, which state,

$$J=\frac{\Delta P}{\mu R_{total}}, \text{ and}$$

$$R_{total}=R_{mem}+R_{cake}+R_{foul}\ .$$

Knowing the membrane resistance and the resistance due to fouling, the cake layer resistance can be identified and then the cake layer thickness can be solved for, through the use of equation 3.11,

$$R_{cake}=\hat{R}_{cake}\delta\ .$$

The cake layer thickness can also be determined through the use of equation 3.36, except rather than solving for a steady state cake layer, the cake layer at a given time is determined. Equation 3.36 is merely the solution for the cake layer thickness as identified in the above steps. Accordingly, equation 3.36 can be re-written in the following form, to solve for the cake layer thickness at a given time,

$$\delta(t)=\frac{\left(R_{mem}^2+2C\hat{R}_{cake}t\right)^{0.5}-R_{mem}}{\hat{R}_{cake}}\ .$$

The amount of cake layer theoretically removed by backflushing is determined through the use of equation 3.39,

$\delta_{removed} = -J_{bf} t_{bf}$, where the negative sign implies that the cake layer is decreasing.

The backflush flux is determined through equations 3.29 or 3.30. In the cases studied the operational time (t_{op}) was always less than the time required to achieve steady state conditions (t_{ss}), therefore the backflush flux equates to,

$$J_{bf} = \left(\frac{J_{PWP} \tau_c t_{op}}{t_{total}^2} \right) \left[\left(1 + \frac{2t_{total}}{\tau_c} \right)^{0.5} - 1 \right]. \qquad (3.29)$$

Sample Calculation: Theoretical Cake Layer Accumulation & Removal, by Backflushing, for the KOCH CM Membrane

Assumptions: A. The dynamic viscosity of water (μ) is equal to 0.000891 Pa*s.

B. The maximum solute volume (ϕ_{max}) is assumed to be 0.58 (Sethi and Wiesner, 1995).

C. The bulk solute volume (ϕ_b) is assumed to be 200 ppm.

The operating pressure used for the experimental run, presented in this sample calculation, was 206KPa (30psi).

As identified in section 5.2.1 the PWP flux for the KOCH CM membrane is approximately 415 L/m2/hr, or roughly $1.15*10^{-4}$ $m^3/m^2/s$.

Therefore the membrane resistance for the KOCH CM membrane is:

$$R_{mem} = \frac{\Delta P}{\mu J_{PWP}}$$

$$= \frac{206734\ Pa}{(0.000891\ Pa*s)\left(1.15*10^{-4}\ m/s\right)}$$

$$= 2.01*10^{12}\ \text{m}^{-1}$$

As shown in Appendix I the radius of the critical particle associated with the KOCH CM membrane is approximately 0.042 microns.

Therefore the specific cake layer resistance is:

$$\hat{R}_{cake} = \frac{37.5\phi_{\max}^2}{a_p^2(1-\phi_{\max})^3}$$

$$= \frac{37.5*0.58^2}{\left(4.2*10^{-8}\right)^2(1-0.58)^3}$$

$$= 9.65*10^{16}\ \text{m}^{-2}$$

As identified in section 3.6 the constant, identified in equation 3.33, is equivalent to:

$$C = \frac{\Delta P\phi_b}{\mu(\phi_{\max}-\phi_b)}$$

$$= \frac{206735*0.0002}{0.000891(0.58-0.0002)}$$

$$= 80{,}036$$

The most common experimental run conducted was that having a 120 seconds total operational cycle, divided into a 115 second operational time and a 5 second backflush. For this condition the cake layer formed during the operational phase is:

$$\delta = \frac{\left(R_{mem}^2 + 2C\hat{R}_{cake}t\right)^{0.5} - R_{mem}}{\hat{R}_{cake}}$$

$$= \frac{\left(\left[2.01*10^{12}\right]^2 + 2*80036*\left(9.65*10^{16}\right)*115\right)^{0.5} - \left(2.01*10^{12}\right)}{9.65*10^{16}}$$

$$= 4.16*10^{-6}\ \text{m} = 4.16\ \text{microns}$$

Since the operational time is less than the time required for a steady state cake layer to form the backflush flux (J_{bf}) is equal to:

$$J_{bf} = \left(\frac{J_{PWP} \tau_c t_{op}}{t_{total}^2} \right) \left[\left(1 + \frac{2t_{total}}{\tau_c} \right)^{0.5} - 1 \right]$$

In the above equation the time constant associated with membrane flux decline is:

$$\tau_c = \frac{R_{mem} (\phi_{max} - \phi_b)}{J_{PWP} \hat{R}_{cake} \phi_b}$$

$$= \frac{(2.01 * 10^{12})(0.58 - 0.0002)}{(1.15 * 10^{-4})(9.65 * 10^{16}) 0.0002}$$

$$= 525.02$$

Thus, the backflush flux is equal to:

$$J_{bf} = \left(\frac{(1.15 * 10^{-4})(525.02)(115)}{120^2} \right) \left[\left(1 + \frac{2 * 120}{525.02} \right)^{0.5} - 1 \right]$$

$$= 5.43 * 10^{-4} \text{ m}^3/\text{m}^2/\text{s}$$

Therefore, theoretically, the amount of cake layer removed, during this 5 second backflush would be:

$$\delta_{removed} = - J_{bf} t_{bf}$$

$$= - (5.43 * 10^{-4}) * 5$$

$$= -0.00271 \text{ m} = -2{,}710 \text{ microns}$$

Since the value of the removed cake layer exceeds the value of the cake layer, formed during the operational cycle, then theoretically, the entire cake layer should be removed.

APPENDIX K:

TRANSPORT CANADA CERTIFICATION OF THE CANADIAN NAVY HYDROMEM OILY WASTEWATER SEPARATOR

K-2

CANADA

Certificate number 15/0158
Certificat numéro

CERTIFICATE OF TYPE APPROVAL FOR OIL FILTERING EQUIPMENT
CERTIFICAT D'AGRÉMENT PAR TYPE DU MATÉRIEL DE FILTRAGE DES HYDROCARBURES

(15ppm equipment) *(Matériel à 15ppm)*

BWTS-100

This is to certify that the equipment listed below has been examined and tested in accordance with the requirements of the Specification contained in Part I of the Annex to the Guidelines and Specifications contained in IMO resolution MEPC 60 (33). This certificate is valid only for equipment referred to below.
Il est certifié que le matériel ci-après a été examiné et soumis à des essais conformément aux dispositions des spécifications qui font l'objet de la Partie I de l'Annexe aux Directives et Spécifications contenues dans la résolution MEPC 60 (33) de l'OMI. Le présent certificat n'est valable que pour le matériel du type décrit ci-dessous.

Equipment supplied by *Matériel fourni par*	Water Technology International Corp.
Type and model designation incorporating: *Type et désignation du modèle comprenant*	BWTS-100
* Equipment manufactured by *Dispositif fabriqué par*	Water Technology International Corp.
To specification/drawing numbers *Conformément à la spécification/au schéma n°*	WRI-1998-05-000
* Hydrocylone manufactured by *Hydro-cyclonal fabriqué par*	KREBS Inc.
To specification/drawing numbers *Conformément à la spécification/au schéma n°*	PL2003-WTI (98-08-17)
* Membrane manufactured by *Filtres fabriqués par*	KOCH
To specification/drawing numbers *Conformément à la spécification/au schéma n°*	7001-5002 Rev A (92-08-07) 7004-5002 Rev A (93-11-16)
Control equipment manufactured by *Matériel de contrôle fabriqué par*	Allen BradleySLC 500
To specification/drawing numbers *Conformément à la spécification/au schéma n°*	Parts 35-43
Maximum throughput of system *Débit maximal du dispositif*	0.45 m^3/h

If integral feed pump is not fitted state method proposed for ensuring maximum throughput of system is not exceeded.
Si le dispositif ne comporte pas de pompe d'alimentation, indiquer la méthode envisagée pour s'assurer que le débit maximal du système n'est pas dépassé.

The equipment has been tested with a residual oil having a relative density of not less than ~~0.94*~~ or 0.98* at 15° C.
Le matériel a été mis à l'essai avec des hydrocarbures résiduels ayant une densité relative qui n'était pas inférieure à ~~0.94~~ or 0.98* à 15° C*

* DELETE AS APPROPRIATE
RAYER LA MENTION INUTILE

Test data and results
Les données et résultats des essais. As per Naval Engineering Testing Establishment Certificate #XT322-01-P dated 31 August 1998

LIMITATION
RESTRICTION

A COPY OF THIS TEST CERTIFICATE SHOULD BE CARRIED ABOARD A VESSEL FITTED WITH THIS EQUIPMENT AT ALL TIMES.
UN EXEMPLAIRE DU PRÉSENT CERTIFICAT D'ESSAI DEVRAIT SE TROUVER EN PERMANENCE A BORD D'UN NAVIRE ÉQUIPÉ DE CE MATÉRIEL.

CANADA-MINISTÈRE DES TRANSPORTS-DEPARTMENT OF TRANSPORT
OFFICIAL STAMP
CACHET OFFICIEL

AMSE - C020M(12-98)

David T. Ford — Marine Surveyor Pollution Prevention

(SIGNATURE OF AUTHORIZED INSPECTOR / *SIGNATURE DE L'INSPECTEUR AUTORISÉ*)

DATED THIS *DATE CE* 23 DAY OF *JOUR DE* DECEMBER 1998

Canada

APPENDIX
APPENDICE

MODEL BWTS-100
TEST DATA AND RESULTS OF TEST CONDUCTED ON A FILTERING EQUIPMENT IN ACCORDANCE WITH PART 1 OF THE ANNEX TO THE GUIDELINES AND SPECIFICATIONS CONTAINED IN IMO RESOLUTION MEPC 60 (33)
DONNÉES ET RÉSULTATS DES ESSAIS EFFECTUÉS SUR UN MATÉRIEL DE FILTRAGE DES HYDROCARBURES CONFORMÉMENT A LA PARTIE 1 DE L'ANNEXE DES DIRECTIVES ET SPÉCIFICATIONS CONTENUES DANS LA RÉSOLUTION MEPC 60 (33) DE L'OMI

Equipment submitted by / *Matériel présenté par*: Water Technology International Corp

Test location / *Lieu ou l'essai a été effectué*: 9401 Wanklyn, Lasalle Quebec H8R 1Z2

Method of sample analysis / *Méthode d'analyse des échantillons*: EPA Method 1664

Samples analysed by / *Échantillons analysés par*: Naval Engineering Test Establishment, 9401 Wanklyn, Lasalle, QC H8R1Z2

Environmental testing of the electrical and electronic sections of the equipment has been carried out in accordance with Part 3 of the annex to the Guidelines and Specifications contained in IMO resolution MEPC 60 (33). The equipment functioned satisfactorily on completion of each test specified on the environmental test protocol.
Les essais d'environnement des éléments électriques et électroniques du matériel ont été effectués conformément à la partie 3 de l'annexe aux Directives et Spécifications contenues dans la Résolution MEPC 60 (33) de l'OMI. Le matériel fonctionnait de manière satisfaisante après chacun des essais spécifiés dans le protocole d'essais d'environnement.

Manufacturers' recommendations and information concerning the use of cleansing agents.
Recommandations des fabricants et renseignements concernant l'emploi d'agents de nettoyage.

Note: When the system "High Oil Feed" is activated , the feed to the membrane is diverted to a storage tank.
The "High Oil Feed" automatic function was disabled by WTI during the 25% oil injection test to allow processing of 25% oil in the water by the membrane for test fuel oil A & B.
This function was enabled by WTI for the 100% oil feed test only with test fuel oil A

TRANSPORT CANADA - MINISTÈRE DES TRANSPORTS - DEPARTMENT OF TRANSPORT
OFFICIAL STAMP / CACHET OFFICIEL

David T. Ford
(SIGNATURE OF AUTORIZED INSPECTOR / *SIGNATURE DE L'INSPECTEUR AUTORISÉ*)

DATED THIS 23 DAY OF DECEMBER 19 98
DATÉ CE ——— *JOUR DE* ———

AMSE - A020(10-93)

MODEL BWTS-100

Test oil (A) *Hydrocarbure d'essai*		Test oil (B) *Hydrocarbure d'essai*	
Influent *Affluent* %	Effluent *Effluent* ppm	Influent *Affluent* %	Effluent *Effluent* ppm
0.5 to 1	0	0.5 to 1	0
0.5 to 1	0	0.5 to 1	01
0.5 to 1	4 7	0.5 to 1	01
25	1.9	25	1.8
25	0	25	11.8
25	0	25	2.0
100	0	—	—
100	0	—	—
**	< 1	**	< 1

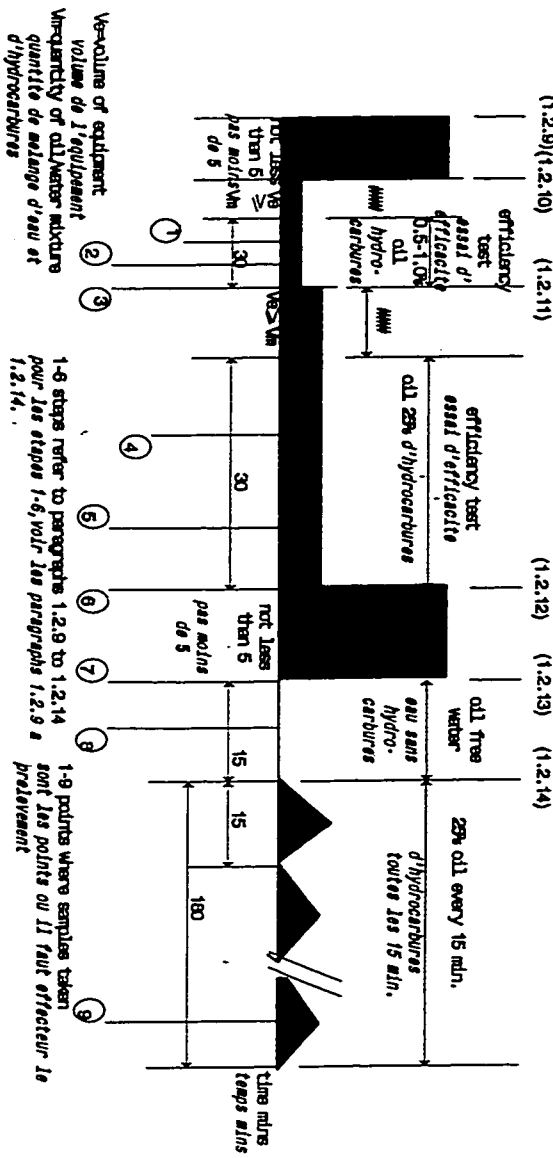

**Test sample (9) taken at the end of final oil phase auto test, paragraph 1.2.14 - Part 1 of the Annex to resolution MEPC 60 (33).
Prélevé à la fin de la dernière phase hydrocarbures de l'auto-essai, paragraphe 1.2.14, Partie 1 de l'annexe à la résolution MEPC 60 (33)

Conditionment

OFFICIAL STAMP
CACHET OFFICIEL
MINISTÈRE DES TRANSPORTS - DEPARTMENT OF TRANSPORT

(SIGNATURE OF AUTHORIZED INSPECTOR / *SIGNATURE DE L' INSPECTEUR AUTORISE*)

DATED THIS _____ DAY OF _____ 19___
DATÉ CE *JOUR DE*